NATIONAL ADVISORY COMMITTEE FOR AERONAUTICS

TECHNICAL NOTE 3114

ANALYSIS OF MULTICELL DELTA WINGS ON CAL-TECH ANALOG COMPUTER

By Richard H. MacNeal and Stanley U. Benscoter

California Institute of Technology

Washington
December 1953

.B

NATIONAL ADVISORY COMMITTEE FOR AERONAUTICS

TECHNICAL NOTE 3114

ANALYSIS OF MULTICELL DELTA WINGS ON CAL-TECH ANALOG COMPUTER

By Richard H. MacNeal and Stanley U. Benscoter

SUMMARY

Using the Cal-Tech analog computer, structural analyses have been made of two delta wings with 45° leading edges. One of these has a constant-depth rectangular cross section and the other has a biconvex cross section that is linearly tapered in the spanwise direction. The wings extend through the fuselage and are rigidly supported along two lines at the faces of the fuselage.

Deflections and all internal forces have been calculated for concentrated static loads. Vibration modes are also presented. The effects of neglecting shearing strains in the ribs and spars and also of assuming the ribs to be rigid have been investigated by modifying the electric circuits to correspond to these simplifications.

INTRODUCTION

The structural analysis of thin multicell wings of nonrectangular plan form presents a difficult problem, particularly when high accuracy is desired. Two delta wings with 45° leading edges have been analyzed on the Cal-Tech analog computer for concentrated statical loads applied at points at the intersections of ribs and spars. Vibration modes have also been calculated. One of these wings has a rectangular cross section while the other has a biconvex cross section and is linearly tapered from fuselage face to tip. Except for the leading-edge spar, the spars are not swept. The wings extend through the fuselage and are rigidly supported along two lines at the faces of the fuselage.

The structural theory and analogous circuits for rectangular bays of multicell wings are given in reference 1. Additional structural theory required for the analysis of the leading edge of a delta wing is developed in this paper.

The main purpose of this paper is to present the results of measurements made on the Cal-Tech computer. The diagrams present only a small

portion of the data which were obtained from the computer and which are given in complete form in the tables.

The effects of certain simplifications in the structural theory have been obtained by modifying the electrical circuits to correspond to these simplifications. The error due to neglecting the effect of shearing strains in the ribs and spars was investigated. The effect of assuming the ribs to be rigid was also determined.

The present investigation was conducted at the California Institute of Technology under the sponsorship and with the financial assistance of the National Advisory Committee for Aeronautics.

SYMBOLS

A	cross-sectional area of flange
A_s	cross-sectional area of leading-edge spar flange
A_x	cross-sectional area of spar flange in spanwise direction
A_y	cross-sectional area of rib flange
E	Young's modulus
F_s	total force in leading-edge flange
F_x	total force in spar flange in spanwise direction
F_y	total force in rib flange
G	shearing modulus of elasticity
i	rib number
j	spar number
M_{ij}	bending moment in ith rib at jth spar
M_{ji}	bending moment in jth spar at ith rib
m	spanwise bay number
n	chordwise bay number
P	load; also a point on plan form

P_{ij}	load at intersection of ith rib and jth spar
Q	total shearing force on segment of length λ, parallel or perpendicular to ribs
S	plan-form area
s	coordinate parallel to free edge
T	total tangential force on free edge of a triangular panel
T_{mn}	twisting moment on spanwise cross section at center of cell mn
T_{nm}	twisting moment on chordwise cross section at center of cell mn
t	thickness of skin; also coordinate perpendicular to free edge
t_1, t_2, t_3, t_4	transformers
U	strain energy in portion of actual structure
U_i	strain energy in portion of idealized structure
$(u_x)_B$	displacement in x-direction at point B
V_{in}	shear in ith rib in nth chordwise bay
V_{jm}	shear in jth spar in mth spanwise bay
w	deflection
w^*	deflection without shearing strains
w_{ij}	deflection at intersection of ith rib and jth spar
x	coordinate in spanwise direction
y	coordinate in chordwise direction
β_i	chordwise rotation of normal in ith rib
β_j	spanwise rotation of normal in jth spar
β_s	rotation of normal in leading-edge spar
β_{in}	rotation of normal in ith rib at center of nth chordwise bay

β_{jm}	rotation of normal in jth spar at center of mth spanwise bay
$(\beta_s)_{ij}$	rotation of normal in leading-edge spar at intersection of ith rib and jth spar
γ	shearing strain
γ_i	shearing strain in idealized structure
ΔM_s	increment in bending moment in leading-edge spar
λ	length of a bay
λ_m	length of mth bay
λ_n	length of nth bay
μ	Poisson's ratio
σ_x	spanwise normal stress
σ_y	chordwise normal stress
τ	shearing stress

DESCRIPTION OF STRUCTURES

The structural plan forms of the delta wings which are herein analyzed have an aspect ratio of 3. The dimensions of the structure could not be chosen by a simple application of beam theory as was done in reference 2. Consequently the dimensions have been chosen to be approximately the same in the root region as those used in reference 2 for the wing of aspect ratio 2. This provides a very thin wing such as would be used for highly supersonic flight. As in reference 2 the wing is assumed to be supported rigidly along two parallel straight lines at the faces of the fuselage. The sweepback angle of the leading edge has been chosen to be 45° for convenience in the analysis although this is not essential.

Two wings have been analyzed, one with a rectangular cross section and one with a biconvex cross section. The wing with a rectangular section is shown in figure 1. Since the plan form does not have a spanwise axis of symmetry the available electrical equipment limits the number of spars to five rather than seven as were used in reference 2.

Consequently each interior spar web in the structure that has been analyzed should be regarded as being equivalent to three spar webs in the wing as it would be built. The spar webs shown in figure 1 are approximately 50 percent thicker than those which were used in reference 2. The positions of the equivalent ribs and spars have been chosen so that they will intersect on the leading edge for convenience in the analysis. As may be seen in figure 1 the pointed portions of the delta wing have been omitted in the fuselage bay and at the tip. This was believed to provide a more practical structural plan form.

The structural layout for the wing with a biconvex section is shown in figure 2. Every streamwise cross section of the wing is a symmetrical, parabolic, biconvex section. From the dimensions shown in figure 2 it can be seen that the maximum thickness at the root is 5 percent of the theoretical aerodynamic chord. This percentage thickness is maintained along the span. Thus the thickness of the wing varies in both spanwise and chordwise directions.

Since the structure is symmetrical about the plane of symmetry of the aircraft, the analysis has been carried out on half of the wing. The points at which various quantities have been determined were numbered as shown in figure 3.

The stiffness constants which enter into the difference equations are determined for these wings in the same manner as was used in reference 2 for straight wings except along the outboard leading edge. In the wing with a biconvex section the stiffness properties vary in both spanwise and chordwise directions. To determine the spanwise bending constant to be used in the difference equations the reciprocal of the spanwise stiffness of an idealized spar was integrated over the length of the bay. A similar procedure was used for the chordwise bending constants. Twisting constants were computed by using the depth of the wing at the center of a panel. A structural theory for the region of the leading edge will be given in the next section.

The wings are assumed to be constructed of an aluminum alloy having the following physical properties:

$$E = 10.4 \times 10^6 \text{ psi}$$

$$G = 4.0 \times 10^6 \text{ psi}$$

$$\mu = 0.3$$

Specific weight = 0.107 lb/cu in.

STRUCTURAL THEORY FOR LEADING EDGE

Except in the neighborhood of the leading edge, the structural theory used in the analysis of the delta wing is the same as that which was used in the analysis of the rectangular wing (ref. 2). This theory is described in detail in reference 1.

The leading-edge spar is a structural member having properties exactly like those of the other ribs and spars. It carries shear and a small amount of bending moment but has no torsional rigidity of itself. Since it is continuously fastened to the skin, shear force can be transmitted to it by the skin.

The leading-edge spar requires special treatment because it is skewed with respect to the other spars and creates a group of triangular skin panels along the leading edge. Most of the bending stiffness of the wing studied in this report is in the skin which is relatively thick. It is desirable that a structural theory which treats the diagonal leading edge should give accurate results for the thick-skin case, and also for the thin-skin case when most of the normal stress-carrying area is concentrated in spar flanges. This attribute is possessed by the theory developed in reference 2 and also, it is believed, by the diagonal-edge theory to be presented here. Other features that the leading-edge theory should have are that it be consistent with the previously developed rectangular-panel theory (the location of points where rotations are defined, concentration of normal stress-carrying area into spar flanges, etc.) and also that it be representable by a simple configuration of electric-circuit elements..

Figure 4(a) shows a portion of the plan form near the leading edge. The solid lines represent ribs and spars, while the dashed lines separate the regions for which concentrated spar and rib flanges are computed. In order to determine relations between internal forces and displacements in the form of difference equations it is necessary to assume that a uniform state of stress exists in the skin over a region containing several adjacent panels. This is one of the sources of error in the difference equations. The skin acts both as shear-carrying material and as normal-stress-carrying material. Because of the uniform state of stress these two actions may be considered independently. When the skin is considered to be shear-carrying material it may be subdivided into panels which are entirely different from the panels into which it is subdivided when considered as normal-stress-carrying material.

Figures 4(b) and 4(c) show, respectively, a skin panel bounded by ribs and spars which is subjected to tangential shear forces on its four sides, and a dashed-line skin panel which is subjected to normal forces on its four sides. In both cases a displacement at the midpoint of each

side in the direction of the applied force is defined in the process of forming difference equations for the idealized structure. The panels in figures 4(b) and 4(c) are in equilibrium under the action of the forces which are shown because of the assumption of a uniform state of stress over the region containing these panels.

The idealized structure for the dashed-line rectangular panel consists of a pair of concentrated flanges intersecting at the center of the panel. The distributed forces on the edges of the panel are concentrated in these flanges. The idealized structure for the solid-line rectangular panel consists of a skin panel which carries shear stresses but not normal stresses. External tangential forces act on the idealized panel at the center of each side.

The above description of the formation of the idealized structure, being based on the assumption of a uniform state of stress, suggests that either the computed force must be interpreted as an average value over the panel or as the first term in a Taylor series expansion about a convenient point. The second interpretation must be adopted in order to satisfy the internal equilibrium equations for the idealized structure. The computed forces must be interpreted as being the values at the centers of the appropriate rectangles. This interpretation determines the proper method of computing the stiffness constants for the structure. From the computed forces in the idealized structure at the centers of the panels one may compute the unit stresses in the actual structure. The state of stress at an internal point, such as point P in figures 4(a), 4(b), and 4(c), may be obtained by simple interpolation.

The requirement that the diagonal-edge theory be consistent with the rectangular-panel theory fixes the location and the types of forces acting across the boundaries of the triangular panels, as shown in figures 4(d) and 4(e). The two groups of forces shown are independently in equilibrium. The shearing stresses and normal stresses which act on planes parallel and perpendicular to the leading edge are to be considered as having independent action. This is possible because of the sweep angle of 45° of the leading edge as well as the assumption of a uniform state of stress. It is assumed throughout this paper that no external bending moments are applied normal to the edge. The tangential force along the edge is applied to the dashed-line triangle and is in equilibrium with normal forces across the other two sides. The tangential forces acting on the solid-line triangle are held in equilibrium by normal forces acting on the same sides. A major difficulty is presented in connection with these panels because adjacent solid-line rectangular panels in the idealized structure are subjected to tangential forces only, so that the normal forces on the triangles must be reacted at the corners or be treated in a fundamentally different manner. A discussion of this difficult problem will be deferred until after the discussion of the dashed-line triangular panels (fig. 5).

The distributed forces acting on the triangular panel, which are redrawn in figure 5(a), are replaced by concentrated forces, as shown in figure 5(b), which shows their magnitudes for the case of a 45° leading edge. (A 45° leading edge will be assumed in all of the following analysis.) The panel itself is replaced by a pair of spar flanges which are extensions of the flanges for the rectangular bays and which intersect at the leading edge (fig. 5(c)).

The cross-sectional area of the idealized flanges can be calculated from a consideration of the strain energy in the dashed-line triangle. If the triangle is in a uniform state of stress then the strain energy stored in the triangle of plan-form area S is:

$$U = \frac{St}{2E}\left(\sigma_x^2 + \sigma_y^2 - 2\mu\sigma_x\sigma_y\right) \tag{1}$$

For a 45° triangle,

$$S = \frac{\lambda^2}{2} \tag{2a}$$

and

$$\sigma_x = -\sigma_y = \frac{T}{\lambda t\sqrt{2}} \tag{2b}$$

With these formulas the strain energy becomes

$$U = \frac{T^2}{4tE}(1 + \mu) \tag{3}$$

The strain energy in the idealized flanges, both of which have a cross-sectional area A, is

$$U_i = \left(\frac{T}{\sqrt{2}}\right)^2\left(\frac{1}{EA}\right)\left(\frac{\lambda}{2}\right) \tag{4}$$

In order that U_i be equal to U, the cross-sectional area of the idealized flange must be

$$A = \frac{\lambda t}{1 + \mu} \tag{5}$$

The distributed forces on the sides of the solid-line triangle are shown in figure 6(a). On planes perpendicular to the free edge, there exists normal force without tangential force as shown in figure 6(b). Hence for the purpose of computing stress-displacement relationships,

the state of stress in the triangle may be regarded as a tension or compression parallel to the free edge. In figure 6(c), the distributed forces are concentrated at the midpoints of the sides. As previously mentioned, there are no idealized flanges to carry normal forces at the points required in figure 6(c) and this method of concentration will not be used. In figure 6(d), the distributed forces have been replaced by concentrated forces acting at the corners in a direction parallel to the edge. In so doing the total normal force acting across a line drawn perpendicular to the leading edge at its midpoint has been preserved. The material in the triangle is replaced by a flange for the leading-edge spar in figure 6(e). If the cross-sectional area of the flange is $\lambda t/2\sqrt{2}$, then the strain energy in the flange will be the same as the strain energy in the triangle, provided that the triangle is in a state of uniform tension or compression parallel to the leading edge. This cross-sectional area is the same as that of a strip of skin of width $\lambda/2\sqrt{2}$.

The complete idealized structure for the skin is shown in figure 7. All normal stresses are concentrated in flanges for the ribs, spars, and leading-edge spar. The rectangular panels carry shearing stresses only while the triangular panels carry no stresses at all. Shearing strain of a triangular panel is resisted by truss action of the flanges surrounding it. Equivalent trusses have been used previously in the solution of problems in elasticity by Hrennikoff (ref. 3).

Since the foregoing derivation is something less than rigorous, it could be made more convincing if it were shown to give correct results in a few cases. Consider the structure that is formed by cutting the structure of figure 7 along a line $\lambda/2\sqrt{2}$ from the leading edge and connecting it to another similar structure, as shown in figure 8(a), thus forming a simple truss. This structure is supposed to be equivalent to a strip of skin of width $\lambda/\sqrt{2}$ for all kinds of loads, except perhaps for normal loads perpendicular to the long edges, which were not considered in the derivation.

If the strip is subjected to a uniform tension in the s-direction, the equivalent structure will give the correct strain in the s-direction because the cross-sectional area of the flanges parallel to the edge is equal to the cross-sectional area of the strip and also because the other flanges carry no load. The strain in the t-direction is incorrect, Poisson's ratio being equal to unity for the idealized structure.

If the strip is subjected to uniform shear forces along its edges, the forces acting on a strip of length $\lambda\sqrt{2}$ are as shown in figure 8(b) and the forces acting on the same length of the idealized structure are as shown in figure 8(a).

The cross-sectional areas of the flanges of the idealized structure are:

$$\left.\begin{aligned} A_x &= t\lambda/(1+\mu) \\ A_y &= t\lambda/(1+\mu) \\ A_s &= t\lambda/2\sqrt{2} \end{aligned}\right\} \tag{6}$$

The forces existing in these flanges are:

$$\left.\begin{aligned} F_x &= T/\sqrt{2} \qquad \text{(tension)} \\ F_y &= -T/\sqrt{2} \qquad \text{(compression)} \\ F_s &= 0 \end{aligned}\right\} \tag{7}$$

For the strip, the shearing strain is (see fig. 8(b)):

$$\gamma = \frac{T}{\sqrt{2}\lambda tG} \tag{8}$$

For the idealized structure the shearing strain is (see fig. 8(c)):

$$\gamma_i = \frac{(u_x)_B\sqrt{2}}{\lambda/\sqrt{2}} = \frac{2(u_x)_B}{\lambda} \tag{9}$$

The increase in length of flange AB is given by

$$(u_x)_B = \frac{F_x\lambda}{EA_x} \tag{10}$$

Substituting equations (6) and (7) into equation (10) gives

$$(u_x)_B = \frac{T(1+\mu)}{\sqrt{2}\,Et} \tag{11}$$

Substituting equation (11) into equation (9) gives

$$\gamma_i = \left(\frac{T}{\sqrt{2}}\lambda t\right)\frac{2(1+\mu)}{E} = \frac{T}{\sqrt{2}\,\lambda t G} \tag{12}$$

Hence the idealized structure gives the correct shearing strain when subjected to uniform shearing forces. It can also be shown that the idealized structure, when connected to parallel vertical webs, gives correct results for the bending and Saint Venant torsion of a 4-flange box. It is also evident that, when the spars and ribs have heavy flanges, the idealized structure will give better results than in the case of very light flanges analyzed here. The technique presented here can be used when the sweep angle is not 45°, although in this more general case the equivalent flange areas for the ribs and spars as given in equation (6) are incorrect.

The manner in which the equivalent flanges of the edge member interact with the vertical shear webs has been treated by the same technique as that given in reference 1.

At points where the ribs and spars intersect the leading edge a transformer is required to effect the connection between the members. The transformer simultaneously satisfies the equations of equilibrium of the joint and the equations of continuity at the joint. If ΔM_s is the jump in the bending moment in the leading-edge member the equations of equilibrium of the joint are as follows:

$$M_{ij} = -M_{ji} = \frac{\Delta M_s}{\sqrt{2}} \tag{13}$$

The condition of continuity at the joint gives the following relation between the rotations of the normals in the members where the subscript ij indicates the intersection of the ith rib and jth spar:

$$(\beta_s)_{ij} = \frac{1}{\sqrt{2}}(\beta_j - \beta_i)_{ij} \tag{14}$$

The slope of the leading-edge spar must be defined at the points where the ribs and spars intersect the leading edge. Since the displacement must also be defined at this same point a slightly different form of the beam analogy must be used along the leading edge (see fig. 9) from that which is explained in reference 4. In this form, the circuit is loaded at the center taps of the transformers. This form has been found

to give very good results in beam problems. A similar but somewhat more accurate circuit is discussed in reference 5.

The complete electrical circuit for the leading edge, as incorporated into the circuit for the delta wing as a whole, is shown in figures 9, 10, and 11.

The idealized structure of figure 7 has been used at points along the leading edge except at the root and tip. At these latter points the dashed-line triangular panels of figure 4 have a corner cut off as shown in figure 5(d) for the tip point. Since the plan-form area of the triangle has been reduced by one-fourth, the cross-sectional areas of the equivalent flanges have been arbitrarily reduced by the same amount.

LOADING CONDITIONS

Since the plan form of each wing has an axis of symmetry lying in the plane of symmetry of the airplane, the loading may be divided into symmetric and antisymmetric parts. Results for an unsymmetric loading can be obtained by superimposing results for the symmetric and antisymmetric loadings. For the two types of loading the boundary conditions along the center line of the airplane are different. These conditions are the same as those for the wing of rectangular plan form and are completely discussed in reference 2.

For the static-loading condition the loads are applied in symmetric or antisymmetric pairs as concentrated forces at the intersection of the ribs and spars. The code numbers for the load points and the points where deflections and internal forces are measured are shown in figure 3.

For symmetric loads, each point of the plan form has been loaded and also a couple, consisting of a positive load at point 91 and a negative load at point 93, has been applied. Deflections and all internal forces have been measured for loads applied outboard of the support. For points loaded inboard of the support only deflections have been measured. For antisymmetric loads, loads at points 91 and 75 and the tip couple have been applied. In these cases deflections and all internal forces have been measured. All of the above measurements were made for both the wing of rectangular cross section and the wing of biconvex cross section.

Additional measurements were made on the wing of rectangular cross section with symmetric loads in order to investigate the effects of certain simplifications in the structural theory. In one group of tests, the shearing stiffnesses of the ribs and spars were made infinite. This was accomplished by setting the resistors corresponding to these shearing stiffnesses to zero. In another group of tests the ribs were given

infinite bending stiffness and infinite shearing stiffness. This was accomplished electrically by removing the resistors corresponding to the shearing stiffness of the ribs and by connecting together the nodes corresponding to the chordwise rotations of the normals in any one cross section. In a third group of tests the ribs were given infinite bending stiffness but finite shearing stiffness of the ribs was retained. In these additional tests deflections and all internal forces were measured for loads at points 91 and 75 and also for the tip couple.

TREATMENT OF DATA FROM COMPUTING MACHINE

The data taken from the analog computer should be regarded as experimental data, subject to the same errors of observation and approximation as any other experimental data. The sources and magnitudes of these errors are fully discussed in reference 2.

The data appearing in the tables have been corrected so that the total bending moment at the line of the support and the total shear in the bay just outboard of the support satisfy statical relations.

The deflections in this report are given in inches for a load of 1 kip. The internal forces correspond to a load of 1 pound. The internal forces given in the tables are total forces rather than force densities. They are the forces that would be measured in the idealized structure. Additional interpolation and calculations are required to obtain the stresses existing at points in the actual structure. These calculations can be performed with the aid of figures 1 and 2 which show the dimensions and cross-sectional properties of the structure.

ELECTRIC CIRCUITS

The complete electric circuit is shown in figures 9, 10, and 11. Figure 9 shows the circuit in which deflections and shears are measured. It also shows the circuit in which bending moments in the leading edge are measured. Points lettered (a), (b), (c), and (d) are connected to points similarly lettered in figure 10. These connections provide the means for transferring moments from the leading-edge member to the idealized flanges of the ribs and spars. Figure 10 shows the circuit in which spanwise rotations of the normal, spanwise bending moments, and chordwise twisting moments are measured. Figure 11 shows the circuits in which chordwise rotations of the normal, chordwise bending moments, and spanwise twisting moments are measured.

These circuits have been constructed in accordance with the theory developed in reference 1 and the structural theory for the leading edge developed in this report. Circuit changes required to alter the symmetry condition along the center line of the airplane are indicated in the figures.

PRESENTATION OF RESULTS

The data taken from the analog computer are presented by means of tables and diagrams. All of the data are given in tables 1 to 6. For each loading condition deflections, shears, spanwise and chordwise bending moments, and spanwise twisting moments will be found in the tables. These tables are recommended to those readers who wish to study the results seriously. Not all of the data taken can, for reasons of space limitations, be presented in diagrams. The data so presented have been chosen to illustrate points of interest, particularly the effects of simplifications in the structural theory.

The internal forces for 12 loading conditions are given in planform diagrams in figures 12 to 23. These diagrams are of three kinds: one kind shows the distribution of shears in the ribs and spars (figs. 12 to 15); the second kind shows the distribution of spanwise bending moments and chordwise twisting moments (figs. 16 to 19); while the third kind shows chordwise bending moments and spanwise twisting moments (figs. 20 to 23). These diagrams should give the reader a good idea of the distribution and interdependence of the internal forces. The arrows show the paths along which the forces are transmitted. In the shear-distribution diagrams, the inflow at each junction should equal the outflow. In the other two types of diagrams, inflow and outflow will not balance because the increments in moments due to rib and spar shear are not shown in the diagrams.

Chordwise distributions of deflections and internal forces as well as vibration modes and other miscellaneous curves are given in figures 28 to 38.

DEFLECTIONS

Chordwise deflection curves for the wing of rectangular section are compared in figure 24 for symmetrical loads applied at points 91 and 93. In general the curves show deflections of nearly equal magnitude in the two cases. For a load at point 93 the tip rib has almost no rotation indicating that the "elastic axis" passes near this point. It will be observed that the ribs show very little curvature for a load at point 91.

This circumstance is regarded as fortuitous and goes far to explain the excellence of the results obtained with rigid ribs for loads at this point. A similar comparison for wings of biconvex section is made in figure 25. Deflections obtained with rigid and elastic ribs for a symmetric load at point 75 are compared in figure 26. The agreement appears to be good. A similar comparison is shown in figure 27 for a symmetric tip couple. The angle of twist at the tip is 30 percent less with rigid ribs than it is with elastic ribs. A considerable curvature of the elastic ribs is evident. The effects of the omission of shearing strains in the ribs and spars are shown in figure 28. The effects are seen to be of the order of 10 percent or less. The omission of shearing strains seems to affect the angle of twist more severely than the bending deflections and to produce severe distortions near the point of application of the load.

SHEARS

The distribution of shears is illustrated in plan-form diagrams, figures 12 to 15. Two general observations concerning these diagrams are that the paths chosen by the shears through the ribs and spars are sometimes quite unexpected and that the shear shows a decided preference for flowing along the leading-edge spar. The leading-edge spar appears to be a more important means than the ribs for distributing shears among the various spars. The theory of least work is an aid to the understanding of the odd patterns of shear distribution. Very little strain energy is stored in the shearing of the ribs and spars, while most of the strain energy is stored in the bending of the spars. Consequently the shear will be distributed in such a way as to cause an even distribution of bending moment among the spars, and, as a result, the chordwise shear paths lying farthest from the root will be preferred, even to the point where shear in the inboard ribs flows in the reverse directions.

Figure 13 shows that the omission of shearing strains, or the assumption of rigid ribs, produces moderate changes in the distribution of shear for a load at point 91. For a tip couple, the assumption of rigid ribs produces a radical change in the distribution of shear as shown in figure 14.

SPANWISE BENDING MOMENTS

Spanwise bending moments are shown in plan-form diagrams in figures 16 to 19. These diagrams show how the shearing of the skin panels serves to distribute the spanwise bending moments. In figure 16, it will be observed that the chordwise location of the load has a moderate effect

on the distribution of bending moment at the line of support. This same fact is illustrated in figure 29(a). Figure 29(a) also shows that, for a wing of rectangular section loaded at the tip, the maximum stress along the support occurs at the trailing edge and that the stress at the leading edge is small. For a wing of biconvex section the point of maximum stress is shifted forward by approximately 30 percent as shown in figure 29(b).

Figure 17 shows that the omission of shearing strains and the assumption of rigid ribs give excellent spanwise bending moments for a load at point 91. Figure 30(a) shows that, for a load at point 75, the assumption of rigid ribs gives errors in the bending-moment distribution at the support of about 10 percent. For a tip couple (fig. 30(b)) the assumption of rigid ribs causes considerably larger percentage errors in the differential bending stresses in the spars; however, these stresses are small.

A few additional comments concerning the effects of shearing strains and rigid ribs appear to be worth while. From the differential equations of plate theory it can easily be shown that, when shearing strains due to vertical shearing stresses on a cross section are neglected, an assumption of linear transverse variation of vertical deflections (rigid ribs) implies a linear transverse distribution of axial displacements and axial normal stresses at every section. An inspection of figure 30 shows that the distribution of normal stress was not found to have a linear variation under the assumption of rigid ribs but, instead, shows much better agreement with the correct solution than could have been obtained from a linear distribution. This nonlinearity of the normal stress distribution is due to the inclusion of the effects of shearing strains in the spars.

A study of several loading conditions indicates that, except for pure torsional loading, the shearing strains in the ribs and spars have only a minor effect on the distribution of spanwise normal stresses when the ribs are elastic. However, from the previous discussion, it is seen that serious error in the distribution of spanwise normal stress may result if both an assumption of rigid ribs and an assumption of zero shearing strains in the spars are made. In other words if either one assumption or the other is made serious error will not result but if both are made serious error may result. Hence if one wishes to develop an approximate engineering method of analysis based on the assumption of rigid ribs the effect of shearing strains in the spars must be taken into account to obtain satisfactory accuracy. In this connection it should be noted that, when vertical shearing strains are taken into account, the assumption of rigid ribs does not determine a distribution of axial displacements or axial stresses. In this case one may make an independent assumption regarding axial displacements or these displacements may be computed accurately. This freedom to make independent

assumptions regarding chordwise distributions of deflections and axial displacements becomes advantageous in the development of practical engineering methods of approximate analysis.

TWISTING MOMENTS

Spanwise and chordwise twisting moments are numerically equal because the twisting-moment panels are square. For a symmetric torque load applied at the tip it can be seen in figure 18(a) that the sum of the twisting moments in the rectangular bays just outboard of the support is 37 percent of the applied torque rather than 50 percent which would be expected for a cantilever beam and also that the twisting moment is much larger near the trailing edge than it is near the leading edge. In figure 35 the twisting moments in these bays are compared with those for the basic wing of rectangular section for the cases when shearing strains in the ribs and spars are omitted and when the ribs are assumed to be rigid.

The omission of shearing strain does not have much effect on the distribution of twisting moment but the assumption of rigid ribs has a very large effect. If shearing strain did not exist in the spars, the assumption of rigid ribs would give equal twisting moments in all of the bays. For a load at point 91, it is seen in figure 17 that large twisting moments are produced by the eccentricity of the load and also that the assumption of rigid ribs gives good results in this case.

CHORDWISE BENDING MOMENTS

The bending moments in the ribs are illustrated in plan-form diagrams in figures 20 to 23. In all cases, the bending moments in the ribs are small. The chordwise bending moments are compared for the cases of rigid and elastic ribs in figure 32. In the rigid-rib case, the bending moments were not measured on the computer but were calculated from equilibrium equations. The chordwise bending moments for the case of rigid ribs shown in figure 32 are in equilibrium with twisting moments and rib shears. They are not equal to Poisson's ratio times the spanwise bending moments. It is seen that for a load at point 91, as for all other quantities, the assumption of rigid ribs gives good results. For a load at point 75 the assumption of rigid ribs gives excessively poor results, exaggerating the maximum bending moment by more than a factor of two.

VIBRATION MODES

Vibration modes were measured in the same way for the delta wing as they were for the wing of rectangular plan form so that the remarks in reference 2 concerning vibration modes apply to the delta wing. Symmetric and antisymmetric vibration modes were measured for both the wing of rectangular cross section and the wing of biconvex cross section. Frequencies and deflections are recorded in tables 5 and 6. Symmetric modes for the wing with rectangular cross section are illustrated in figure 33 by means of contour drawings. The first and fourth modes may be described as the first and second bending modes. The second and third modes, which are only 20 percent apart in frequency, seem to combine torsion of the outboard wing with large bending amplitudes of the fuselage carry-through bay. In the antisymmetric case these two modes merge into a single more normal torsion mode. The difficulties that would be involved in replacing the delta wing by an equivalent beam for dynamic analyses are made evident by the contour lines.

CONCLUSIONS

The foregoing discussion of the results is based on the data presented in the figures which include only a small portion of all the data taken. The reader will find that the data in the tables will permit him to make a more thorough study of any particular case in which he may be interested. The problems analyzed in this paper utilized the Cal-Tech analog computer for 2 weeks and the amount of data taken was limited by the speed at which the operator could record the results.

1. For loads in the tip region of the delta wing of rectangular cross section, the highest values of normal and shearing stresses occur near the intersection of the trailing edge and the line of support. For the wing of biconvex cross section the maximum spanwise normal stress occurs about 30 percent farther forward.

2. For the wings analyzed in this paper which have homogeneous skin coverings without heavy concentrated flanges, it has been found that the shearing stresses in the skin and chordwise normal stresses are small compared with the maximum spanwise normal stresses, even for the loads of greatest eccentricity. It has also been found that the leading-edge spar carries considerable shear for loads near the tip and that it is an important agent in the distribution of spanwise bending moments.

3. The effects of neglecting shearing strains in the ribs and spars and also of assuming the ribs to be rigid have been investigated by modifying the electric curcuits to correspond to these simplifications. It

has been found that the omission of shearing strains produces errors in the deflections and in the distribution of spanwise normal stresses of the order of 8 percent or less. The assumption of rigid ribs gives good results for the average deflection of any chordwise cross section and for the distribution of spanwise normal stresses; it gives poor and qualitatively incorrect results for the distribution of shearing stresses in the skin and chordwise normal stresses. It also gives poor results for torsional deflections due to a couple applied to the tip. An evaluation of the effect of either assumption on the distribution of shears in the ribs and spars is difficult to make since the magnitude of the discrepancy appears to depend strongly on the locations of the load and of the point where the shear is measured.

It should be emphasized that the conclusions concerning the effects of these assumptions cannot be applied to an analysis in which both the assumption of rigid ribs and the assumption of no shearing strains in the spars are made simultaneously. The results given in this paper indicate that, for wings of low aspect ratio, the elastic camber of the ribs has a significant influence upon the deflections and internal stress distributions.

California Institute of Technology,
Pasadena, Calif., January 9, 1953.

REFERENCES

1. Benscoter, Stanley U., and MacNeal, Richard H.: Equivalent Plate Theory for a Straight Multicell Wing. NACA TN 2786, 1952.

2. Benscoter, Stanley U., and MacNeal, Richard H.: Analysis of Straight Multicell Wings on Cal-Tech Analog Computer. NACA TN 3113, 1953.

3. Hrennikoff, A.: Solution of Problems of Elasticity by the Framework Method. Jour. Appl. Mech., vol. 8, no. 4, Dec. 1941, pp. A-169 - A-175.

4. Benscoter, Stanley U., and MacNeal, Richard H.: Introduction to Electrical-Circuit Analogies for Beam Analysis. NACA TN 2785, 1952.

5. Russell, W. T., and MacNeal, R. H.: An Improved Electrical Analogy for the Analysis of Beams in Bending. Jour. Appl. Mech., vol. 20, no. 3, Sept. 1953, pp. 349-354.

TABLE 1

WING OF RECTANGULAR SECTION WITH SYMMETRIC LOADS

(a) Deflections

Deflection point	Deflection, in./kip, at loading point -														
	11	13	15	17	19	51	53	55	57	71	73	75	91	93	Tip couple
11	0.0248	0.0106	0.0052	0.0032	0.0026	-0.0095	-0.0078	-0.0062	-0.0048	-0.0170	-0.0152	-0.0128	-0.0249	-0.0226	-0.0020
13		.0130	.0065	.0039	.0032	-.0073	-.0067	-.0058	-.0047	-.0140	-.0130	-.0116	-.0207	-.0196	-.0010
15			.0115	.0065	.0052	-.0055	-.0056	-.0058	-.0055	-.0111	-.0113	-.0114	-.0172	-.0173	.0003
17				.0130	.0106	-.0042	-.0048	-.0056	-.0067	-.0089	-.0099	-.0110	-.0141	-.0150	.0011
19					.0253	-.0038	-.0046	-.0059	-.0079	-.0083	-.0096	-.0112	-.0132	-.0148	.0015
51						.0291	.0168	.0108	.0072	.0418	.0314	.0227	.0550	.0444	.0103
53							.0182	.0125	.0094	.0316	.0299	.0252	.0447	.0426	.0023
55								.0164	.0122	.0228	.0248	.0268	.0352	.0374	-.0022
57									.0171	.0164	.0196	.0238	.0257	.0292	-.0037
71										.0938	.0696	.0522	.1308	.1058	.0233
73											.0688	.0571	.1059	.1018	.0038
75												.0632	.0832	.0895	-.0061
91													.2204	.1788	.0401
93														.1777	.0017

TABLE 1.- Continued

WING OF RECTANGULAR SECTION WITH SYMMETRIC LOADS

(b) Spanwise shears

Shear point	Spanwise shear, lb/lb, at loading point -									
	51	53	55	57	71	73	75	91	93	Tip couple
21	-0.011	0.023	0.030	0.028	0.010	0.040	0.055	0.034	0.062	-0.027
23	-.036	-.049	-.009	.008	-.077	-.071	-.034	-.115	-.099	-.016
25	-.001	-.014	-.043	-.008	-.024	-.042	-.060	-.052	-.074	.021
27	.016	.006	-.013	-.046	.022	.001	-.034	.025	-.001	.025
29	.031	.033	.034	.017	.068	.071	.072	.106	.111	-.003
41	.627	.176	.038	-.015	.489	.204	.035	.421	.177	.237
43	.276	.545	.196	.095	.334	.393	.256	.321	.332	-.010
45	.079	.179	.521	.202	.121	.219	.340	.150	.246	-.093
47	.027	.071	.151	.401	.069	.142	.250	.118	.198	-.078
61	-.101	.042	.014	-.007	.591	.191	.044	.483	.206	.267
63	.051	-.142	.040	.049	.254	.476	.212	.244	.307	-.060
65	.024	.021	-.162	.101	.082	.149	.355	.142	.228	-.082
81	-.019	.004	0	-.002	-.095	.031	.010	.615	.177	.419
83	-.007	-.043	.018	.017	-.007	-.184	.110	.151	.372	-.214
[a]48	-.008	.028	.095	.318	-.013	.043	.119	-.011	.048	-.058
[a]66	.018	.069	.099	-.150	.068	.184	.392	.129	.258	-.128
[a]84	.018	.033	-.025	-.020	.083	.138	-.130	.238	.457	-.212

[a]Leading-edge spar.

TABLE 1.- Continued

WING OF RECTANGULAR SECTION WITH SYMMETRIC LOADS

(c) Chordwise shears

Shear point	Chordwise shear, lb/lb, at loading point -									
	51	53	55	57	71	73	75	91	93	Tip couple
12	0.011	-0.023	-0.030	-0.028	-0.010	-0.041	-0.055	-0.035	-0.062	0.027
14	.047	.025	-.021	-.036	.067	.030	-.021	.080	.036	.043
16	.048	.039	.022	-.028	.091	.072	.041	.133	.110	.022
18	.032	.033	.035	.017	.069	.071	.073	.107	.111	-.003
52	-.282	.134	.024	-.008	-.104	.013	-.011	-.063	-.032	-.032
54	-.056	-.190	.179	.037	-.028	-.069	.035	.013	-.007	.020
56	-.001	-.031	-.149	.140	.011	0	.023	.020	.011	.009
72	-.084	.038	.013	-.005	-.335	.159	.034	-.132	.028	-.155
74	-.025	-.058	.035	.026	-.070	-.198	.138	-.037	-.037	0
92	-.016	.005	.002	0	-.089	.035	.012	-.414	.185	-.576

TABLE 1.- Continued

WING OF RECTANGULAR SECTION WITH SYMMETRIC LOADS

(d) Spanwise bending moments

Moment point	Spanwise bending moment, in-lb/lb, at loading point -									
	51	53	55	57	71	73	75	91	93	Tip couple
11	-3.93	-3.09	-2.38	-1.83	-7.00	-6.05	-5.03	-9.97	-8.94	-0.99
13	-6.39	-6.04	-4.99	-4.07	-12.35	-11.56	-10.32	-18.19	-17.18	-.88
15	-4.76	-5.01	-5.42	-4.92	-9.88	-10.18	-10.46	-14.99	-15.40	.41
17	-3.55	-4.11	-4.99	-6.05	-7.61	-8.61	-9.84	-11.95	-12.97	1.09
19	-1.41	-1.74	-2.26	-3.18	-3.09	-3.60	-4.34	-4.90	-5.48	.59
31	-5.39	-3.23	-2.03	-1.34	-8.64	-6.41	-4.66	-11.68	-9.48	-2.22
33	-6.77	-6.98	-4.88	-3.52	-13.50	-12.71	-10.55	-19.91	-18.66	-1.16
35	-4.40	-5.07	-6.36	-4.80	-9.88	-10.73	-11.64	-15.58	-16.59	1.06
37	-2.80	-3.67	-4.99	-6.86	-6.49	-7.99	-10.08	-10.37	-12.10	1.74
39	-.64	-1.04	-1.73	-3.48	-1.49	-2.16	-3.07	-2.47	-3.17	.73
51	3.09	.20	-.63	-.65	-3.50	-2.98	-2.76	-7.95	-6.87	-1.10
53	.16	2.46	-.69	-1.20	-6.76	-6.55	-5.97	-14.50	-14.14	-.27
55	-1.84	-1.20	2.31	-.24	-6.78	-6.99	-7.09	-12.60	-13.43	.83
57	-.23	-.66	-.85	-.62	-1.11	-2.05	-3.40	-2.24	-3.34	1.12
71	.44	.23	-.14	-.15	3.13	0	-.90	-4.99	-4.00	-.93
73	.24	.13	-.13	.03	-.70	1.72	-.98	-9.71	-10.30	.65
75	.18	-.46	-.91	.93	-.53	-1.72	-1.56	-2.92	-5.28	2.33
93	.21	-.41	.11	.20	.47	-1.33	.52	.80	-3.25	3.97
[a]48	-1.03	-1.09	-1.10	-.41	-2.30	-2.45	-2.68	-3.65	-3.86	.20
[a]66	-1.23	-.66	.45	1.08	-3.14	-2.14	-.30	-5.22	-4.31	-.89
[a]84	-.51	.14	.22	0	-1.75	0	1.19	-4.19	-1.67	-2.50

[a]Leading-edge spar.

TABLE 1.- Continued

WING OF RECTANGULAR SECTION WITH SYMMETRIC LOADS

(e) Chordwise bending moments

Moment point	Chordwise bending moment, in-lb/lb, at loading point -									
	51	53	55	57	71	73	75	91	93	Tip couple
13	-1.02	-1.07	-0.88	-0.65	-2.06	-2.01	-1.81	-3.11	-3.00	-0.09
15	-.95	-1.12	-1.28	-1.05	-2.10	-2.30	-2.45	-3.32	-3.50	.19
17	-.52	-.67	-.89	-1.02	-1.19	-1.43	-1.73	-1.95	-2.23	.27
53	-2.02	2.05	.05	-.52	-2.66	.17	-.43	-3.23	-1.02	-2.21
55	-1.74	-.25	2.76	-.27	-2.99	-1.00	1.28	-3.95	-1.63	-2.30
57	.23	.67	.86	.63	1.11	2.05	3.44	2.25	3.37	-1.12
73	-1.21	1.32	.17	-.56	-2.60	3.48	.47	-3.14	2.42	-5.51
75	-.17	.46	.93	-.91	.53	1.73	1.60	2.93	5.35	-2.34
93	-.20	.43	-.09	-.19	-.47	1.37	-.47	-.75	3.31	-4.05

TABLE 1.- Concluded

WING OF RECTANGULAR SECTION WITH SYMMETRIC LOADS

(f) Spanwise twisting moments

Moment point	Spanwise twisting moment, in-lb/lb, at loading point -									
	51	53	55	57	71	73	75	91	93	Tip couple
22	-1.25	-0.59	-0.27	-0.07	-1.85	-1.19	-0.70	-2.43	-1.75	-0.63
24	-.90	-.57	.04	.32	-1.40	-.89	-.20	-1.83	-1.22	-.60
26	-.54	-.35	-.07	.59	-.93	-.61	-.12	-1.29	-.92	-.37
28	-.13	-.01	.18	.67	-.20	-.02	.24	-.25	-.04	-.20
42	-4.28	-.18	.65	.99	-4.78	-.78	1.17	-4.81	-.97	-3.77
44	-2.96	-1.82	.87	1.38	-4.68	-2.46	.63	-5.83	-3.08	-2.66
46	-2.00	-1.55	-1.10	1.87	-3.92	-3.05	-1.66	-5.84	-4.81	-.97
62	-.58	-.83	.21	.63	-5.41	-.90	.94	-6.89	-1.41	-5.37
64	-1.54	-.33	-.05	.87	-4.54	-2.28	1.60	-6.90	-3.63	-3.22
82	-.10	-.33	.12	.17	-1.30	-.68	.70	-7.47	.39	-7.70

TABLE 2

WING OF BICONVEX SECTION WITH SYMMETRIC LOADS

(a) Deflections

Deflection point	Deflection, in./kip, at loading point -														
	11	13	15	17	19	51	53	55	57	71	73	75	91	93	Tip couple
11	0.0450	0.0160	0.0076	0.0046	0.0036	-0.0134	-0.0105	-0.0082	-0.0065	-0.0235	-0.0204	-0.0175	-0.0333	-0.0305	-0.0029
13		.0169	.0085	.0054	.0045	-.0093	-.0085	-.0072	-.0061	-.0178	-.0165	-.0151	-.0262	-.0248	-.0011
15			.0131	.0085	.0076	-.0068	-.0069	-.0070	-.0069	-.0140	-.0140	-.0142	-.0212	-.0211	.0003
17				.0171	.0162	-.0054	-.0061	-.0069	-.0085	-.0116	-.0125	-.0139	-.0176	-.0188	.0011
19					.0456	-.0053	-.0063	-.0078	-.0114	-.0116	-.0131	-.0152	-.0176	-.0194	.0017
51						.0511	.0240	.0139	.0088	.0654	.0436	.0288	.0795	.0596	.0198
53							.0251	.0162	.0116	.0440	.0407	.0327	.0614	.0574	.0042
55								.0214	.0158	.0287	.0316	.0346	.0443	.0478	-.0034
57									.0259	.0194	.0240	.0312	.0301	.0354	-.0051
71										.1585	.1031	.0700	.2098	.1574	.0524
73											.1000	.0784	.1571	.1498	.0072
75												.0912	.1142	.1268	-.0122
91													.3983	.2863	.1078
93														.2901	-.0009

TABLE 2.- Continued

WING OF BICONVEX SECTION WITH SYMMETRIC LOADS

(b) Spanwise shears

Shear point	Spanwise shear, lb/lb, at loading point -									
	51	53	55	57	71	73	75	91	93	Tip couple
21	-0.022	0.015	0.024	0.0225	-0.001	0.031	0.045	0.022	0.050	-0.029
23	-.036	-.046	-.002	.0175	-.085	-.072	-.025	-.126	-.103	-.021
25	-.001	-.020	-.054	-.0085	-.032	-.056	-.082	-.069	-.099	.030
27	.035	.025	.010	-.0275	.064	.043	.007	.089	.068	.021
29	.024	.024	.022	-.005	.052	.052	.053	.080	.082	-.001
41	.507	.113	.013	-.020	.340	.110	-.013	.252	.057	.188
43	.390	.586	.194	.075	.468	.450	.252	.460	.395	.061
45	.107	.234	.600	.267	.180	.318	.481	.254	.399	-.142
47	.010	.061	.144	.446	.040	.125	.257	.075	.164	-.087
61	-.100	.020	.002	-.0095	.514	.129	.013	.378	.114	.253
63	.076	-.090	.027	.0285	.377	.571	.233	.403	.436	-.032
65	.018	.029	-.090	.1055	.090	.192	.449	.185	.329	-.139
81	-.012	-.001	-.002	-.002	-.075	.013	-.007	.613	.138	.458
83	.002	-.022	.011	-.002	.023	-.115	.090	.239	.478	-.232
[a]48	-.013	.007	.048	.232	-.028	-.003	.024	-.041	-.015	-.024
[a]66	-.004	.034	.055	-.130	.017	.111	.308	.030	.121	-.088
[a]84	.001	.016	-.015	0	.033	.084	-.098	.154	.389	-.230

[a]Leading-edge spar.

TABLE 2.- Continued

WING OF BICONVEX SECTION WITH SYMMETRIC LOADS

(c) Chordwise shears

Shear point	Chordwise shear, lb/lb, at loading point -									
	51	53	55	57	71	73	75	91	93	Tip couple
12	0.022	-0.015	-0.024	-0.023	0.001	-0.031	-0.046	-0.023	-0.051	0.029
14	.058	.031	-.022	-.040	.085	.041	-.021	.103	.051	.049
16	.060	.050	.032	-.032	.117	.097	.061	.173	.152	.020
18	.024	.025	.023	-.004	.053	.054	.055	.082	.083	-.001
52	-.403	.092	.010	-.011	-.178	-.021	-.024	-.126	-.057	-.066
54	-.089	-.239	.177	.036	-.087	-.142	-.005	-.072	-.100	.028
56	0	-.034	-.138	.197	.003	-.012	.026	-.006	-.031	.024
72	-.089	.020	.004	-.008	-.436	.118	.017	-.238	-.027	-.201
74	-.015	-.049	.020	.022	-.077	-.223	.163	-.068	-.066	-.002
92	-.008	.001	-.001	-.001	-.067	.016	-.003	-.421	.147	-.544

TABLE 2.- Continued

WING OF BICONVEX SECTION WITH SYMMETRIC LOADS

(d) Spanwise bending moments

Moment point	Spanwise bending moment, in-lb/lb, at loading point -									
	51	53	55	57	71	73	75	91	93	Tip couple
11	-1.69	-1.24	-0.94	-0.73	-2.92	-2.42	-1.99	-3.99	-3.56	-0.45
13	-6.94	-6.50	-5.36	-4.41	-13.49	-12.50	-11.19	-19.52	-18.70	-.92
15	-6.97	-7.27	-7.70	-7.05	-14.42	-14.62	-15.09	-21.88	-22.64	.57
17	-3.81	-4.35	-5.08	-6.37	-8.05	-8.86	-10.08	-12.35	-13.36	.98
19	-.58	-.71	-.90	-1.41	-1.26	-1.44	-1.69	-1.91	-2.13	.21
31	-3.32	-1.51	-.77	-.43	-4.55	-2.90	-1.76	-5.74	-4.08	-1.52
33	-7.99	-7.77	-5.21	-3.58	-15.82	-14.51	-11.55	-23.23	-21.39	-1.68
35	-6.23	-7.11	-8.72	-6.57	-13.90	-15.03	-16.22	-21.88	-23.37	1.55
37	-2.36	-3.27	-4.55	-7.08	-5.45	-6.96	-9.44	-8.69	-10.36	1.69
39	-.10	-.34	-.74	-2.34	-.27	-.59	-1.03	-.46	-.79	.34
51	2.42	.25	-.16	-.18	-2.42	-1.60	-1.23	-5.09	-3.80	-1.23
53	-.10	1.91	-.56	-.89	-9.03	-8.44	-6.63	-18.67	-17.92	-.92
55	-1.65	-1.31	1.41	-.47	-7.21	-7.86	-8.79	-13.79	-15.44	1.61
57	.08	-.34	-.65	-.62	-.30	-1.15	-2.66	-.77	-1.69	.94
71	.15	.12	-.03	-.01	2.32	.15	-.33	-4.63	-2.92	-1.66
73	.13	.14	-.09	.13	-.95	1.15	-.82	-11.94	-12.29	.36
75	.27	-.27	-.44	.86	-.03	-1.24	-1.51	-1.78	-4.32	2.47
93	.16	-.15	.08	.07	.39	-.70	.55	.59	-2.75	3.25
[a]48	-.35	-.39	-.39	0	-.79	-.91	-1.15	-1.26	-1.39	.14
[a]66	-.49	-.29	.13	.55	-1.41	-1.05	-.20	-2.52	-2.36	-.14
[a]84	-.20	.01	.09	-.09	-.85	-.10	.64	-2.58	-1.36	-1.25

[a]Leading-edge spar.

TABLE 2.- Continued

WING OF BICONVEX SECTION WITH SYMMETRIC LOADS

(e) Chordwise bending moments

Moment point	Chordwise bending moment, in-lb/lb, at loading point -									
	51	53	55	57	71	73	75	91	93	Tip couple
13	-0.70	-0.87	-0.79	-0.60	-1.64	-1.71	-1.63	-2.53	-2.61	0.06
15	-.99	-1.22	-1.34	-1.09	-2.30	-2.49	-2.66	-3.57	-3.80	.25
17	-.51	-.63	-.75	-.73	-1.17	-1.33	-1.53	-1.83	-2.00	.18
53	-3.71	1.89	-.07	-.50	-4.53	-.34	-.61	-5.11	-1.64	-3.37
55	-2.35	-.66	2.43	-.77	-4.15	-1.92	.51	-5.58	-3.03	-2.46
57	-.08	.34	.65	.64	.30	1.16	2.67	.77	1.71	-.94
73	-1.54	.83	.04	-.49	-3.87	2.89	.10	-5.22	1.00	-6.17
75	-.27	.27	.45	-.83	0	1.25	1.56	1.78	4.37	-2.50
93	-.17	.16	-.06	-.05	-.40	.74	-.48	-.56	2.88	-3.33

TABLE 2.- Concluded

WING OF BICONVEX SECTION WITH SYMMETRIC LOADS

(f) Spanwise twisting moments

Moment point	Spanwise twisting moment, in-lb/lb, at loading point -									
	51	53	55	57	71	73	75	91	93	Tip couple
22	-1.13	-0.57	-0.31	-0.14	-1.63	-1.07	-0.69	-2.05	-1.54	-0.51
24	-1.46	-.96	-.12	.33	-2.40	-1.62	-.60	-3.13	-2.30	-.84
26	-.72	-.45	-.06	.99	-1.26	-.80	-.12	-1.72	-1.27	-.45
28	.01	.12	.29	.81	.08	.23	.42	.17	.31	-.14
42	-4.69	-.53	.37	.64	-4.84	-.93	.78	-4.52	-.90	-3.53
44	-4.71	-2.80	1.10	1.81	-7.45	-4.05	.62	-9.32	-5.23	-4.03
46	-2.26	-1.69	-.99	2.54	-4.41	-3.35	-1.63	-6.46	-5.41	-1.03
62	-.24	-.55	.08	.36	-5.85	-.88	.66	-7.19	-1.42	-5.70
64	-1.55	-.45	0	.79	-5.43	-2.90	1.77	-8.38	-4.66	-3.67
82	.03	-.13	.05	.03	-.89	-.41	.42	-7.70	.08	-7.64

TABLE 3

WING WITH ANTISYMMETRIC LOADS

(a) Deflections

Deflection point	Rectangular section			Biconvex section		
	Deflection, in./kip, at loading point -			Deflection, in./kip, at loading point -		
	91	75	Tip couple	91	75	Tip couple
11	-0.0032	-0.0014	-0.0004	-0.0047	-0.0020	-0.0008
13	-.0025	-.0013	-.0002	-.0032	-.0017	-.0002
15	-.0019	-.0013	.0001	-.0022	-.0016	.0001
17	-.0013	-.0012	.0002	-.0015	-.0014	.0002
19	-.0010	-.0011	.0002	-.0012	-.0015	.0003
51	.0411	.0144	.0099	.0636	.0190	.0195
53	.0319	.0170	.0020	.0465	.0230	.0039
55	.0230	.0187	-.0022	.0303	.0251	-.0034
57	.0143	.0160	-.0034	.0167	.0218	-.0050
71	.1031	.0358	.0226	.1798	.0497	.0524
73	.0804	.0406	.0034	.1256	.0582	.0068
75	.0591	.0463	-.0062	.0843	.0703	-.0125
91	.1821	.0585	.0397	.3508	.0825	.1098
93	.1394	.0650	.0011	.2401	.0965	-.0015

TABLE 3.- Continued

WING WITH ANTISYMMETRIC LOADS

(b) Spanwise shears

Shear point	Rectangular section			Biconvex section		
	Spanwise shear, lb/lb, at loading point -			Spanwise shear, lb/lb, at loading point -		
	91	75	Tip couple	91	75	Tip couple
1	-0.406	-0.172	-0.063	-0.225	-0.091	-0.039
3	-.654	-.341	-.044	-.717	-.373	-.047
5	-.498	-.358	.027	-.675	-.483	.033
7	-.318	-.314	.056	-.317	-.316	.051
9	-.110	-.130	.031	-.053	-.067	.015
21	-.404	-.153	-.075	-.225	-.075	-.054
23	-.690	-.354	-.048	-.769	-.383	-.055
25	-.507	-.381	.036	-.690	-.512	.047
27	-.315	-.330	.065	-.284	-.312	.059
29	-.069	-.101	.028	-.020	-.044	.014
41	.431	.038	.239	.267	-.004	.190
43	.342	.259	-.003	.471	.252	.065
45	.150	.339	-.094	.241	.471	-.144
47	.103	.245	-.081	.057	.247	-.088
61	.486	.046	.268	.378	.015	.251
63	.254	.211	-.058	.409	.233	-.031
65	.146	.351	-.080	.185	.445	-.139
81	.609	.011	.416	.611	-.005	.454
83	.155	.110	-.213	.242	.091	-.232
[a]48	-.026	.118	-.063	-.036	.034	-.028
[a]66	.111	.388	-.133	.025	.306	-.089
[a]84	.233	-.128	-.212	.152	-.096	-.228

[a]Leading-edge spar.

TABLE 3.- Continued

WING WITH ANTISYMMETRIC LOADS

(c) Chordwise shears

Shear point	Rectangular section			Biconvex section		
	Chordwise shear, lb/lb, at loading point -			Chordwise shear, lb/lb, at loading point -		
	91	75	Tip couple	91	75	Tip couple
12	-0.008	-0.020	0.013	-0.001	-0.018	0.015
14	.034	-.007	.017	.051	-.006	.022
16	.047	.014	.007	.070	.024	.008
18	.041	.030	-.002	.032	.022	0
52	-.057	-.009	-.029	-.115	-.019	-.064
54	.029	.035	.024	-.052	.001	.032
56	.032	.023	.013	.001	.025	.027
72	-.127	.034	-.154	-.234	.018	-.203
74	-.028	.138	.002	-.061	.162	-.001
92	-.406	.012	-.578	-.417	-.003	-.544

TABLE 3.- Continued

WING WITH ANTISYMMETRIC LOADS

(d) Spanwise bending moments

Moment point	Rectangular section			Biconvex section		
	Spanwise bending moments, in-lb/lb, at loading point -			Spanwise bending moments, in-lb/lb, at loading point -		
	91	75	Tip couple	91	75	Tip couple
11	-3.85	-1.61	-0.62	-1.71	-0.67	-0.34
13	-6.83	-3.54	-.48	-7.64	-3.85	-.58
15	-5.13	-3.68	.28	-7.22	-5.13	.38
17	-3.30	-3.25	.59	-3.10	-3.22	.55
19	-.99	-1.18	.28	-.35	-.48	.11
31	-12.54	-4.83	-2.46	-6.47	-2.07	-1.68
33	-20.62	-10.57	-1.42	-24.17	-11.65	-1.90
35	-15.26	-11.58	1.15	-20.87	-15.86	1.64
37	-9.48	-9.95	2.03	-7.98	-9.21	1.89
39	-2.09	-3.07	.86	-.52	-1.20	.41
51	-8.26	-2.81	-1.20	-5.22	-1.30	-1.28
53	-14.78	-6.02	-.37	-18.93	-6.68	-.98
55	-12.36	-7.07	.91	-13.62	-8.68	1.68
57	-2.03	-3.37	1.20	-.72	-2.70	.98
71	-5.07	-.92	-.96	-4.65	-.34	-1.69
73	-9.68	-1.01	.63	-11.91	-.87	.36
75	-2.86	-1.56	2.36	-1.77	-1.51	2.52
93	.78	.51	3.98	.55	.53	3.30
[a]48	-3.32	-2.66	.32	-1.23	-1.20	.17
[a]66	-4.99	-.29	-.83	-2.45	-.19	-.13
[a]84	-4.14	1.18	-2.49	-2.57	.63	-1.25

[a]Leading-edge spar.

TABLE 3.- Continued

WING WITH ANTISYMMETRIC LOADS

(e) Chordwise bending moments

Moment point	Rectangular section			Biconvex section		
	Chordwise bending moment, in-lb/lb, at loading point -			Chordwise bending moment, in-lb/lb, at loading point -		
	91	75	Tip couple	91	75	Tip couple
13	-1.36	-0.75	-0.06	-1.28	-0.73	-0.04
15	-1.32	-.93	.05	-1.57	-1.11	.06
17	-.79	-.71	.11	-.76	-.66	.09
53	-3.29	-.43	-2.23	-5.04	-.58	-3.44
55	-3.92	1.30	-2.30	-5.41	.56	-2.48
57	2.02	3.40	-1.20	.72	2.72	-.98
73	-3.19	.47	-5.51	-5.18	.13	-6.17
75	2.86	1.58	-2.37	1.74	1.55	-2.54
93	-.76	-.47	-4.03	-.54	-.48	-3.41

TABLE 3.- Concluded

WING WITH ANTISYMMETRIC LOADS

(f) Spanwise twisting moments

Moment point	Rectangular section			Biconvex section		
	Spanwise twisting moment, in-lb/lb, at loading point -			Spanwise twisting moment, in-lb/lb, at loading point -		
	91	75	Tip couple	91	75	Tip couple
2	0.58	0.28	0.04	1.03	0.49	0.12
4	.12	.08	0	.33	.30	-.04
6	-.04	-.04	.01	-.50	-.30	.02
8	-.25	-.24	.06	-.33	-.38	.08
22	-.64	-.06	-.29	-.19	.10	-.23
24	-.54	.04	-.22	-1.03	.04	-.41
26	-.50	-.10	-.09	-1.07	-.34	-.11
28	-.29	-.16	-.01	-.27	-.17	0
42	-4.39	1.22	-3.66	-4.15	.86	-3.52
44	-5.33	.67	-2.52	-8.75	.69	-3.93
46	-5.35	-1.62	-.83	-6.16	-1.62	-.92
62	-6.67	.95	-5.29	-7.04	.66	-5.69
64	-6.64	1.62	-3.15	-8.16	1.79	-3.69
82	-7.35	.71	-7.66	-7.64	.42	-7.64

TABLE 4

SPECIAL CASES FOR WING OF RECTANGULAR SECTION

WITH SYMMETRIC LOADS

(a) Deflections

Deflection point	[a]Case I			[b]Case II			[c]Case III		
	Deflection, in./kip, at loading point -			Deflection, in./kip, at loading point -			Deflection, in./kip, at loading point -		
	91	75	Tip couple	91	75	Tip couple	91	75	Tip couple
11	-0.0229	-0.0117	-0.0021	-0.0225	-0.0120	-0.0018	-0.0249	-0.0127	-0.0024
13	-.0205	-.0116	-.0011	-.0199	-.0117	-.0009	-.0201	-.0116	-.0010
15	-.0172	-.0115	.0002	-.0172	-.0115	.0001	-.0169	-.0113	.0002
17	-.0139	-.0111	.0012	-.0145	-.0112	.0010	-.0141	-.0111	.0011
19	-.0116	-.0107	.0018	-.0118	-.0109	.0019	-.0130	-.0114	.0016
51	.0546	.0234	.0087	.0541	.0247	.0077	.0509	.0221	.0086
53	.0445	.0243	.0034	.0446	.0246	.0036	.0426	.0239	.0023
55	.0347	.0251	-.0012	.0352	.0244	-.0004	.0343	.0247	-.0017
57	.0257	.0237	-.0041	.0256	.0241	-.0043	.0261	.0230	-.0032
71	.1302	.0523	.0214	.1287	.0529	.0191	.1217	.0505	.0195
73	.1048	.0553	.0066	.1053	.0561	.0078	.1010	.0540	.0044
75	.0832	.0598	-.0040	.0828	.0589	-.0037	.0817	.0564	-.0047
91	.2188	.0822	.0402	.2139	.0837	.0356	.2049	.0810	.0321
93	.1773	.0869	.0070	.1778	.0878	.0089	.1718	.0860	.0049

[a]Case I: Ribs rigid in bending only.

[b]Case II: Ribs rigid in bending and shear.

[c]Case III: No shear strain in ribs or spars.

TABLE 4.- Continued

SPECIAL CASES FOR WING OF RECTANGULAR SECTION

WITH SYMMETRIC LOADS

(b) Spanwise shears

Shear point	[a]Case 1			[b]Case II			[c]Case III		
	Spanwise shear, lb/lb, at loading point -			Spanwise shear, lb/lb, at loading point -			Spanwise shear, lb/lb, at loading point -		
	91	75	Tip couple	91	75	Tip couple	91	75	Tip couple
21	-0.048	0.003	-0.025	-0.040	0.001	-0.020	0.056	0.078	-0.039
23	-.052	.002	-.018	-.089	.001	-.036	-.164	-.051	-.022
25	.001	-.022	.015	-.002	-.018	.014	-.057	-.070	.033
27	.061	-.003	.025	.100	-.005	.043	.023	-.054	.035
29	.035	.019	.002	.029	.020	-.002	.140	.097	-.007
41	.446	.111	.148	.438	.141	.130	.439	.020	.260
43	.298	.223	.071	.312	.219	.078	.321	.283	-.030
45	.138	.223	-.008	.159	.159	.039	.139	.351	-.105
47	.092	.224	-.089	.074	.248	-.115	.167	.239	-.064
61	.476	.037	.219	.467	.013	.204	.513	.049	.277
63	.272	.217	.026	.286	.261	.076	.207	.224	-.085
65	.096	.360	-.097	.075	.375	-.155	.094	.193	-.034
81	.610	-.003	.437	.593	.007	.424	.631	.004	.405
83	.145	.114	-.239	.182	.049	-.219	.063	.131	-.144
[d]48	.025	.218	-.125	.017	.233	-.137	-.067	.108	-.064
[d]66	.153	.382	-.153	.165	.342	-.130	.180	.524	-.160
[d]84	.247	-.124	-.204	.227	-.069	-.209	.317	-.145	-.267

[a]Case I: Ribs rigid in bending only.

[b]Case II: Ribs rigid in bending and shear.

[c]Case III: No shear strain in ribs or spars.

[d]Leading-edge spar.

TABLE 4.- Continued

SPECIAL CASES FOR WING OF RECTANGULAR SECTION

WITH SYMMETRIC LOADS

(c) Chordwise shears

Shear point	[a]Case I			[b]Case II			[c]Case III		
	Chordwise shear, lb/lb, at loading point -			Chordwise shear, lb/lb, at loading point -			Chordwise shear, lb/lb, at loading point -		
	91	75	Tip couple	91	75	Tip couple	91	75	Tip couple
12	0.046	-0.004	0.025	0.039	-0.002	0.019	-0.057	-0.078	0.039
14	.098	-.006	.043	.129	-.002	.055	.105	-.028	.061
16	.098	.017	.027	.131	.016	.041	.162	.043	.028
18	.036	.020	.002	.030	.021	-.002	.140	.097	-.007
52	-.033	.074	-.073	-.036	.129	-.075	-.078	-.032	-.015
54	-.004	.081	-.028	-.010	.084	-.074	.033	.024	.040
56	.038	-.058	.062	.073	-.137	.119	.077	.179	-.031
72	-.135	.037	-.219	-.121	.005	-.219	-.114	.044	-.131
74	-.007	.142	.044	-.019	.217	.075	.034	.139	-.072
92	-.417	.001	-.559	-.434	.009	-.576	-.400	.006	-.594

[a]Case I: Ribs rigid in bending only.

[b]Case II: Ribs rigid in bending and shear.

[c]Case III: No shear strain in ribs or spars.

TABLE 4.- Continued

SPECIAL CASES FOR WING OF RECTANGULAR SECTION

WITH SYMMETRIC LOADS

(d) Spanwise bending moments

Shear point	[a]Case I			[b]Case II			[c]Case III		
	Spanwise bending moment, in-lb/lb, at loading point -			Spanwise bending moment, in-lb/lb, at loading point -			Spanwise bending moment, in-lb/lb, at loading point -		
	91	75	Tip couple	91	75	Tip couple	91	75	Tip couple
11	-9.55	-4.78	-0.97	-9.38	-4.89	-0.83	-10.12	-5.16	-0.99
13	-18.39	-10.26	-1.08	-18.13	-10.36	-.99	-17.53	-10.13	-.84
15	-15.22	-10.36	.28	-15.31	-10.31	.11	-14.77	-10.14	.33
17	-12.08	-9.98	1.26	-12.43	-10.07	1.13	-12.11	-9.83	1.02
19	-4.59	-4.27	.75	-4.72	-4.41	.76	-5.25	-4.72	.66
31	-11.85	-4.79	-2.02	-11.76	-5.02	-1.80	-11.78	-4.16	-2.69
33	-19.85	-10.26	-1.53	-20.14	-10.31	-1.80	-20.15	-10.71	-1.18
35	-15.20	-11.12	.71	-15.33	-10.67	.47	-15.55	-11.65	1.24
37	-10.39	-10.21	1.95	-10.15	-10.26	2.17	-10.76	-10.53	1.89
39	-2.70	-3.63	1.12	-2.62	-3.74	1.21	-1.76	-2.95	.84
51	-7.88	-2.48	-1.44	-7.73	-2.17	-1.30	-7.98	-2.75	-1.07
53	-14.47	-5.73	-.12	-14.59	-5.95	-.48	-14.08	-5.73	-.48
55	-12.43	-7.27	1.02	-12.29	-7.88	1.48	-12.44	-5.98	.60
57	-2.91	-5.04	2.13	-3.01	-4.92	1.96	-2.37	-4.75	1.52
71	-4.94	-.65	-1.41	-4.62	-.55	-1.09	-4.73	-.84	-.78
73	-9.51	-.89	1.02	-9.75	-.36	.95	-9.32	-1.23	-.06
75	-3.51	-1.61	2.83	-3.56	-1.87	2.43	-4.09	-2.77	3.12
93	.87	.69	3.72	1.28	.26	4.02	-.12	.68	4.53
[d]48	-3.53	-2.03	-.21	-3.48	-1.94	-.23	-3.47	-2.67	.27
[d]66	-5.17	-.63	-1.17	-5.21	-.61	-1.22	-5.17	-.29	-.78
[d]84	-4.45	.83	-2.26	-4.73	.70	-2.63	-4.08	1.22	-2.52

[a]Case I: Ribs rigid in bending only.

[b]Case II: Ribs rigid in bending and shear.

[c]Case III: No shear strain in ribs or spars.

[d]Leading-edge spar.

TABLE 4.- Continued

SPECIAL CASES FOR WING OF RECTANGULAR SECTION

WITH SYMMETRIC LOADS

(e) Chordwise bending moments

Moment point	[a]Case III		
	Chordwise bending moment, in-lb/lb, at loading point -		
	91	75	Tip couple
13	-3.96	-2.26	-0.08
15	-3.81	-2.93	.41
17	-2.19	-2.25	.48
53	-3.61	-.76	-1.91
55	-4.12	.14	-1.81
57	2.38	4.77	-1.52
73	-3.08	.76	-4.79
75	4.09	2.82	-3.13
93	.10	-.62	-4.57

[a]Cases I and II were not measured. Case III: No shear strain in ribs or spars.

TABLE 4.- Concluded

SPECIAL CASES FOR WING OF RECTANGULAR SECTION

WITH SYMMETRIC LOADS

(f) Spanwise twisting moments

Moment point	[a]Case I			[b]Case II			[c]Case III		
	Spanwise twisting moment, in-lb/lb, at loading point -			Spanwise twisting moment, in-lb/lb, at loading point			Spanwise twisting moment, in-lb/lb, at loading point -		
	91	75	Tip couple	91	75	Tip couple	91	75	Tip couple
22	-1.28	-0.06	-0.53	-1.56	-0.14	-0.56	-2.79	-0.64	-0.86
24	-1.60	-.02	-.63	-1.77	-.11	-.66	-2.03	-.14	-.75
26	-1.57	-.20	-.50	-1.78	-.17	-.62	-1.64	-.15	-.49
28	-1.16	-.27	-.31	-1.49	-.24	-.47	-.66	.25	-.33
42	-5.10	.08	-2.43	-4.80	0	-2.11	-5.00	1.05	-3.73
44	-5.78	.12	-2.44	-5.59	0	-2.36	-5.32	.41	-2.42
46	-5.78	-.61	-1.96	-5.71	-.33	-2.12	-4.98	-.96	-.92
62	-6.77	1.10	-4.44	-6.50	1.36	-3.93	-7.20	.92	-5.36
64	-7.11	1.56	-3.81	-7.26	1.63	-4.06	-6.61	.79	-3.20
82	-7.45	.67	-7.50	-7.38	.40	-7.47	-8.02	.76	-7.46

[a]Case I: Ribs rigid in bending only.

[b]Case II: Ribs rigid in bending and shear.

[c]Case III: No shear strain in ribs or spars.

TABLE 5

VIBRATION MODES FOR WING OF RECTANGULAR SECTION

Deflection point	Symmetric loads				Antisymmetric loads		
	Mode						
	1	2	3	4	1	2	3
	Frequency, cps						
	46.6	163	206	275	54.8	195	268
1	-1.46	3.00	10.00	-2.34	0	0	0
3	-1.26	3.78	7.51	-2.40	0	0	0
5	-1.10	5.22	4.02	-1.50	0	0	0
7	-.97	6.80	1.04	.14	0	0	0
9	-.96	7.98	-.44	1.22	0	0	0
11	-1.44	2.84	9.44	-2.12	-0.24	-0.064	0.60
13	-1.24	3.54	6.92	-2.06	-.22	.120	.42
15	-1.10	4.96	3.62	-1.30	-.20	.364	.22
17	-.96	6.50	.96	.12	-.14	.496	.144
19	-.96	7.76	-.40	1.14	-.08	.508	.144
51	2.97	2.30	-4.94	-9.35	2.79	3.46	-9.32
53	2.70	-1.05	-.26	-5.40	2.48	-1.30	-5.36
55	2.30	-4.35	3.55	-2.22	1.98	-5.22	-2.08
57	1.80	-5.86	3.90	-1.12	1.39	-5.55	-.88
71	6.44	6.36	-6.15	-5.72	6.39	7.35	-5.54
73	5.96	.12	1.70	-.58	5.73	-1.39	-.40
75	5.20	-5.75	7.13	1.63	4.75	-8.02	1.83
91	10.00	9.90	-5.03	5.93	10.00	9.99	6.11
93	9.37	2.38	3.84	10.00	9.13	-.42	10.00

TABLE 6

VIBRATION MODES FOR WING OF BICONVEX SECTION

Deflection point	Symmetric loads				Antisymmetric loads		
	Mode						
	1	2	3	4	1	2	3
	Frequency, cps						
	41.3	131	167	196	46.5	151	188
1	-1.26	3.24	10.00	-6.82	0	0	0
3	-1.00	2.92	5.80	-3.93	0	0	0
5	-.84	3.24	3.20	-1.38	0	0	0
7	-.76	4.29	2.38	.75	0	0	0
9	-.81	6.06	2.18	2.75	0	0	0
11	-1.24	3.08	9.44	-6.64	-0.18	0.04	0.46
13	-1.00	2.78	5.50	-3.62	-.14	.12	.22
15	-.84	3.08	3.00	-1.28	-.11	.20	.11
17	-.76	4.08	2.20	.68	-.08	.26	.08
19	-.82	5.88	2.04	2.64	-.08	.36	.11
51	2.73	1.00	-7.20	-8.40	2.50	2.18	-8.54
53	2.39	-1.48	-.78	-3.80	2.12	-1.48	-3.80
55	1.92	-3.62	2.84	-1.60	1.58	-3.86	-1.38
57	1.48	-4.71	3.10	-1.31	1.04	-4.20	-.72
71	6.30	5.02	-8.81	-6.77	6.18	6.00	-6.44
73	5.58	-.80	2.31	-1.02	5.23	-1.90	-.70
75	4.62	-5.40	8.18	.95	4.10	-7.00	1.39
91	10.00	9.99	-5.98	6.18	10.00	10.00	5.99
93	9.02	2.12	7.51	10.00	8.79	-.64	10.00

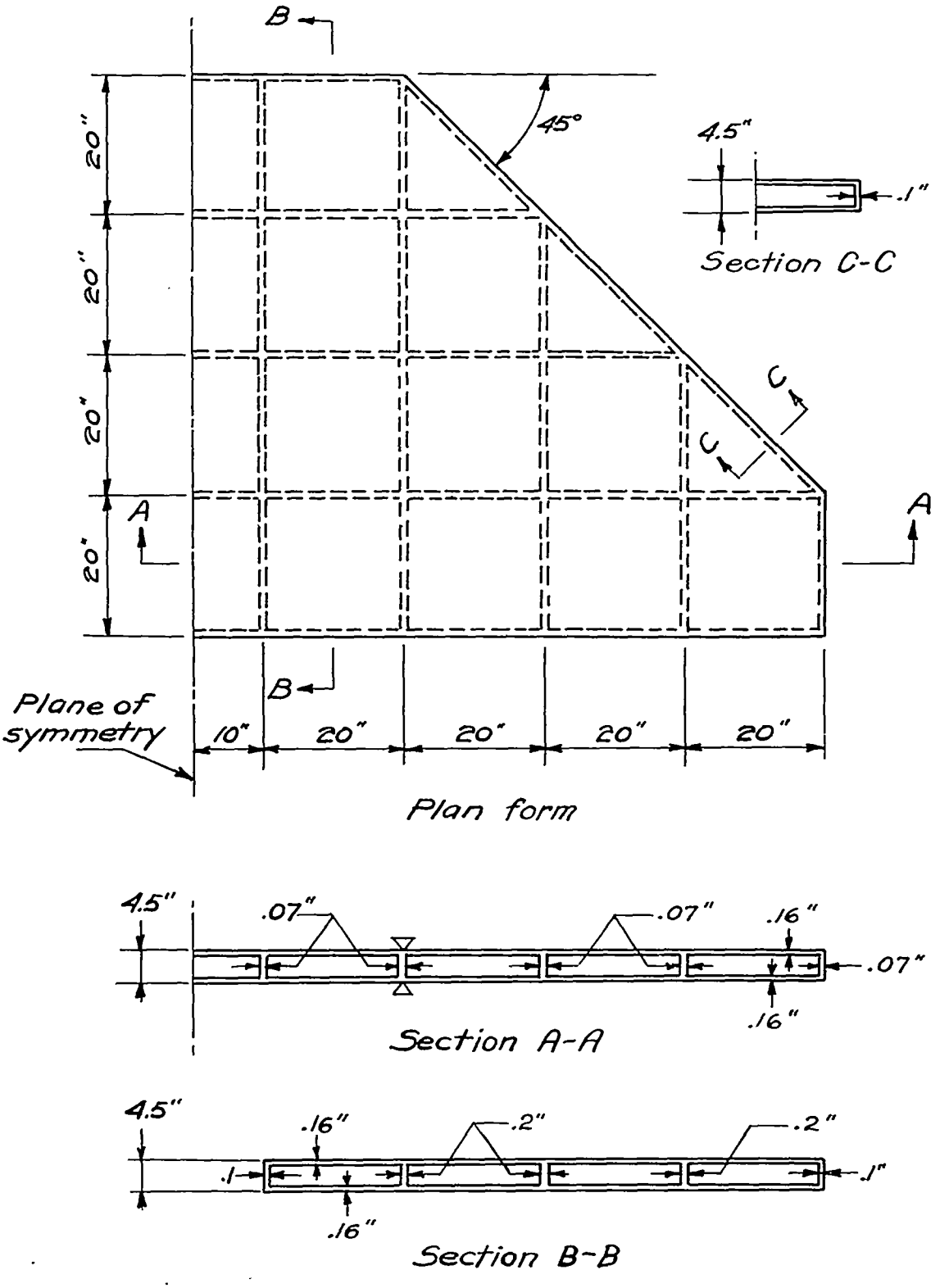

Figure 1.- Wing with rectangular section.

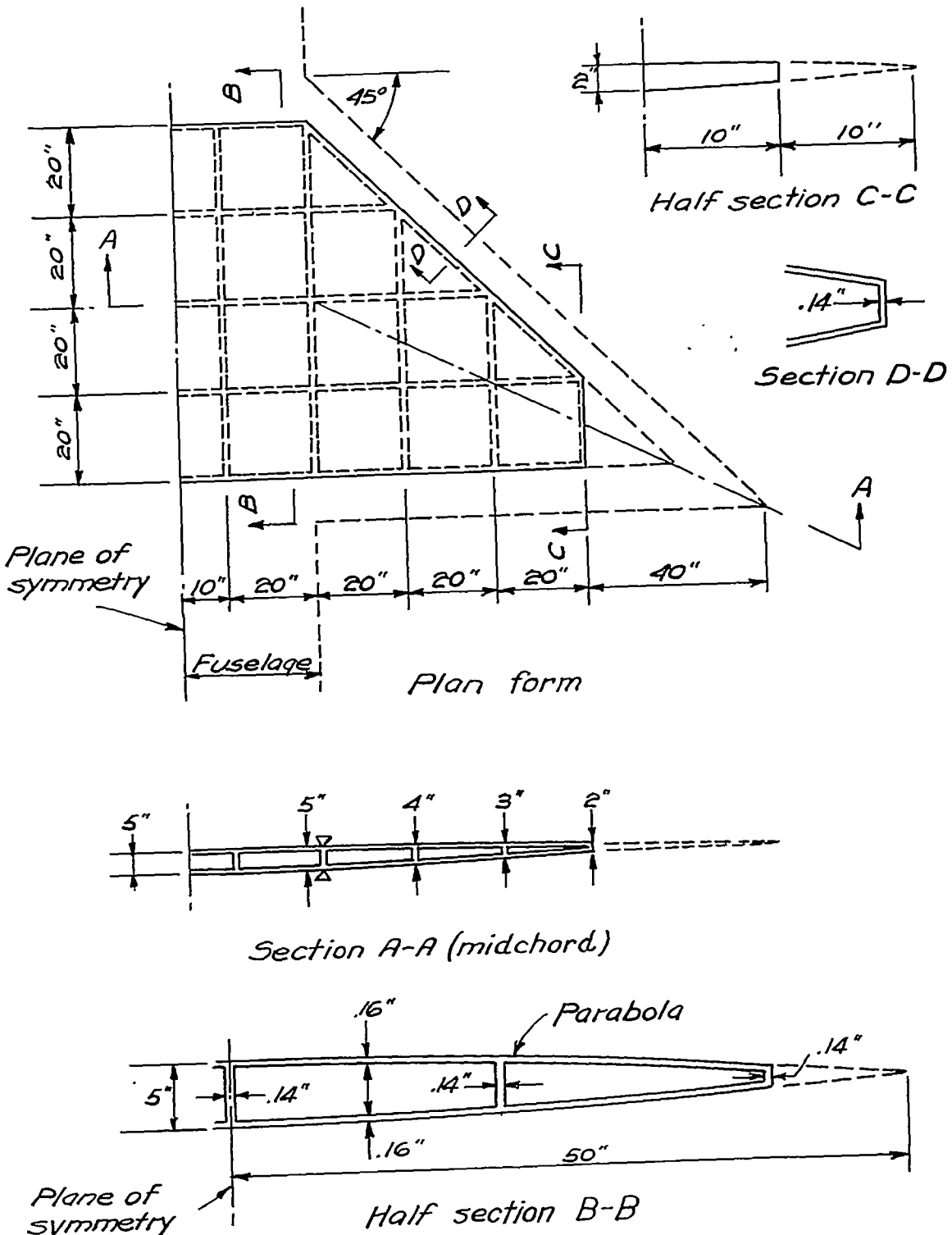

Figure 2.- Wing with biconvex section.

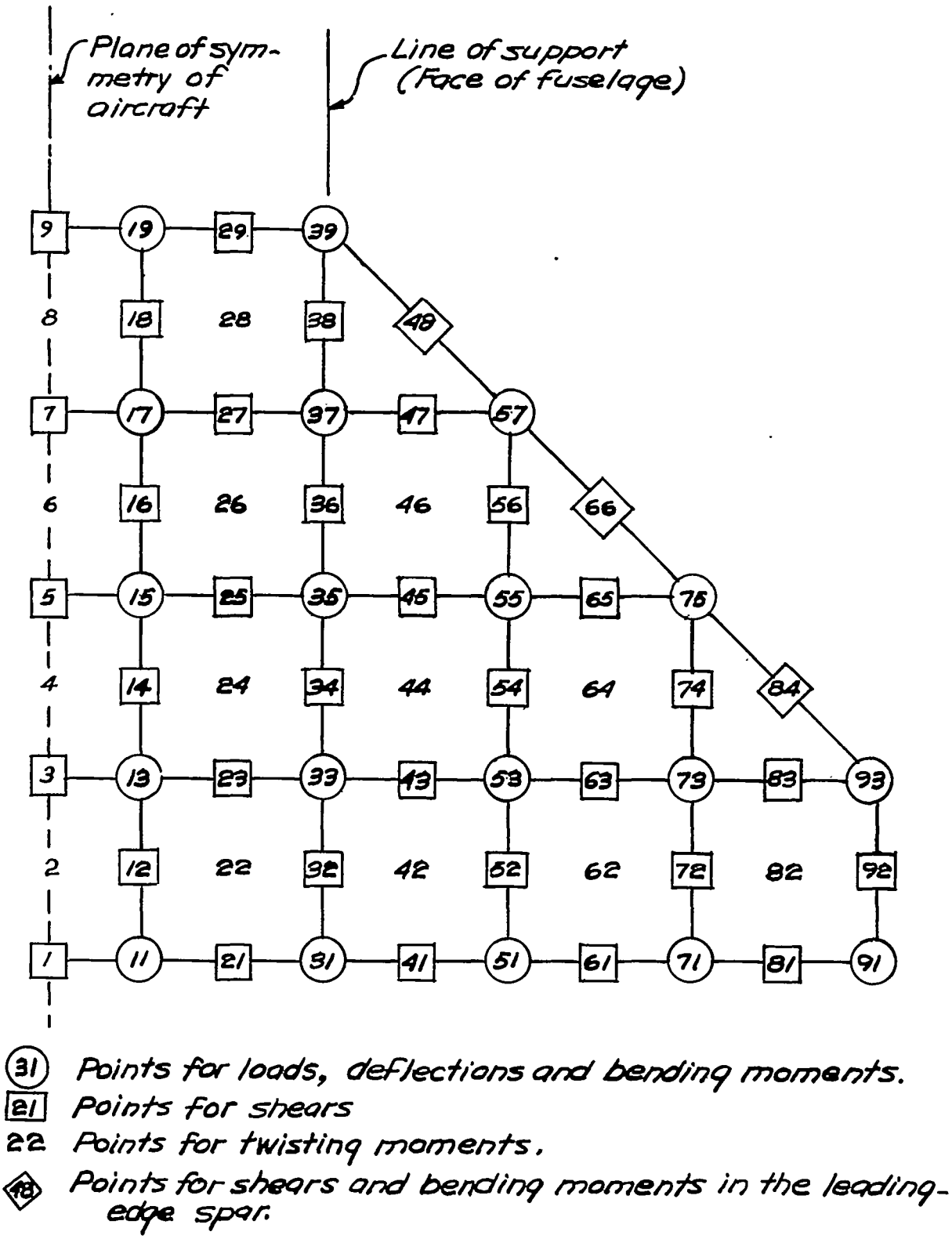

Figure 3.- Numbering of points where quantities are measured.

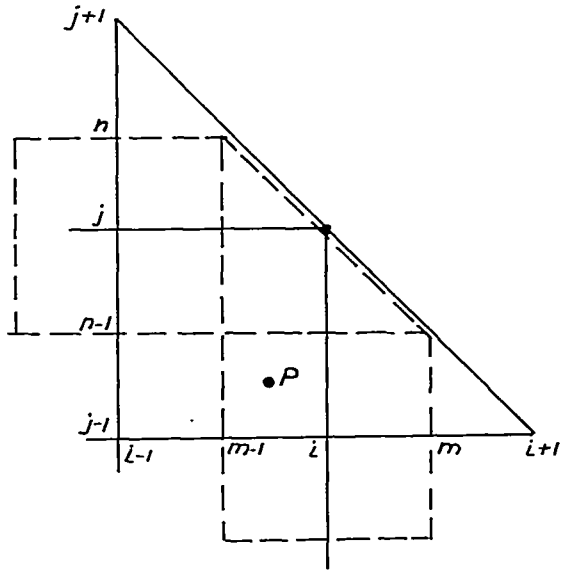

(a) Portion of plan form near leading edge.

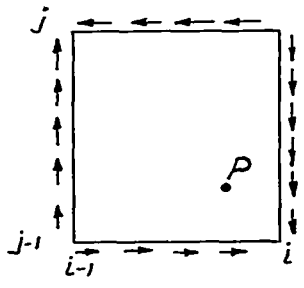

(b) Skin panel subjected to tangential shear forces on four sides.

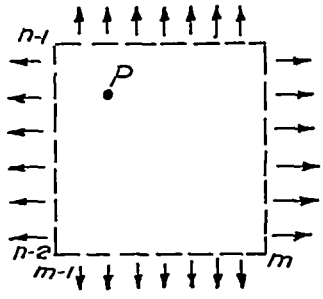

(c) Skin panel subjected to normal forces on four sides.

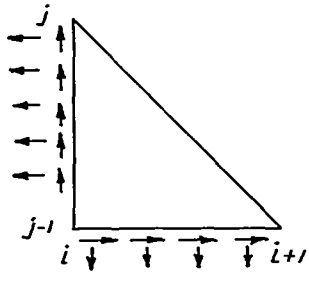

(d) Tangential forces equal to normal forces acting on same sides.

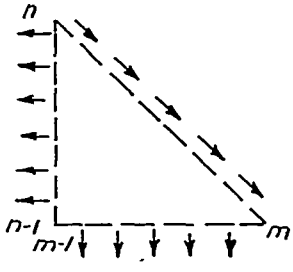

(e) Tangential force along edge equal to normal forces on other two sides.

Figure 4.- Types of panels occurring near leading edge.

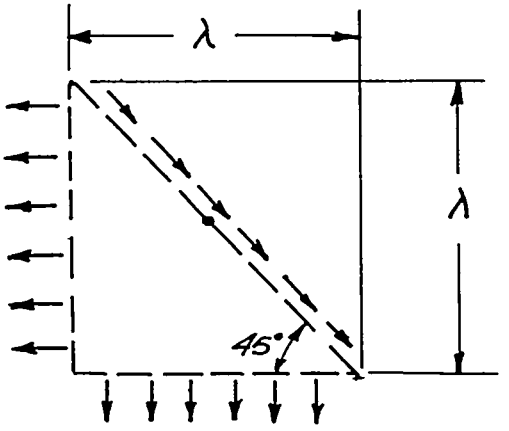

(a) Distributed forces.

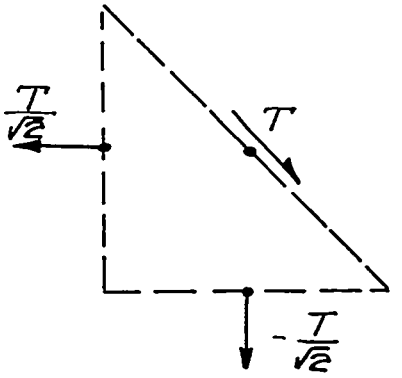

(b) Concentrated forces.

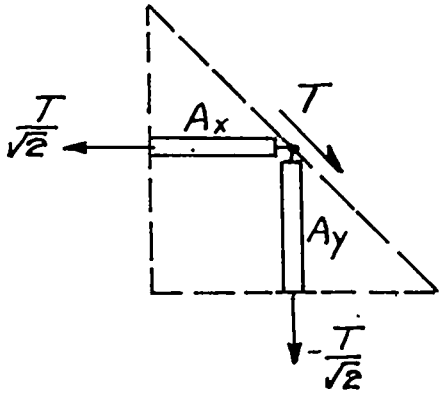

(c) $A_x = A_y = \frac{\lambda t}{1 + \mu}$.

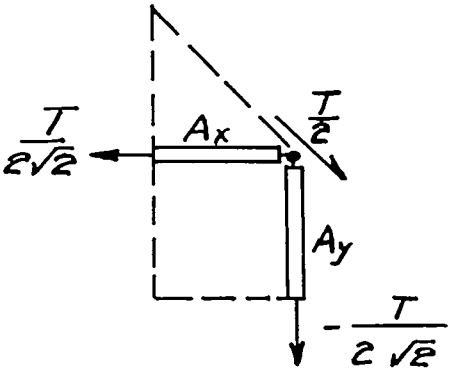

(d) Corner point;
$A_x = A_y = \frac{3}{4} \frac{\lambda t}{1 + \mu}$.

Figure 5.- Steps in idealization of dashed-line triangular panels.

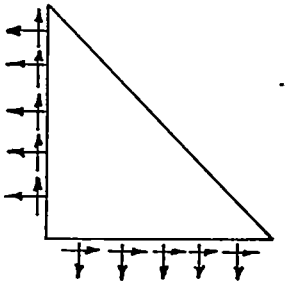

(a) Distributed forces on solid-line triangle.

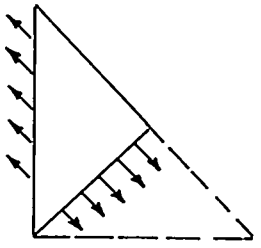

(b) Normal forces on plane perpendicular to leading edge.

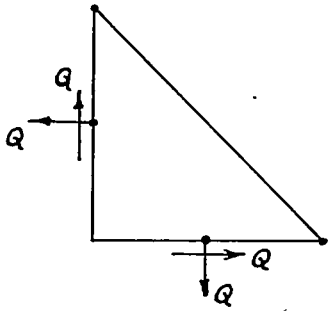

(c) Distributed forces concentrated at midpoints of sides.

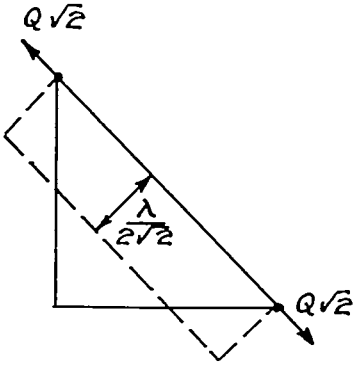

(d) Concentrated forces acting at corner in direction parallel to edge.

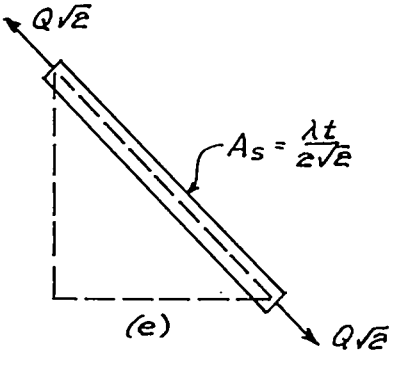

(e) Material in triangle replaced by flange for leading-edge spar.

Figure 6.- Steps in idealization of triangular shear panels.

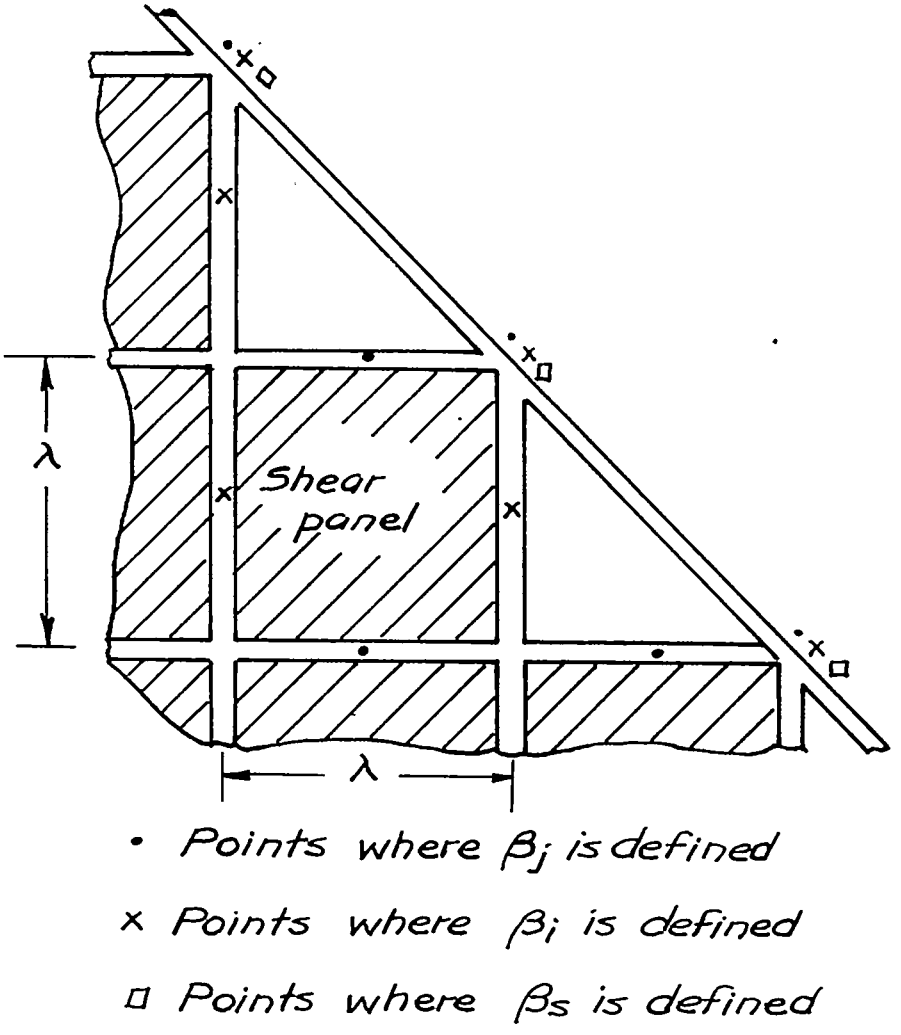

Figure 7.- Complete idealized structure near leading edge.

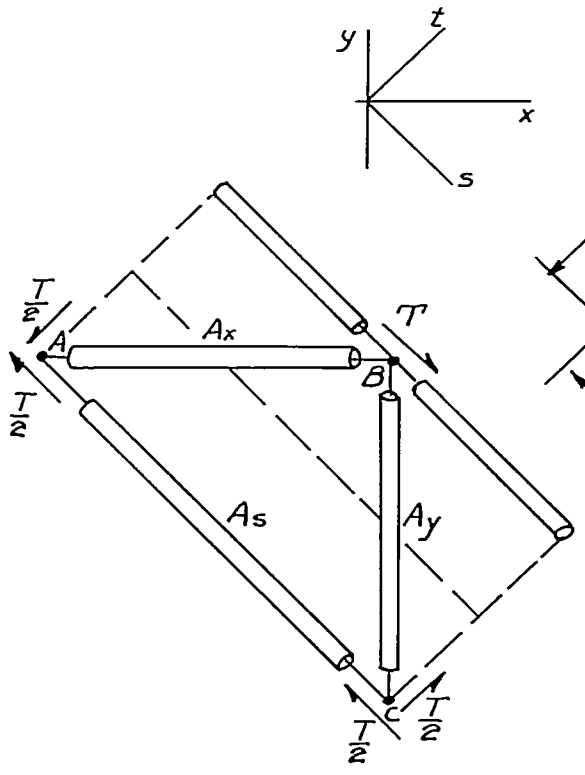

(a) Uniform shear forces acting on idealized structure of length $\lambda\sqrt{2}$.

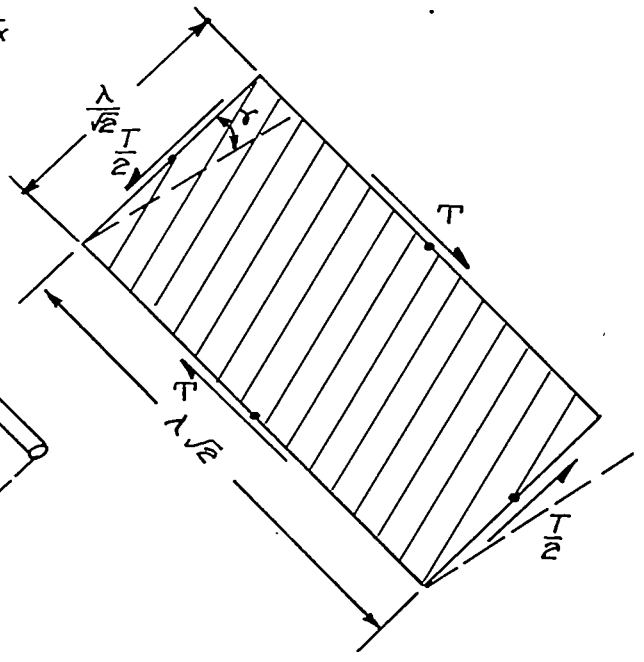

(b) Uniform shear forces acting along edge of strip of length $\lambda\sqrt{2}$.

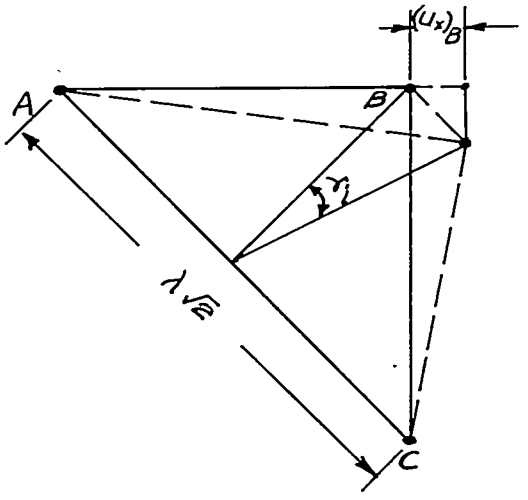

(c) Shearing strain for idealized structure.

Figure 8.- Idealized structure for a strip of skin subjected to shear forces.

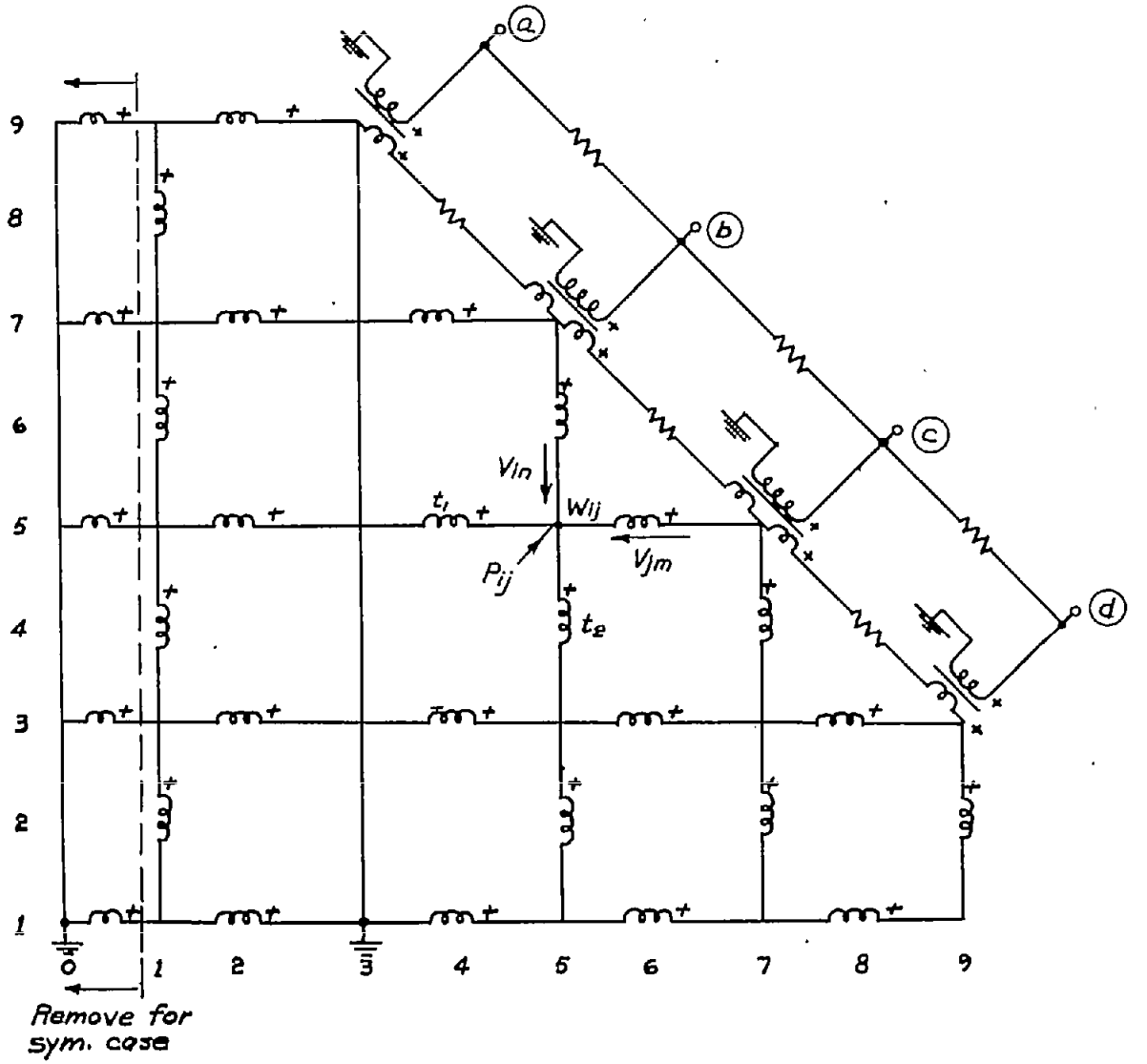

Figure 9.- Circuit for shears and deflections.

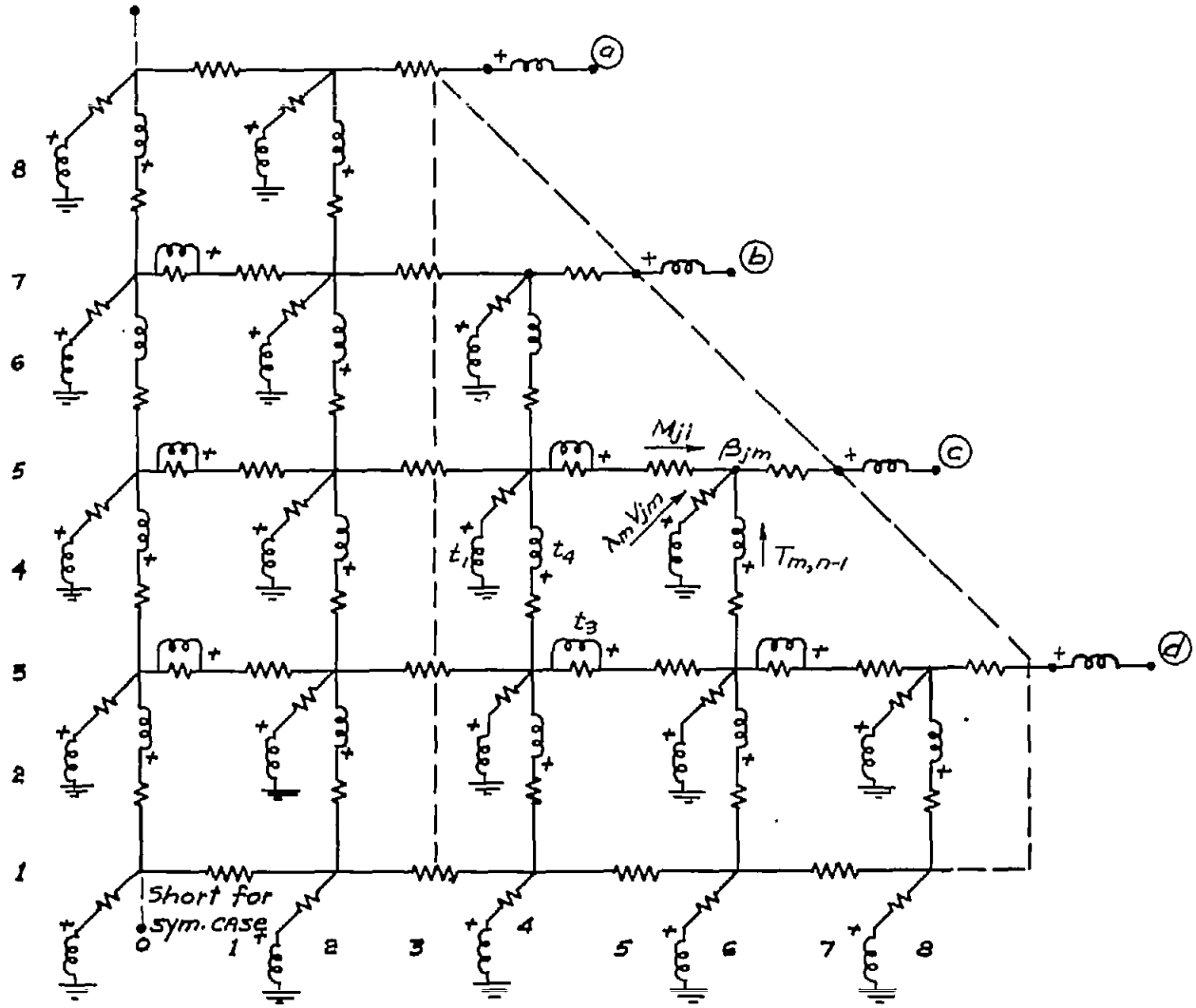

Figure 10.- Circuit for spanwise bending moments and chordwise twisting moments.

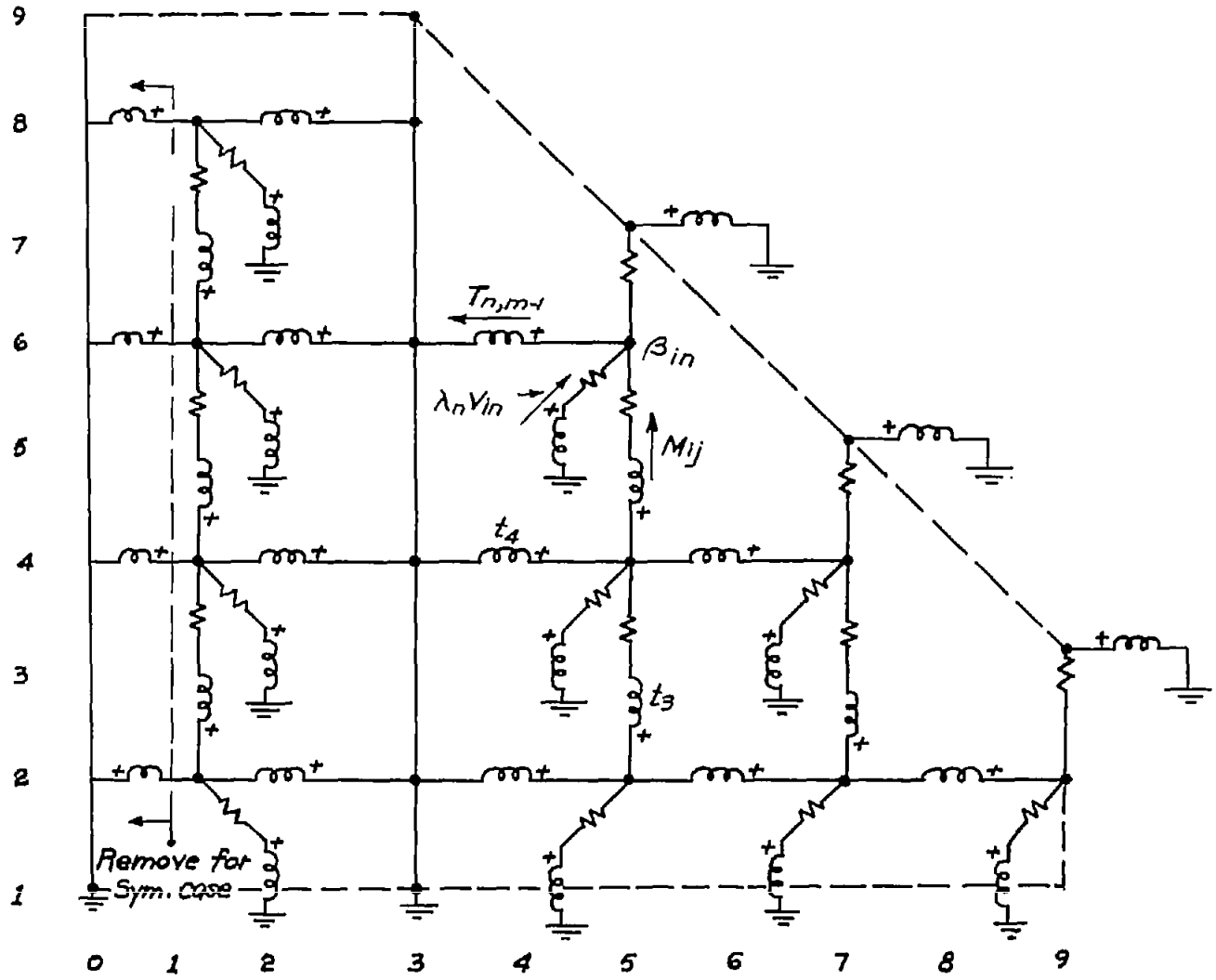

Figure 11.- Circuit for chordwise bending moments and spanwise twisting moments.

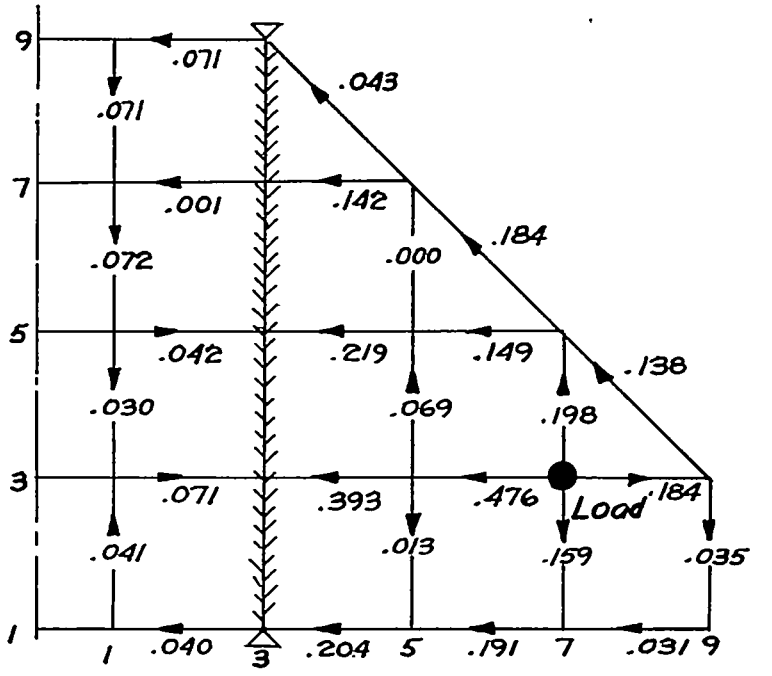

(a) Load at point 73.

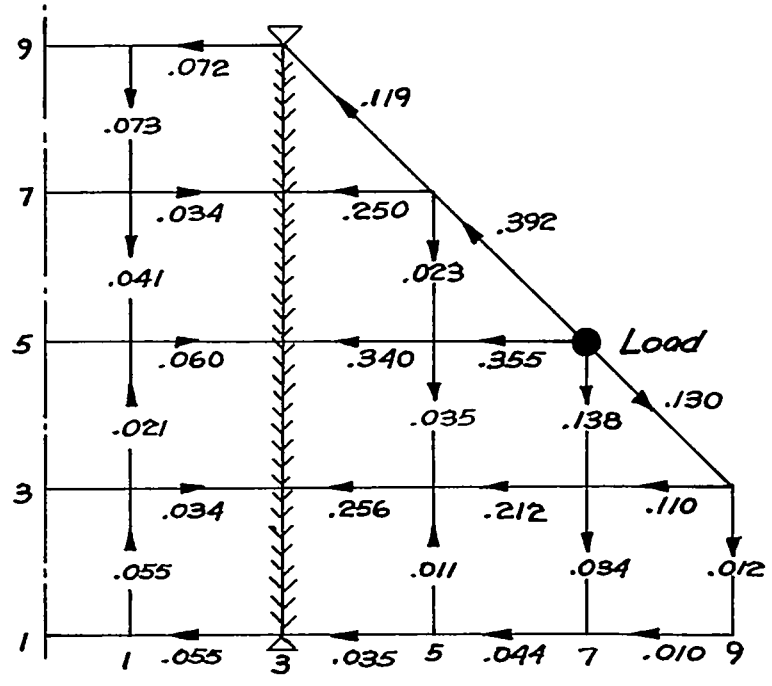

(b) Load at point 75.

Figure 12.- Distribution of shears. Rectangular section; symmetric loads.

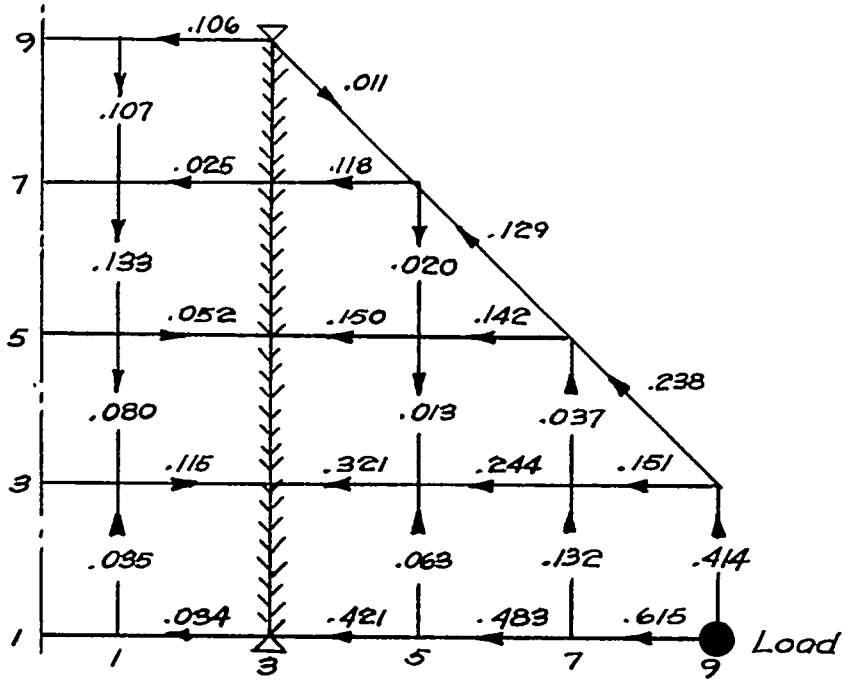

(a) Basic wing with shear strains in ribs and spars.

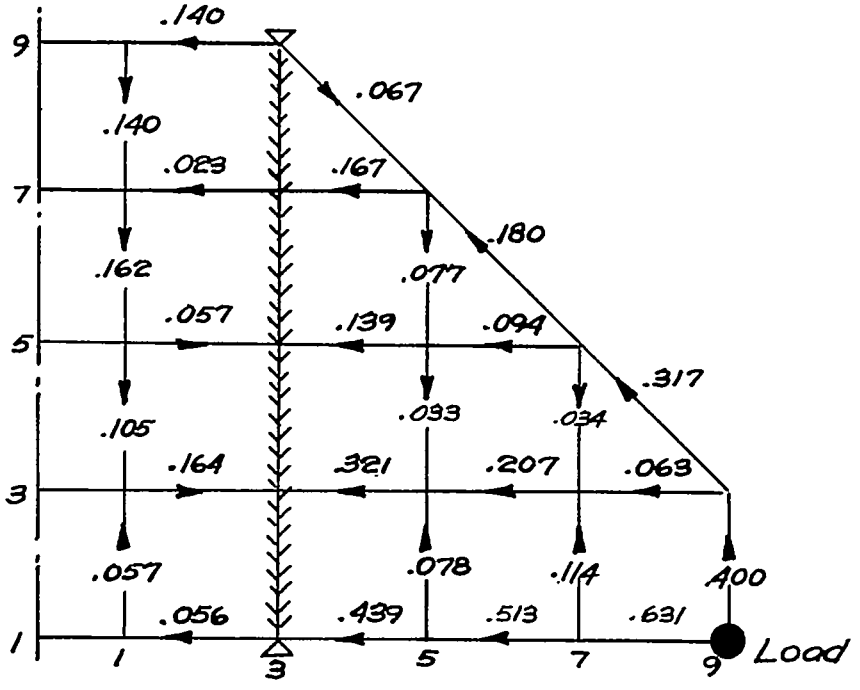

(b) Basic wing without shear strains in ribs and spars.

Figure 13.- Distribution of shears. Rectangular section; symmetric loads at point 91.

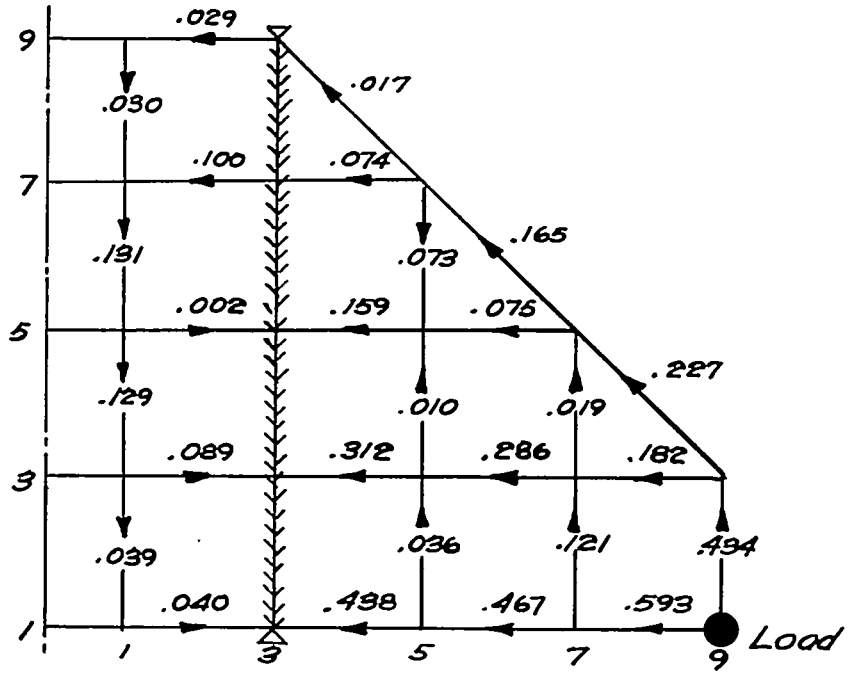

(c) Ribs rigid in bending and shear.

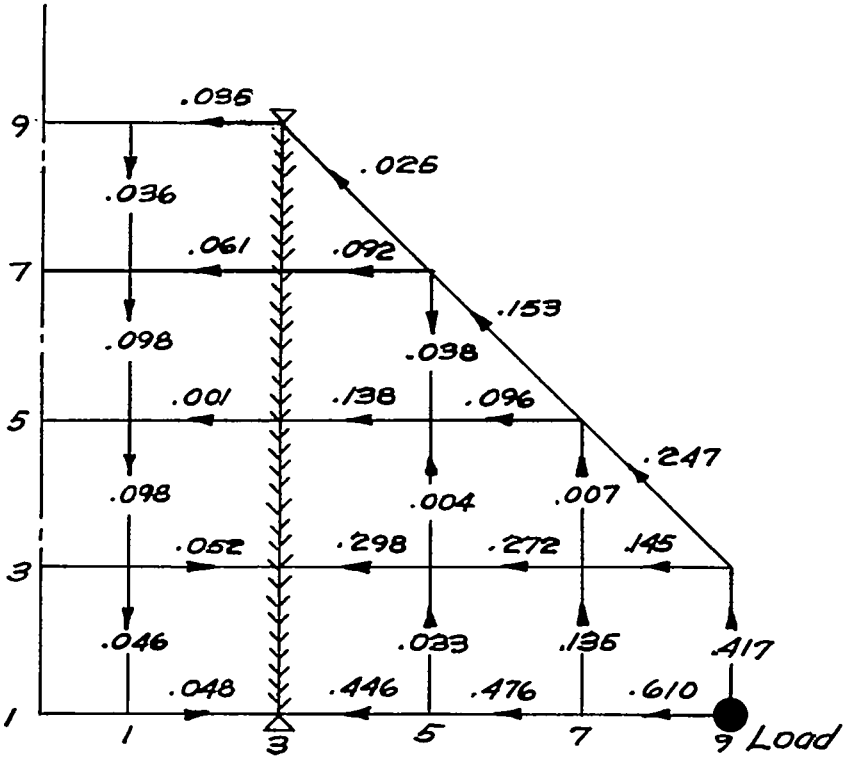

(d) Ribs rigid in bending only.

Figure 13.- Concluded.

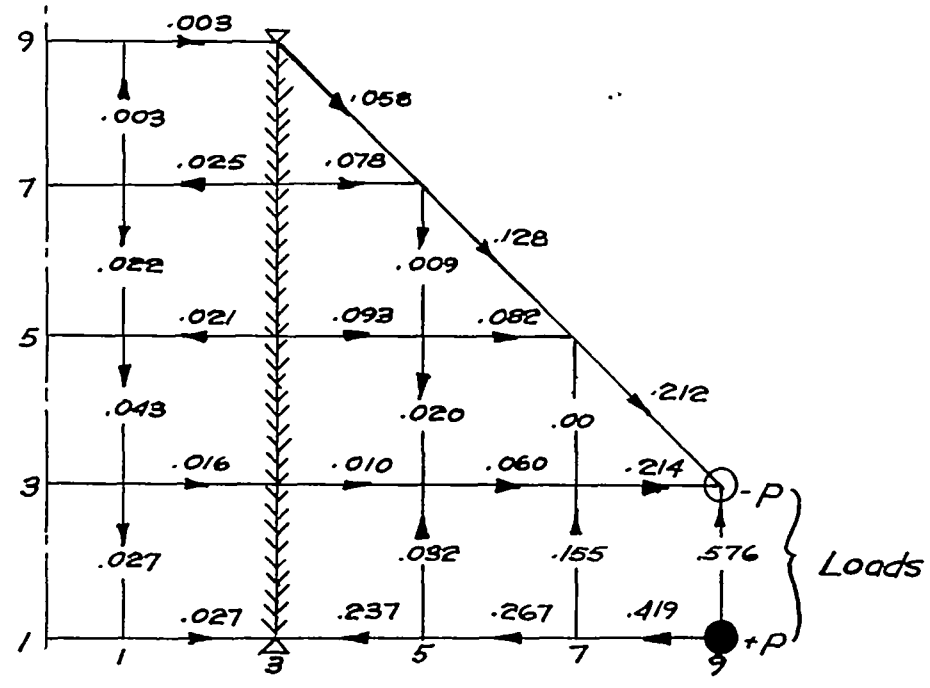

(a) Basic wing with shear strains in ribs and spars.

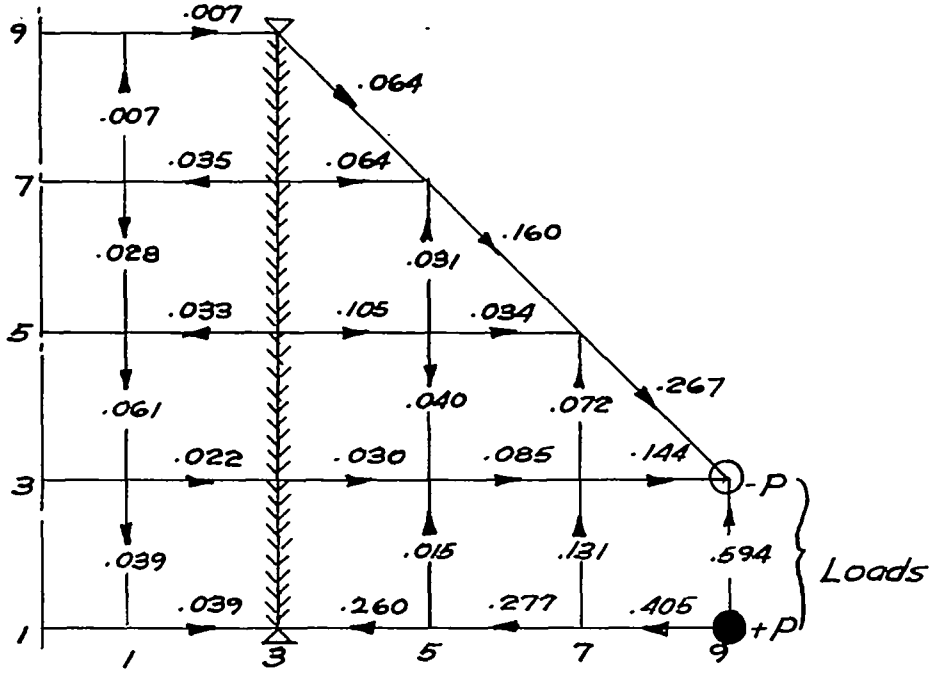

(b) Basic wing without shear strains in ribs and spars.

Figure 14.- Distribution of shears. Rectangular section; symmetric tip couple.

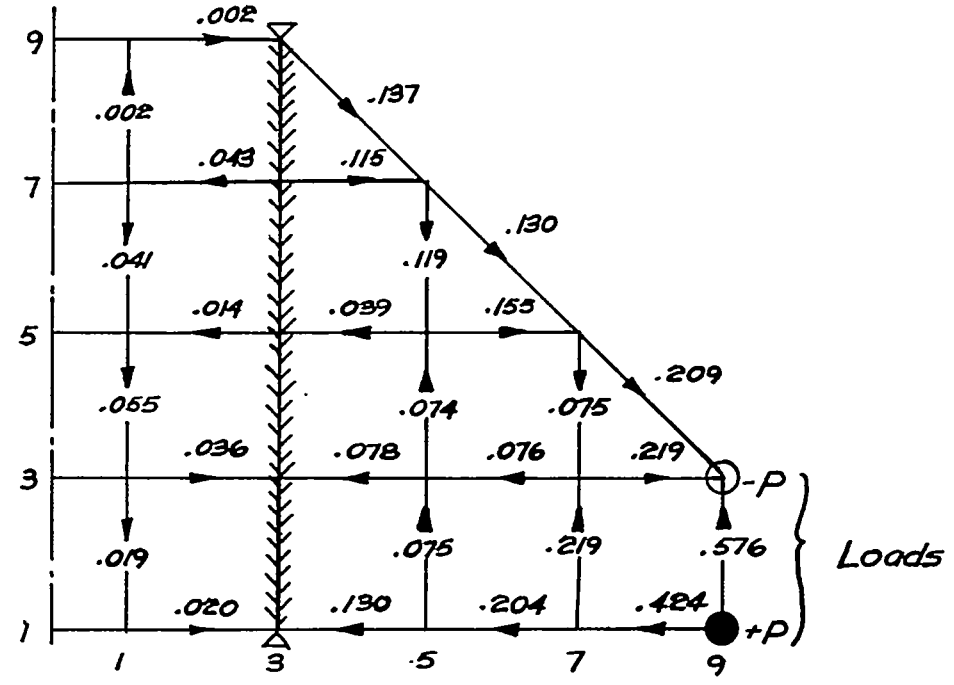

(c) Ribs rigid in bending and shear.

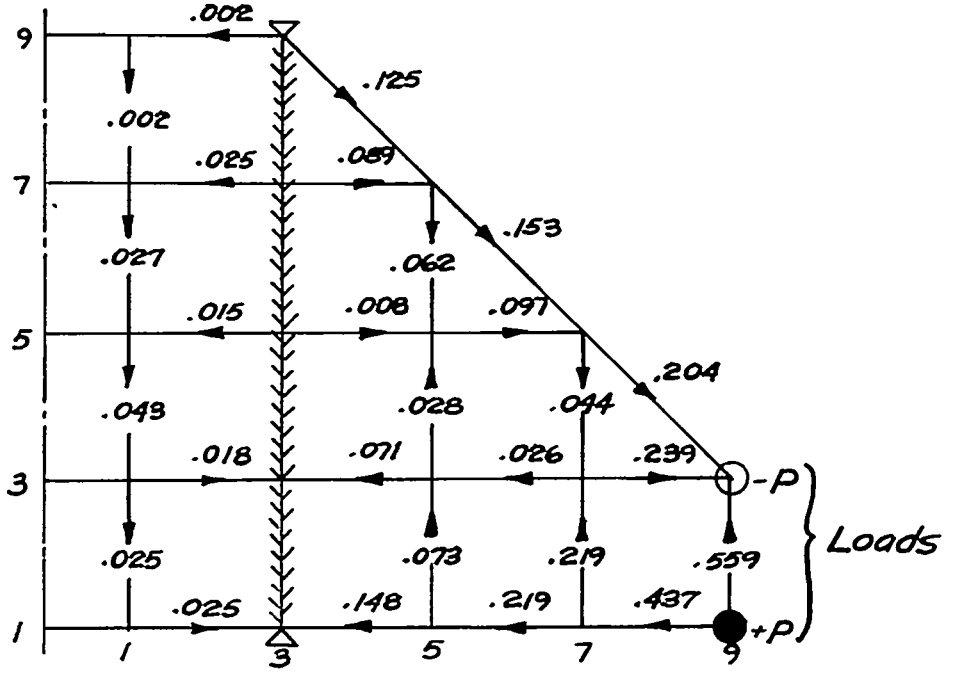

(d) Ribs rigid in bending only.

Figure 14.- Concluded.

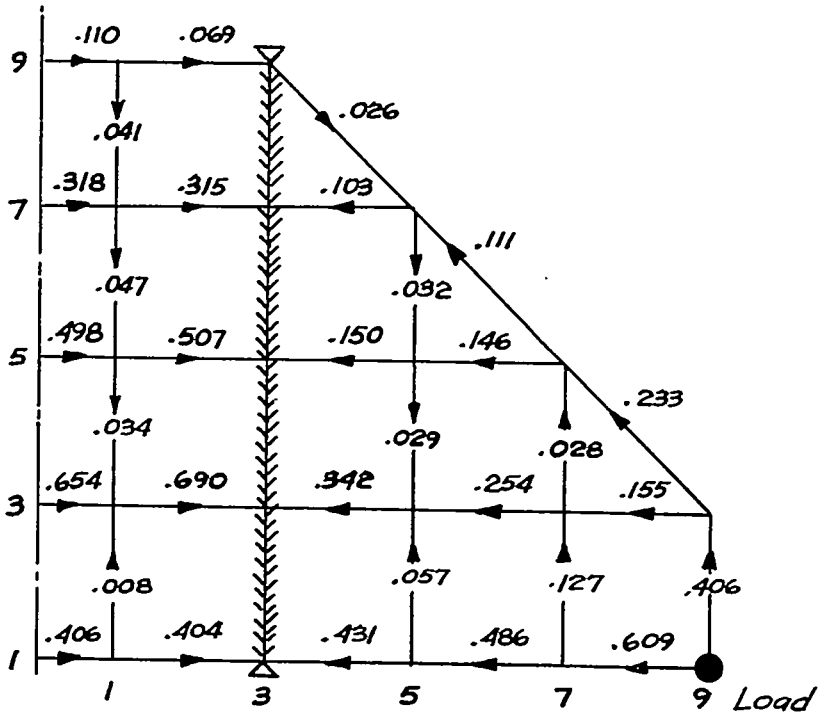

(a) Rectangular section.

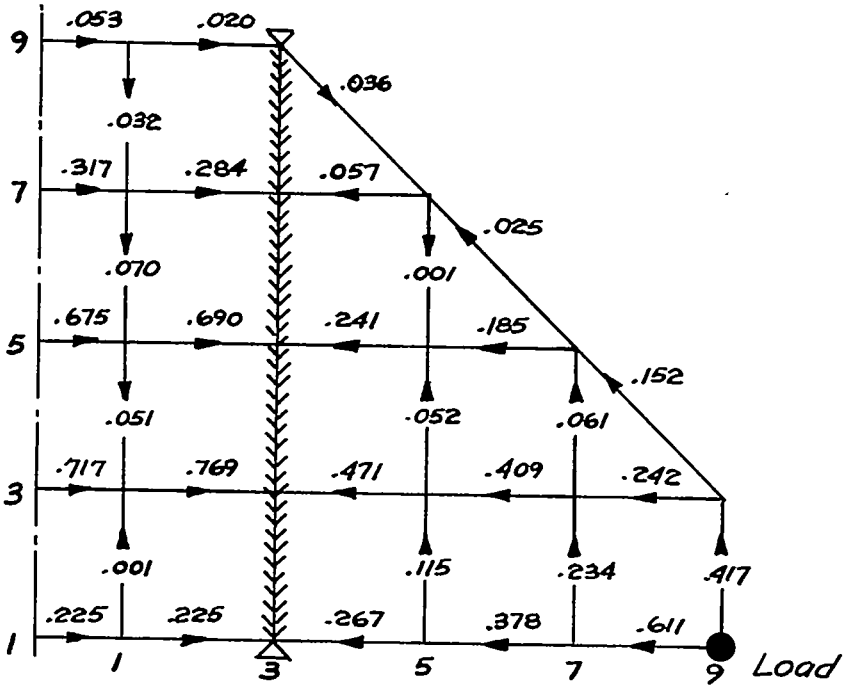

(b) Biconvex section.

Figure 15.- Distribution of shears. Antisymmetric loads at point 91.

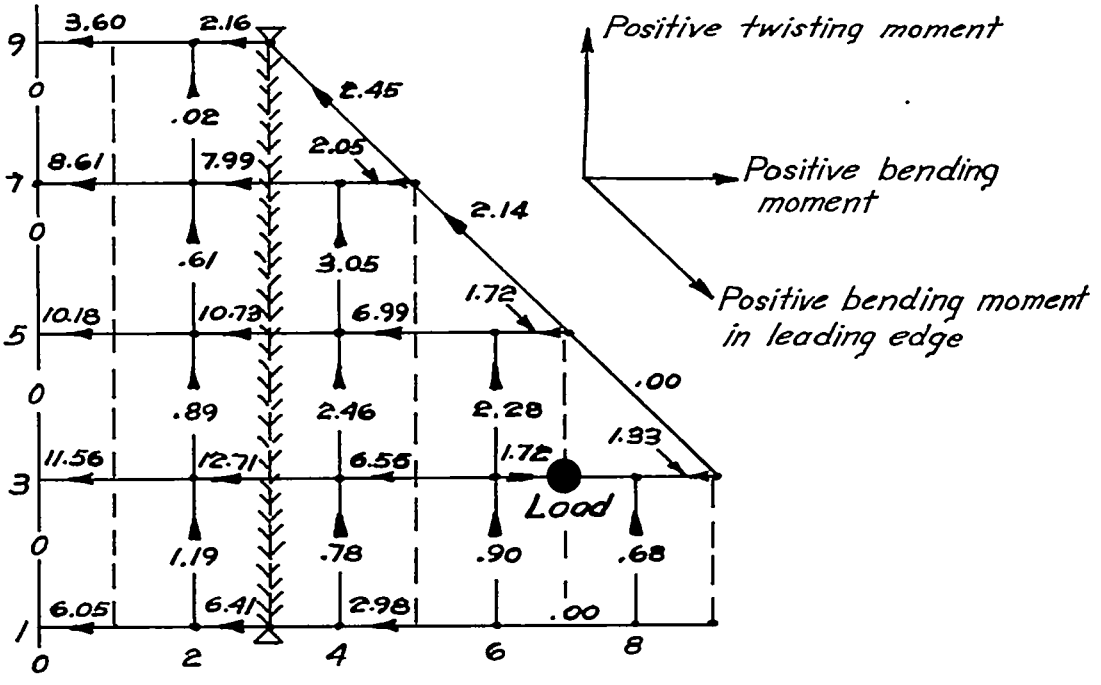

(a) Load at point 73.

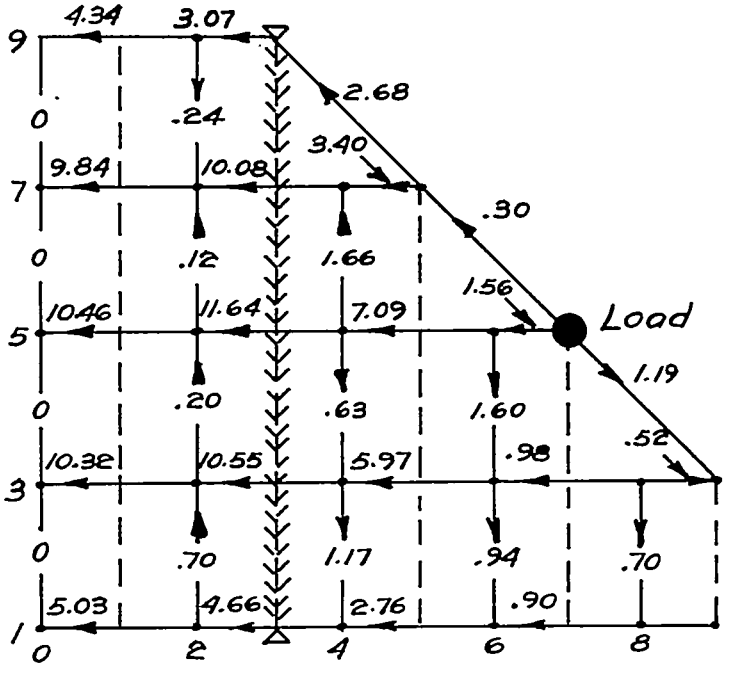

(b) Load at point 75.

Figure 16.- Distribution of spanwise bending moments and chordwise twisting moments. Rectangular section; symmetric loads.

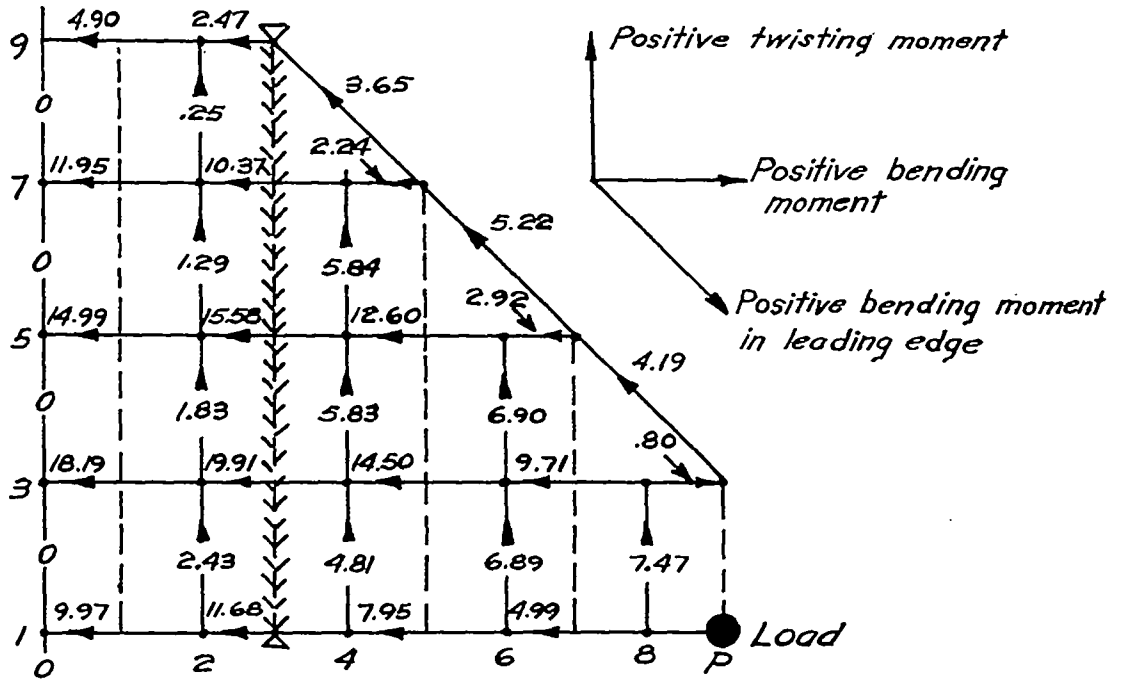

(a) Basic wing with shear strain in ribs and spars.

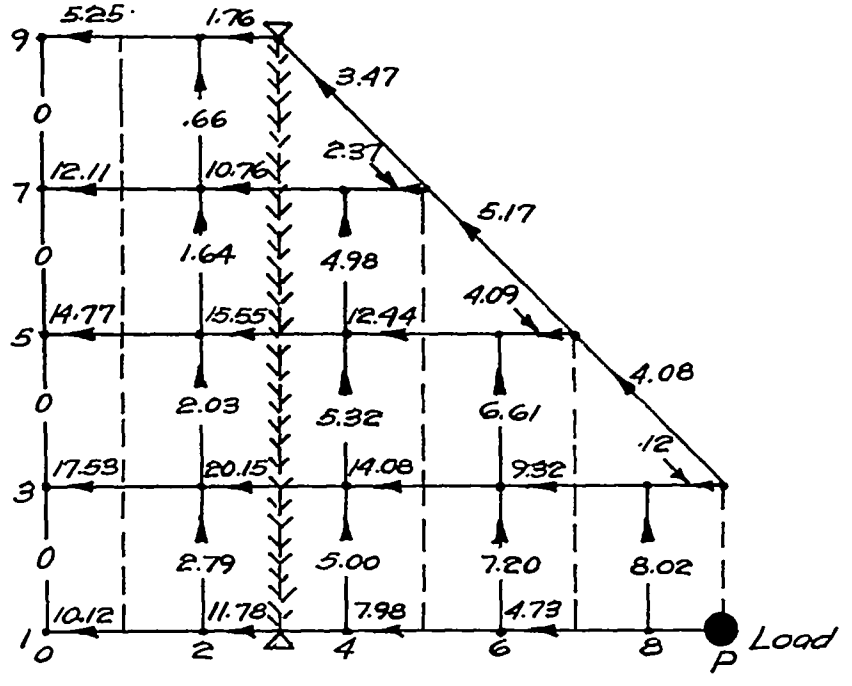

(b) Basic wing without shear strain in ribs or spars.

Figure 17.- Distribution of spanwise bending moments and chordwise twisting moments. Rectangular section; symmetric loads at point 91.

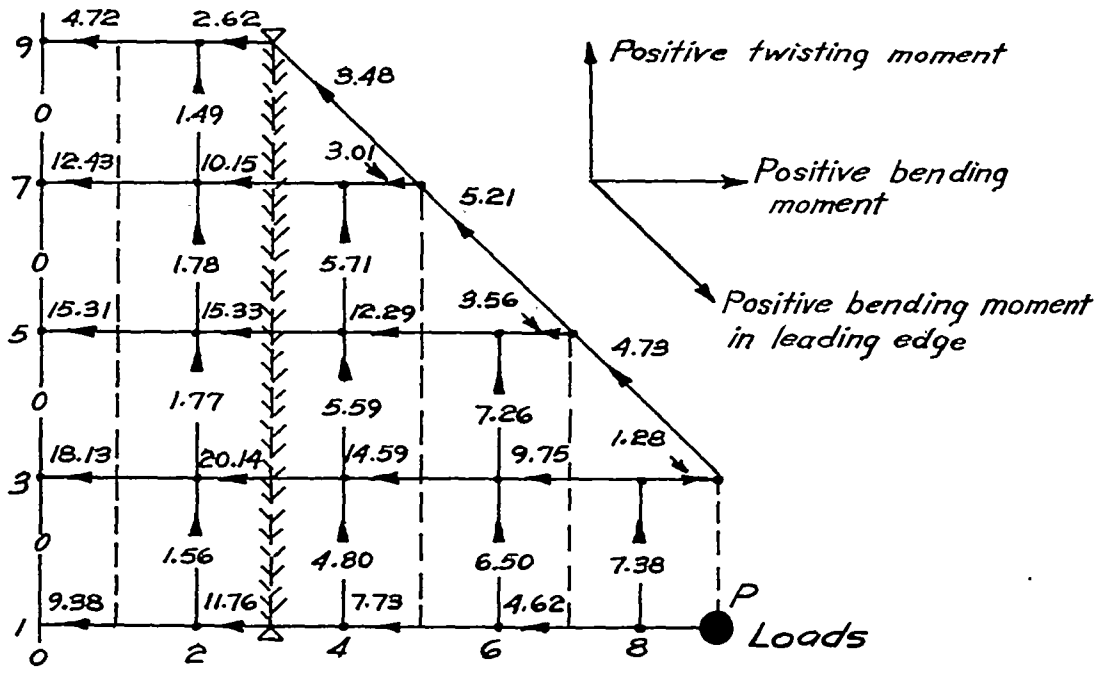

(c) Ribs rigid in bending and shear.

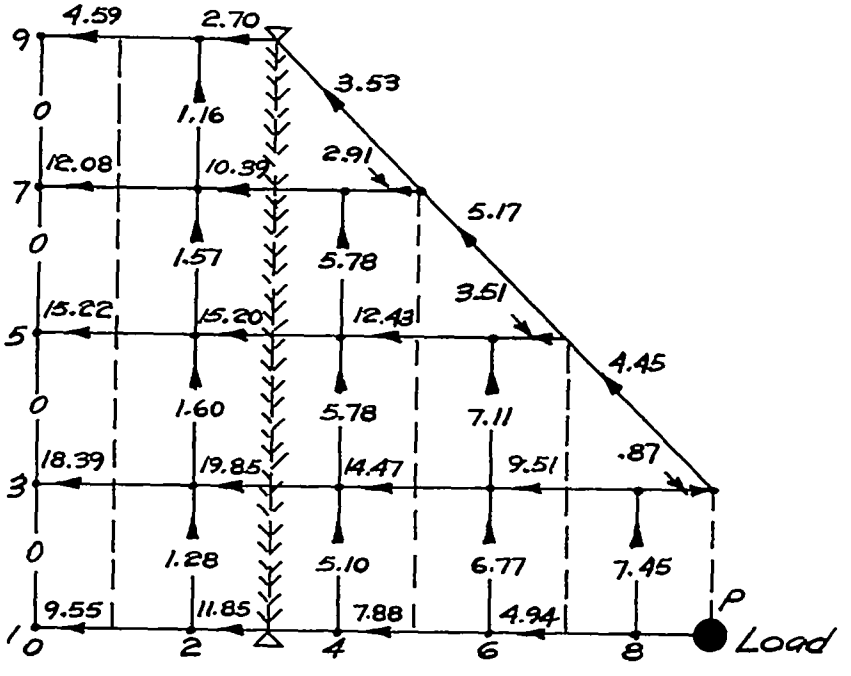

(d) Ribs rigid in bending only.

Figure 17.- Concluded.

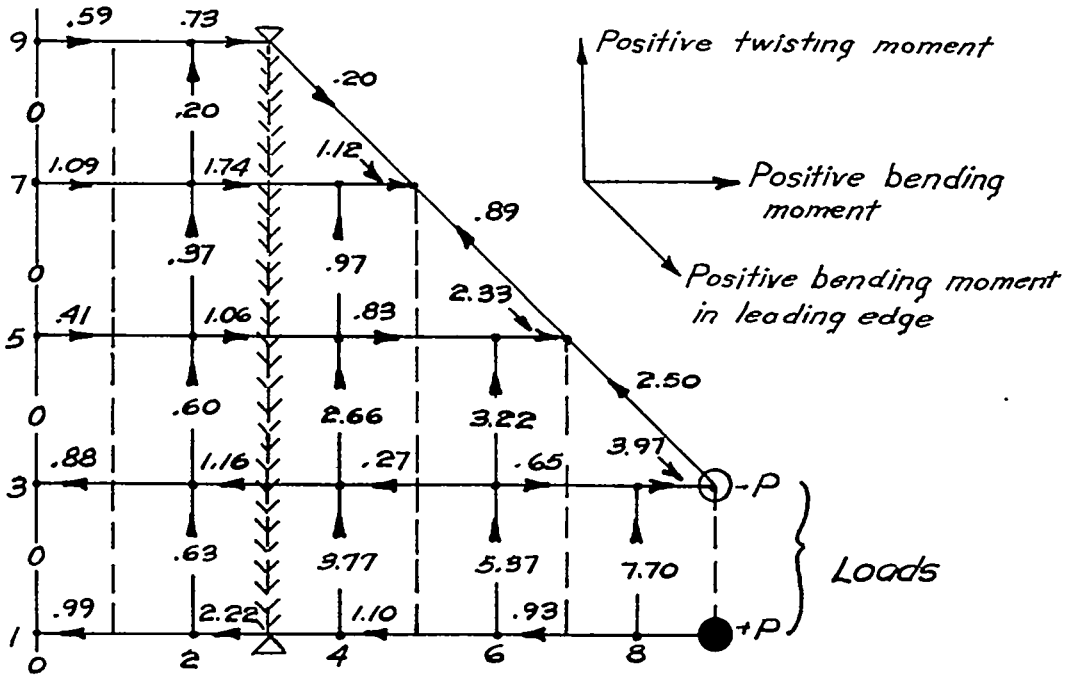

(a) Basic wing with shear strain in ribs and spars.

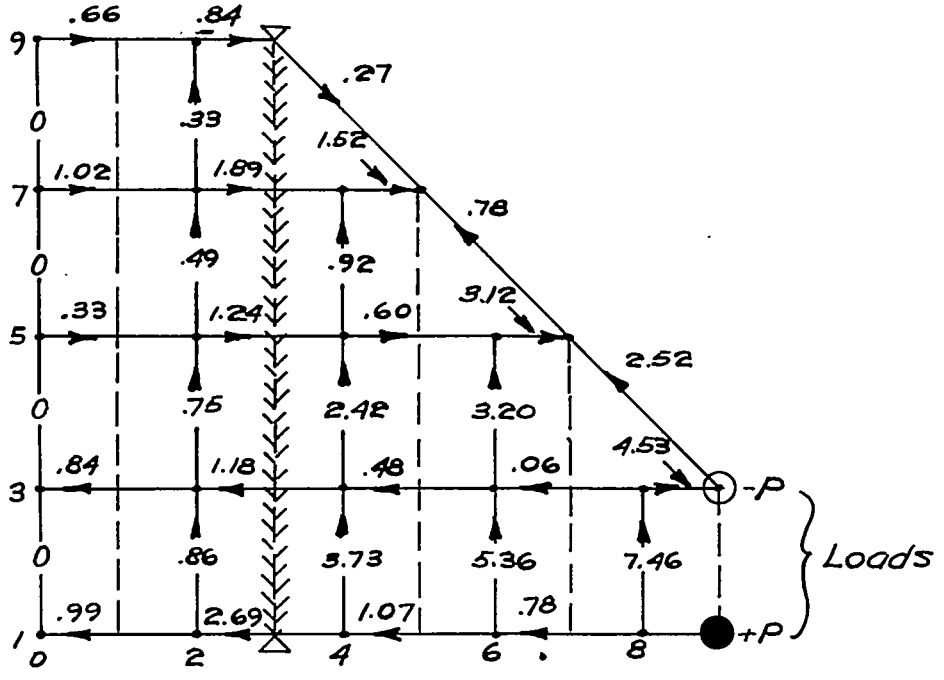

(b) Basic wing without shear strain in ribs or spars.

Figure 18.- Distribution of spanwise bending moments and chordwise twisting moments. Rectangular section; symmetric tip couples.

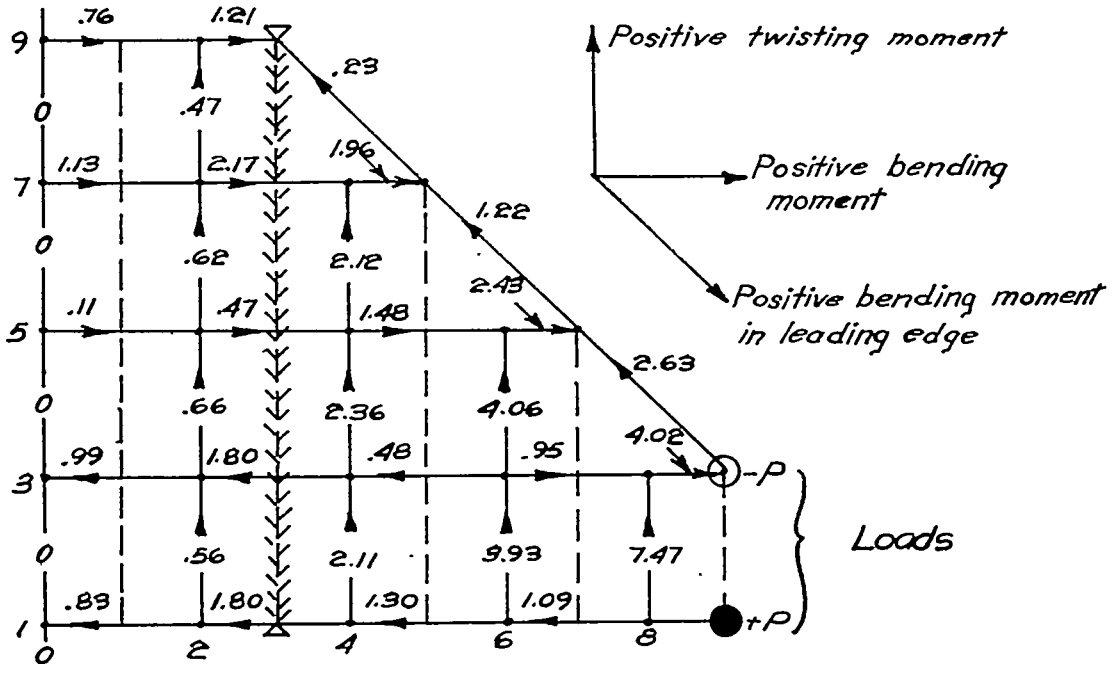

(c) Ribs rigid in bending and shear.

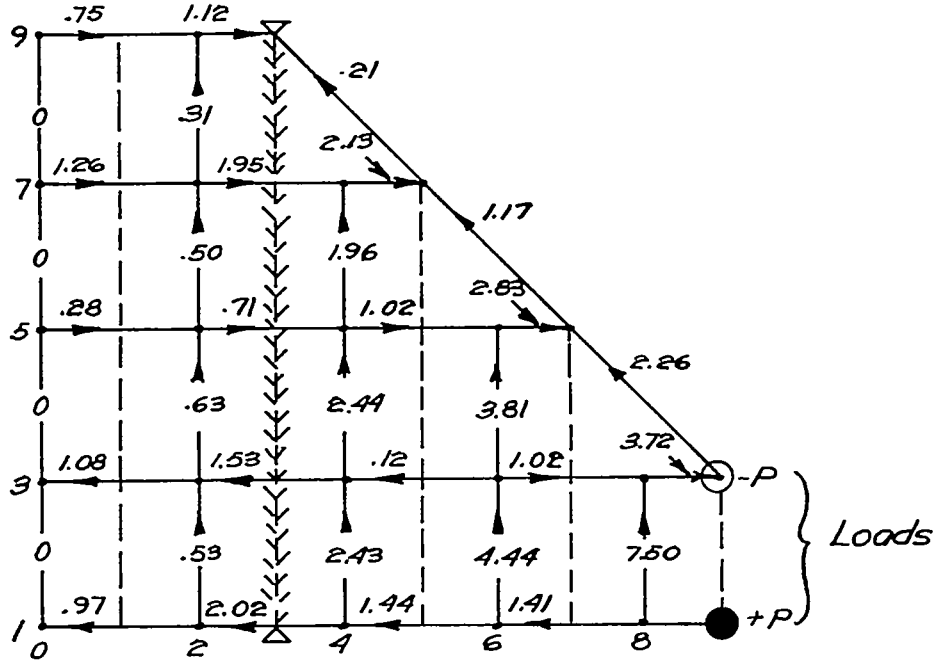

(d) Ribs rigid in bending only.

Figure 18.- Concluded.

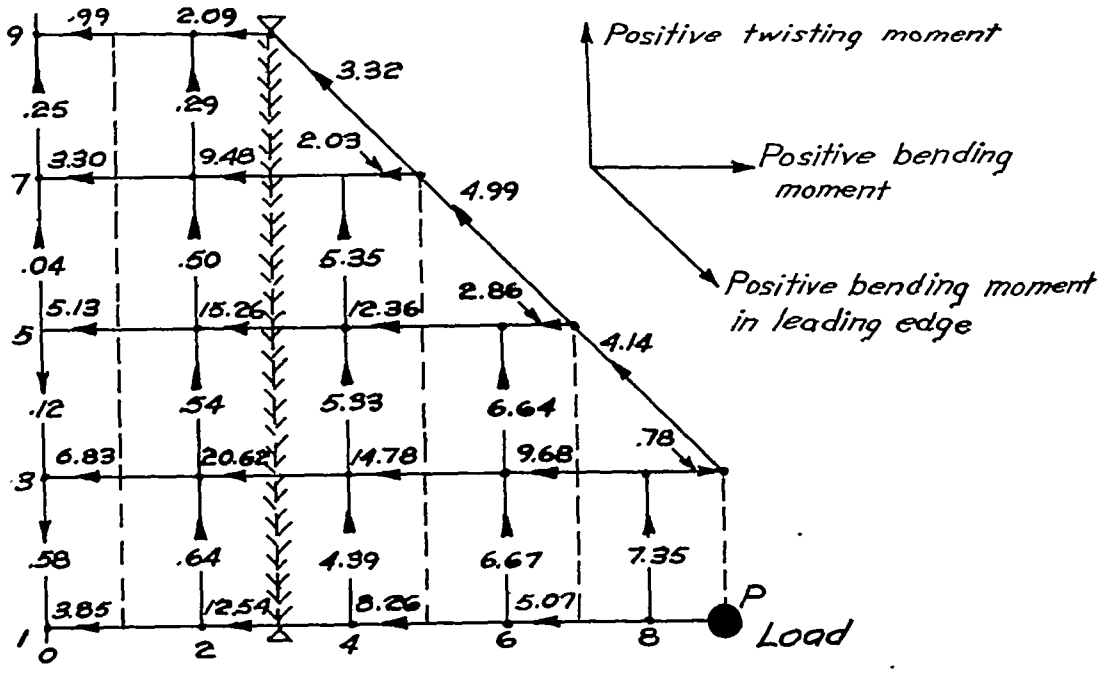

(a) Rectangular section.

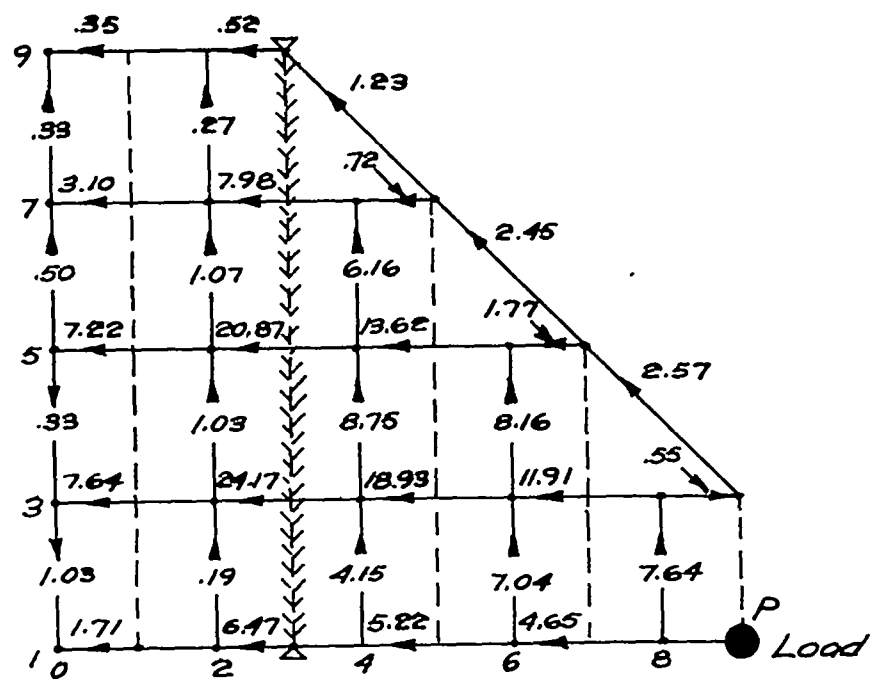

(b) Biconvex section.

Figure 19.- Distribution of spanwise bending moments and chordwise twisting moments. Antisymmetric loads at point 91.

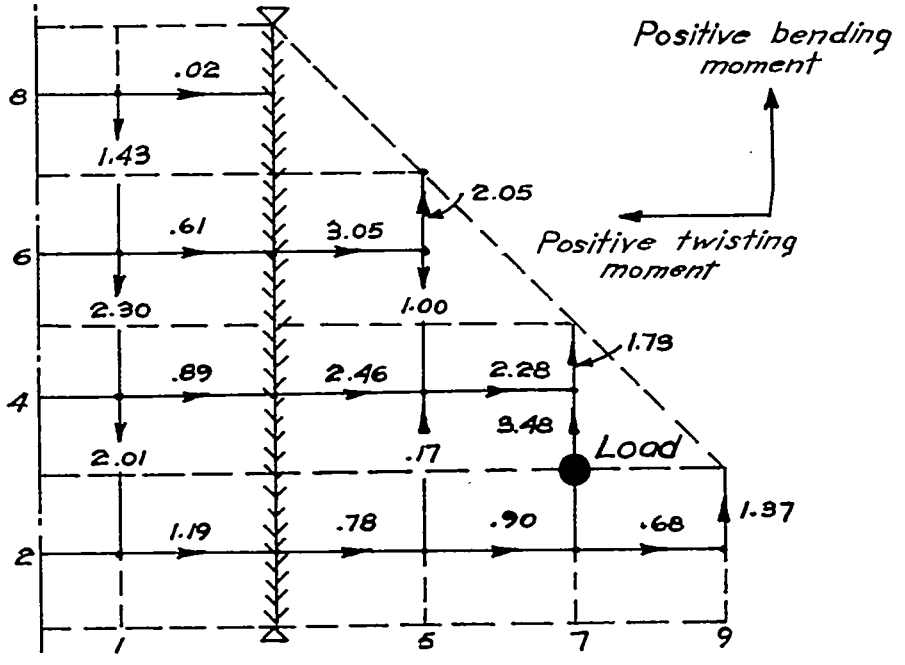

(a) Load at point 73.

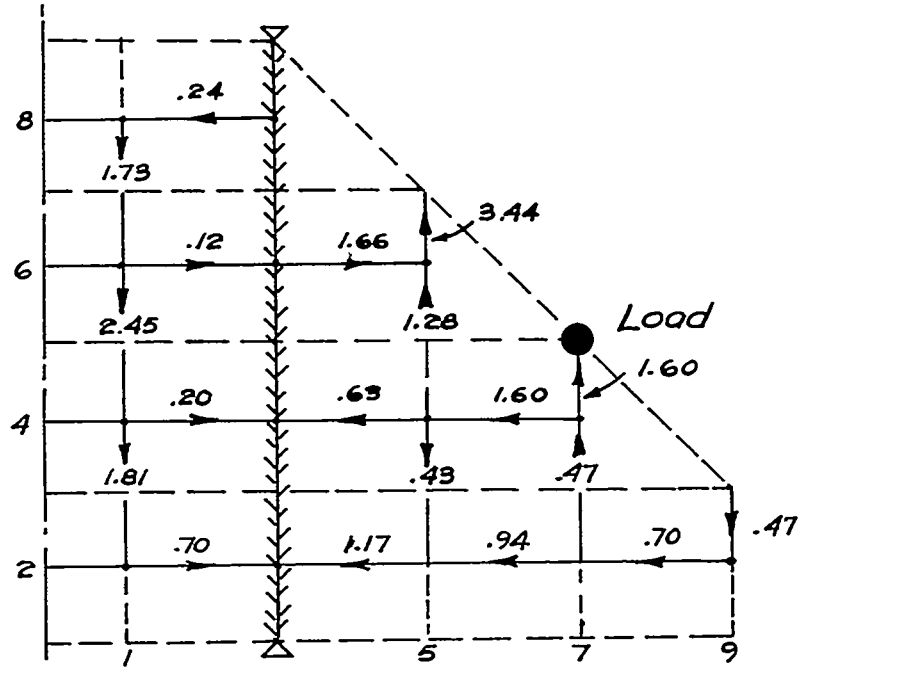

(b) Load at point 75.

Figure 20.- Distribution of chordwise bending moments and spanwise twisting moments. Rectangular section; symmetric loads.

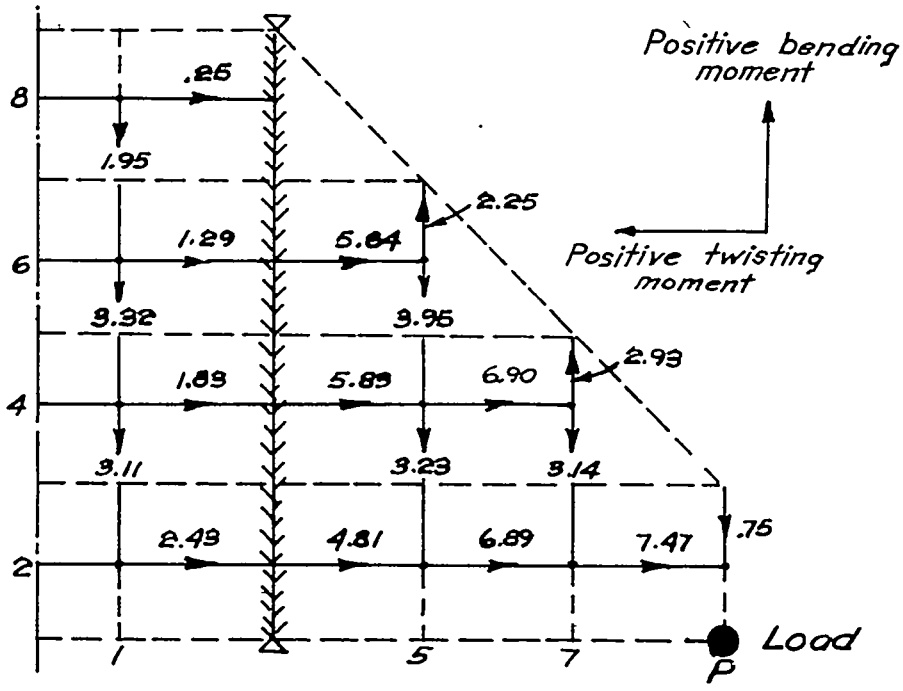

(a) Basic wing with shear strain in ribs and spars.

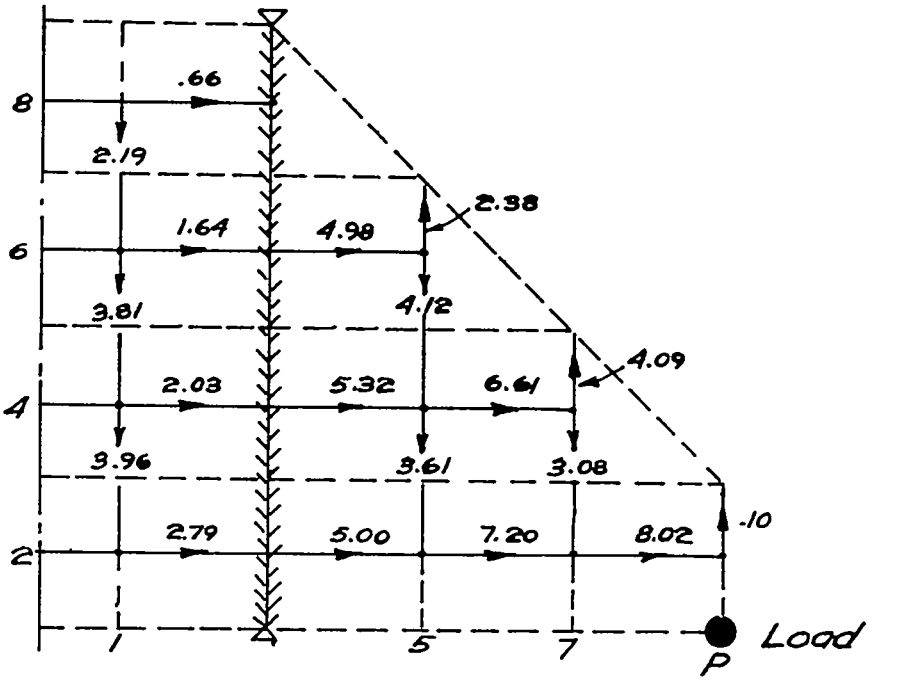

(b) Basic wing without shear strain in ribs or spars.

Figure 21.- Distribution of chordwise bending moments and spanwise twisting moments. Rectangular section; symmetric loads at point 91.

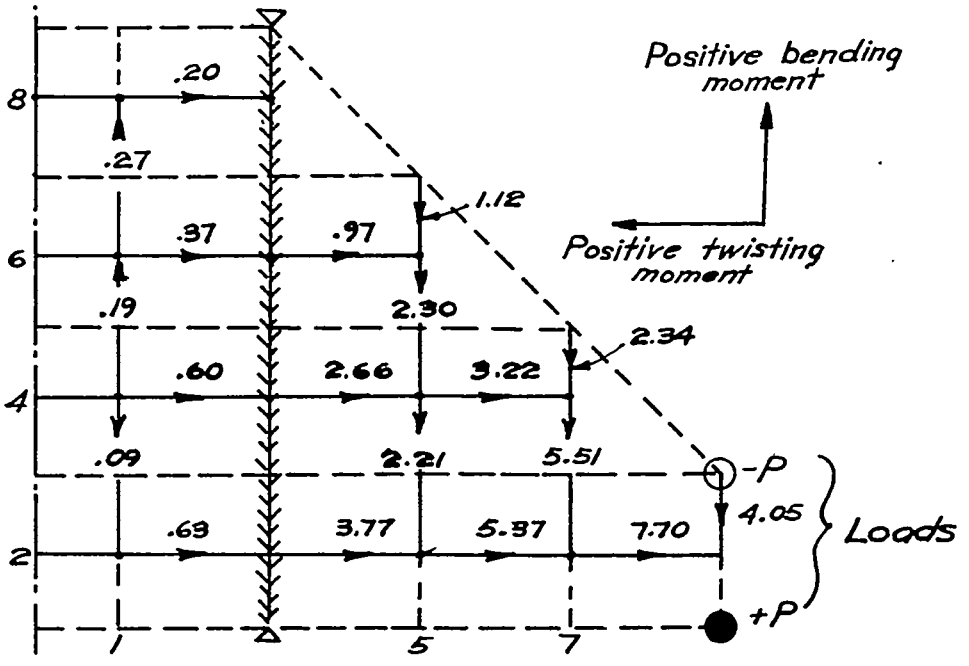

(a) Basic wing with shear strain in ribs and spars.

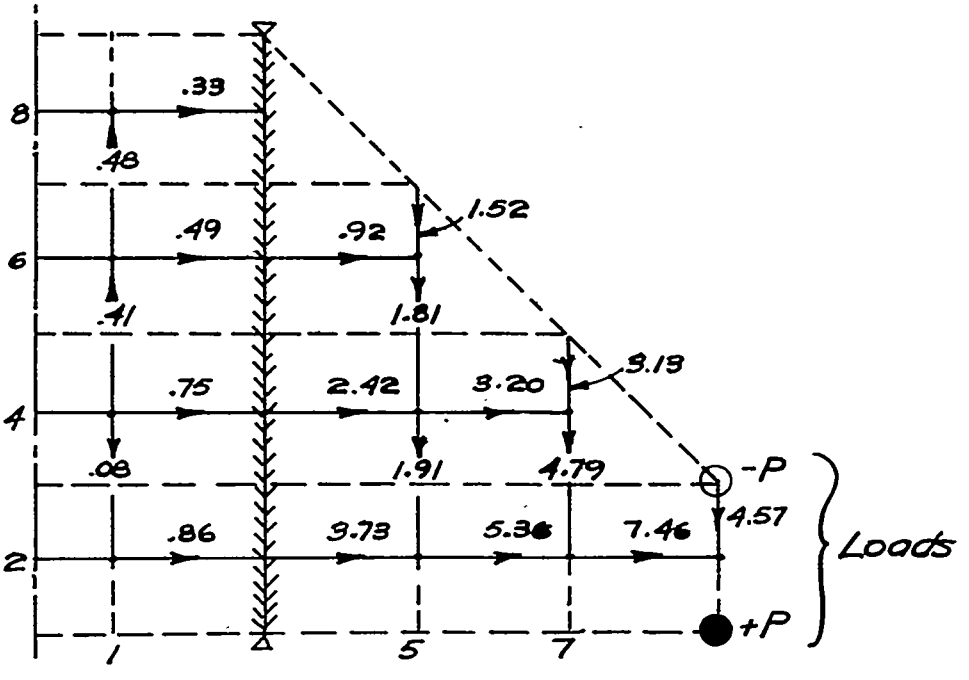

(b) Basic wing without shear strain in ribs or spars.

Figure 22.- Distribution of chordwise bending moments and spanwise twisting moments. Rectangular section; symmetric tip couples.

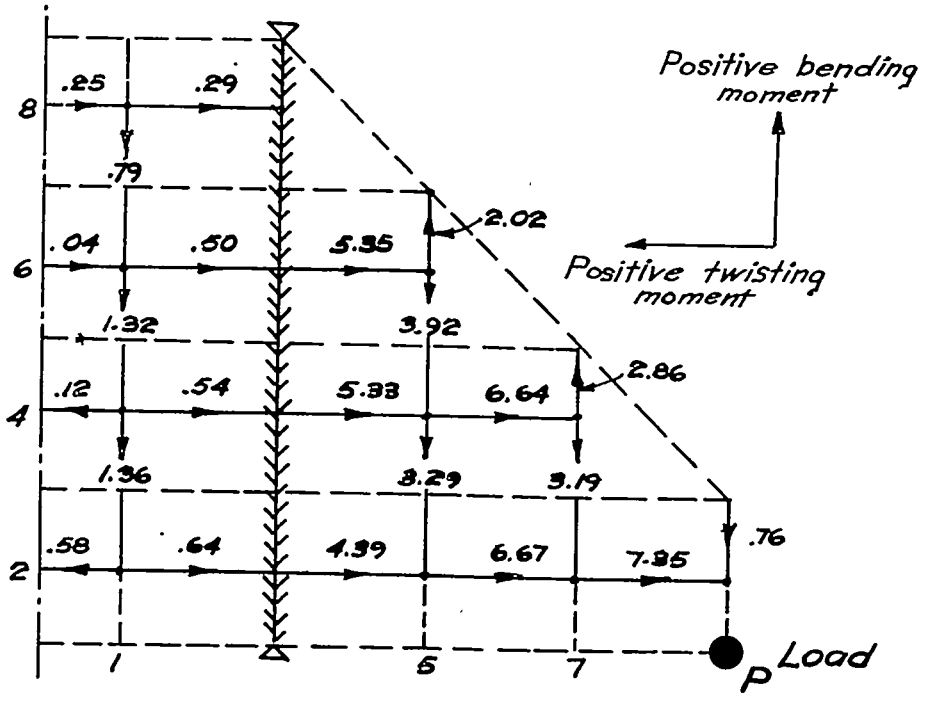

(a) Rectangular section.

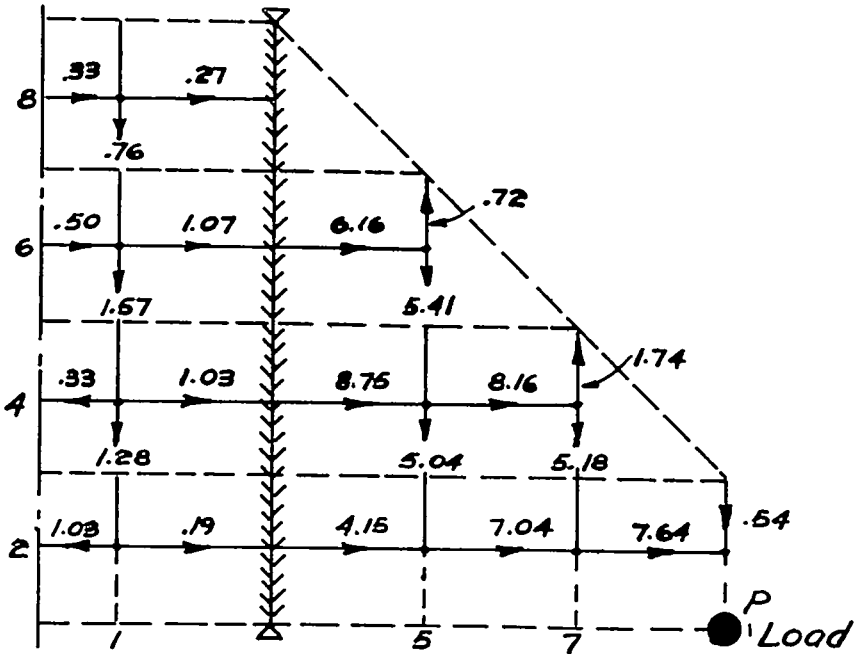

(b) Biconvex section.

Figure 23.- Distribution of chordwise bending moments and spanwise twisting moments. Antisymmetric loads at point 91.

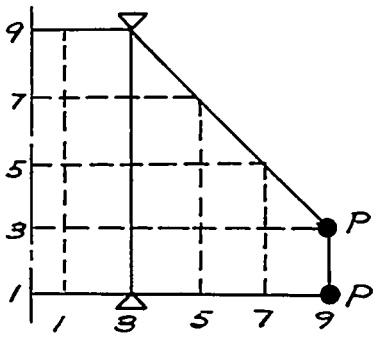

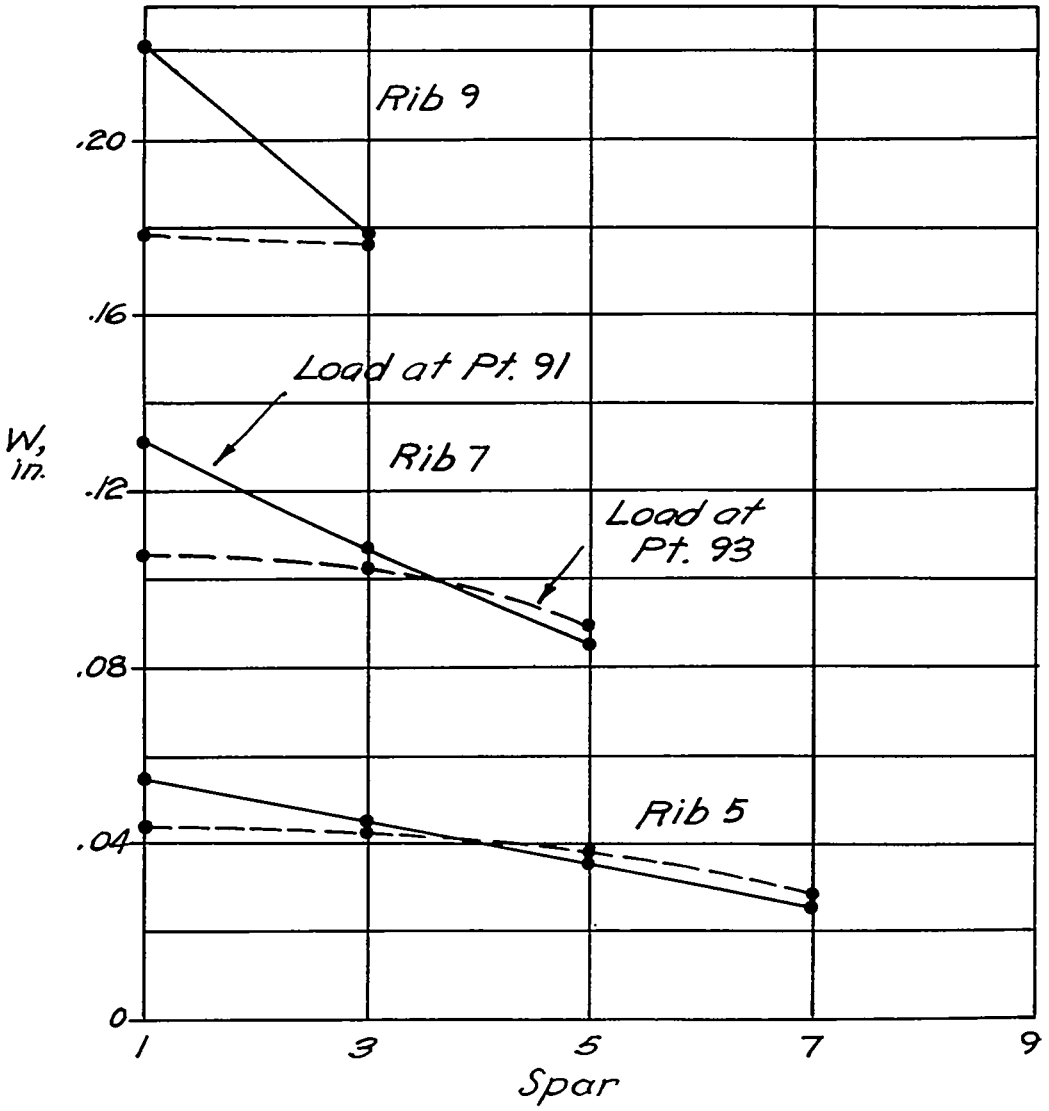

Figure 24.- Chordwise deflections. Rectangular section; symmetric loads; P = 1 kip.

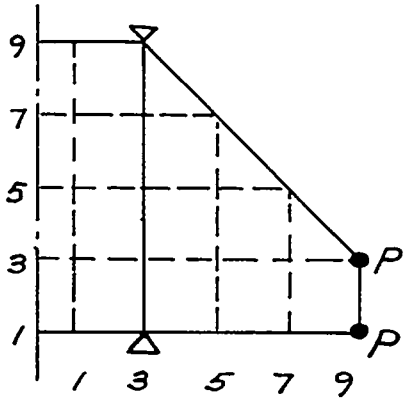

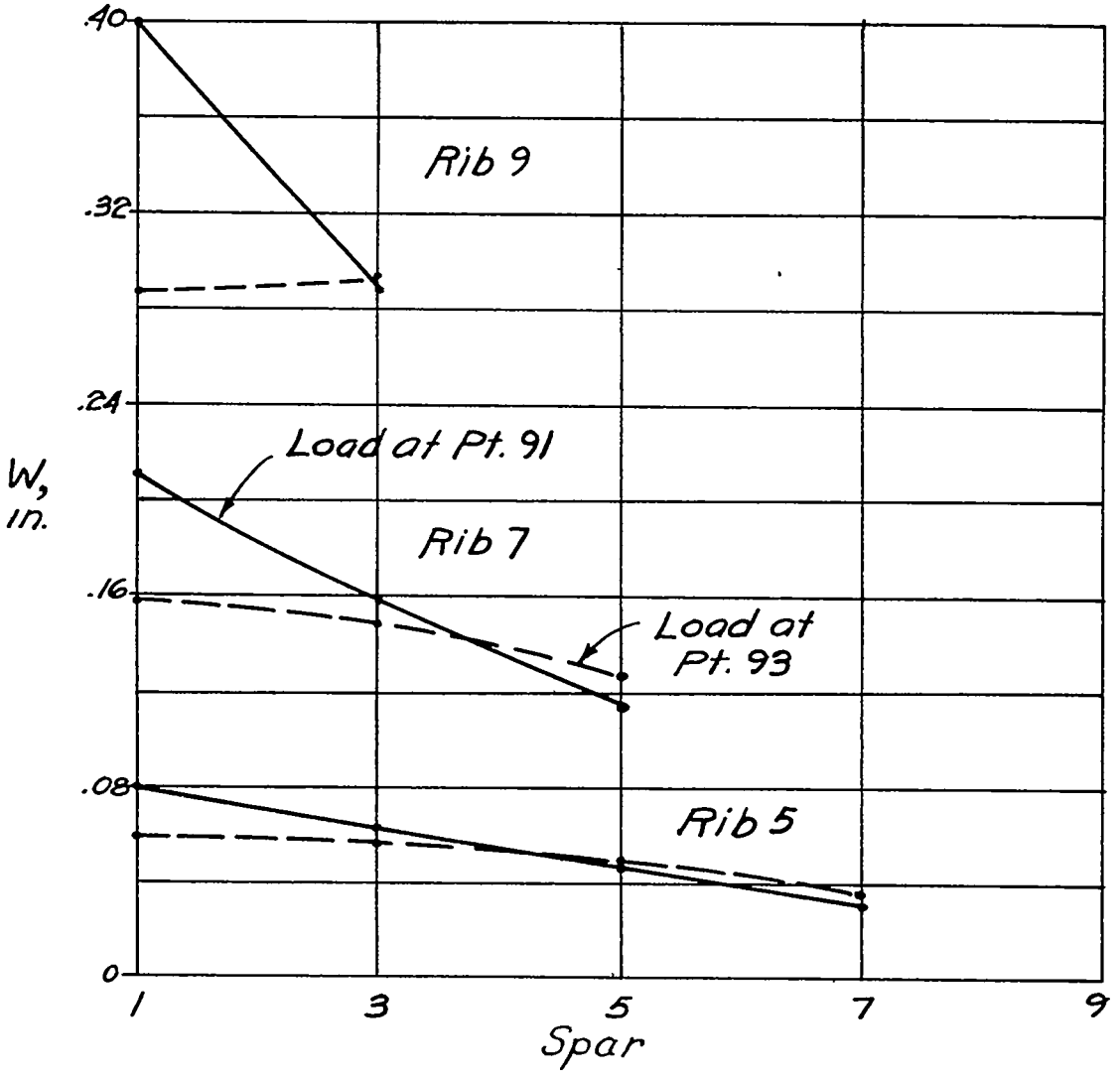

Figure 25.- Chordwise deflections. Biconvex section; symmetric loads; P = 1 kip.

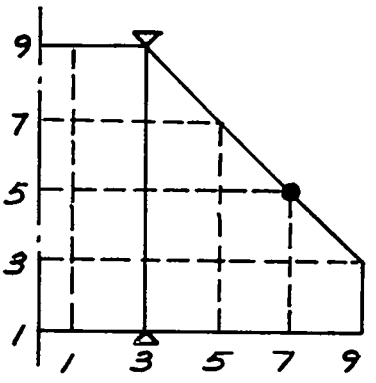

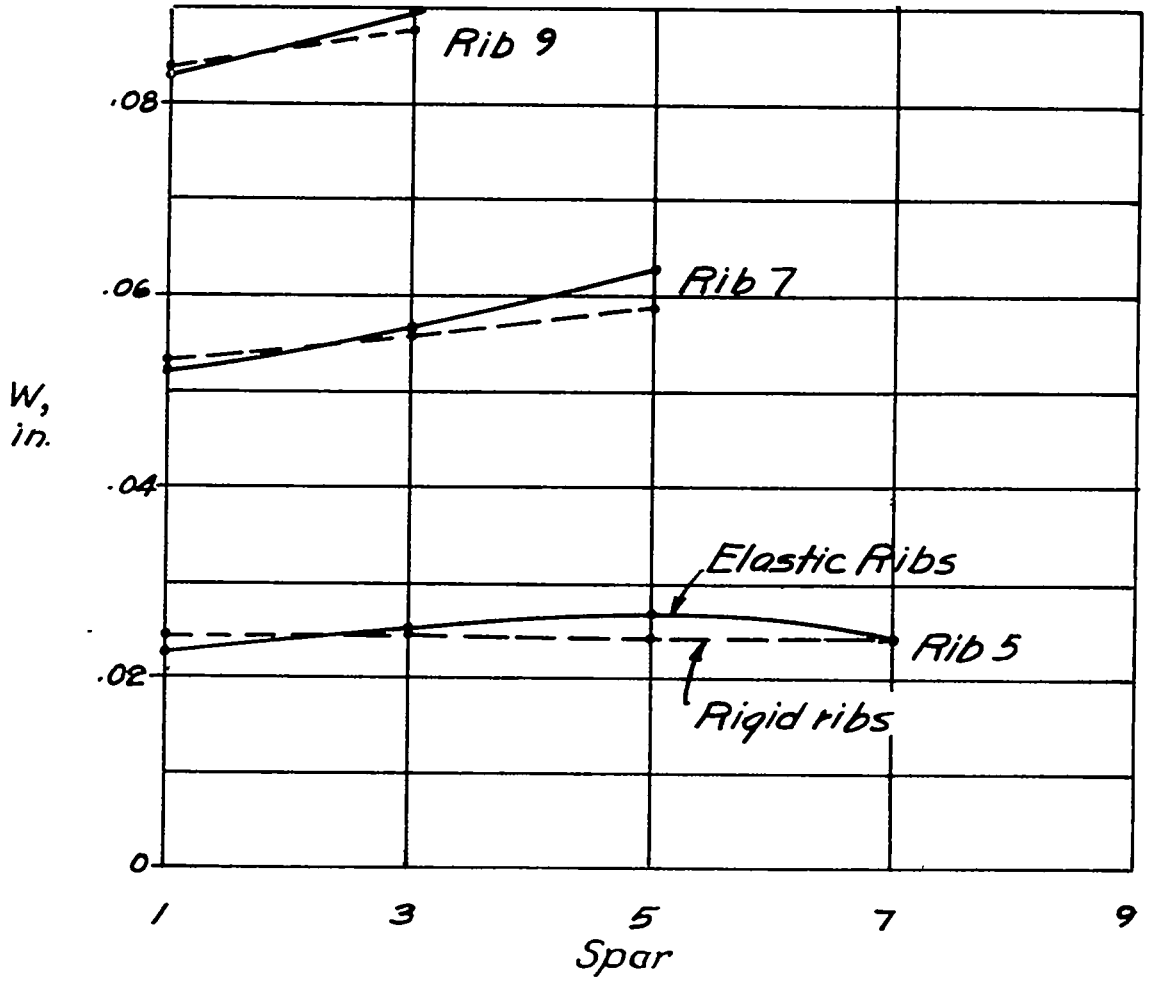

Figure 26.- Chordwise deflections. Rectangular section; symmetric loads at point 75; P = 1 kip.

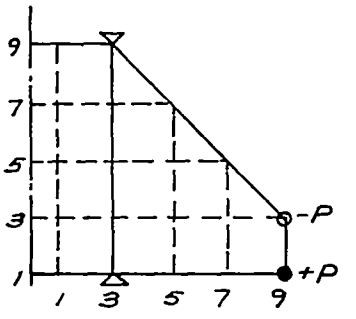

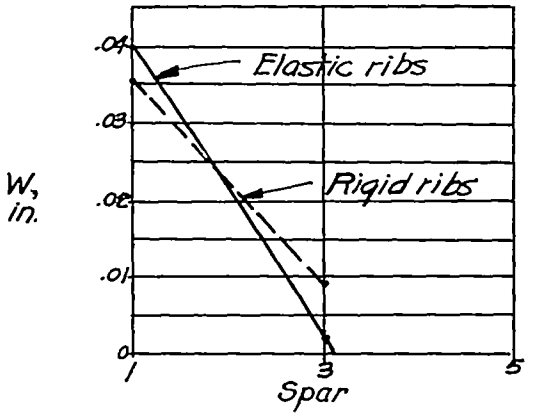

(a) Rib 9.

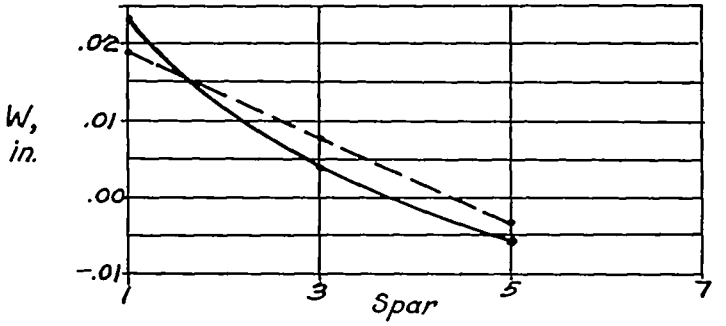

(b) Rib 7.

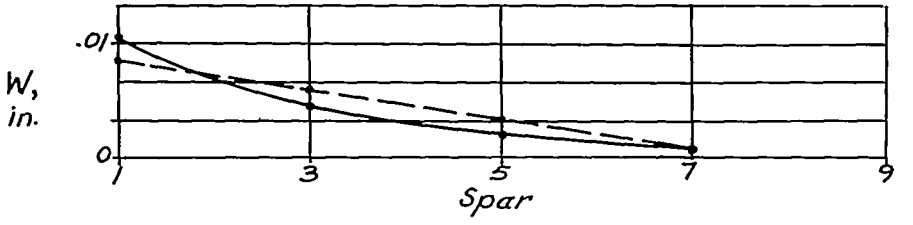

(c) Rib 5.

Figure 27.- Chordwise deflections. Rectangular section; symmetric tip couple; P = 1 kip.

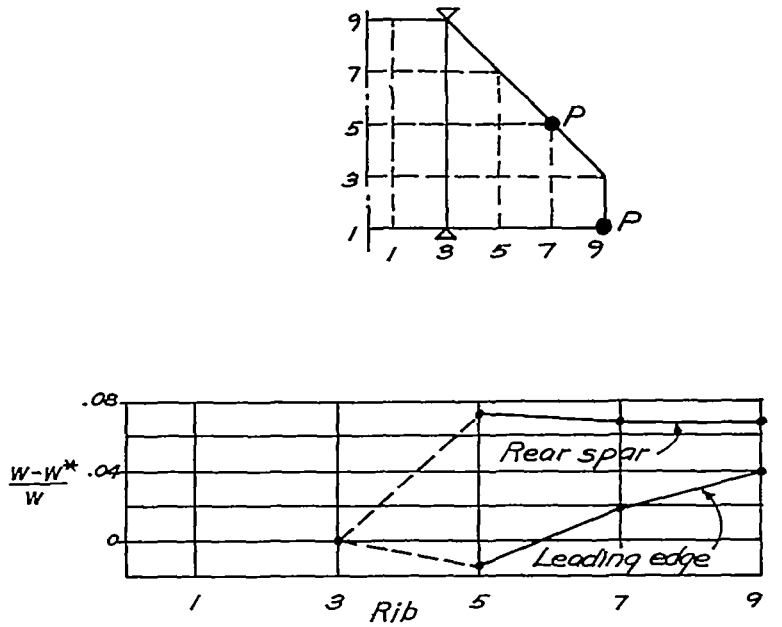

(a) Load at point 91.

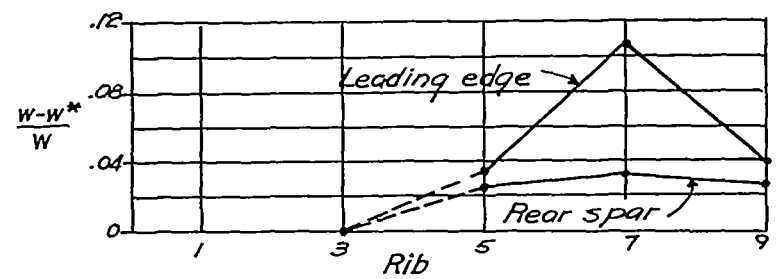

(b) Load at point 75.

Figure 28.- Effect of shearing strains upon deflections. Rectangular section; symmetric loads. w, deflection with shearing strains; w*, deflection without shearing strains.

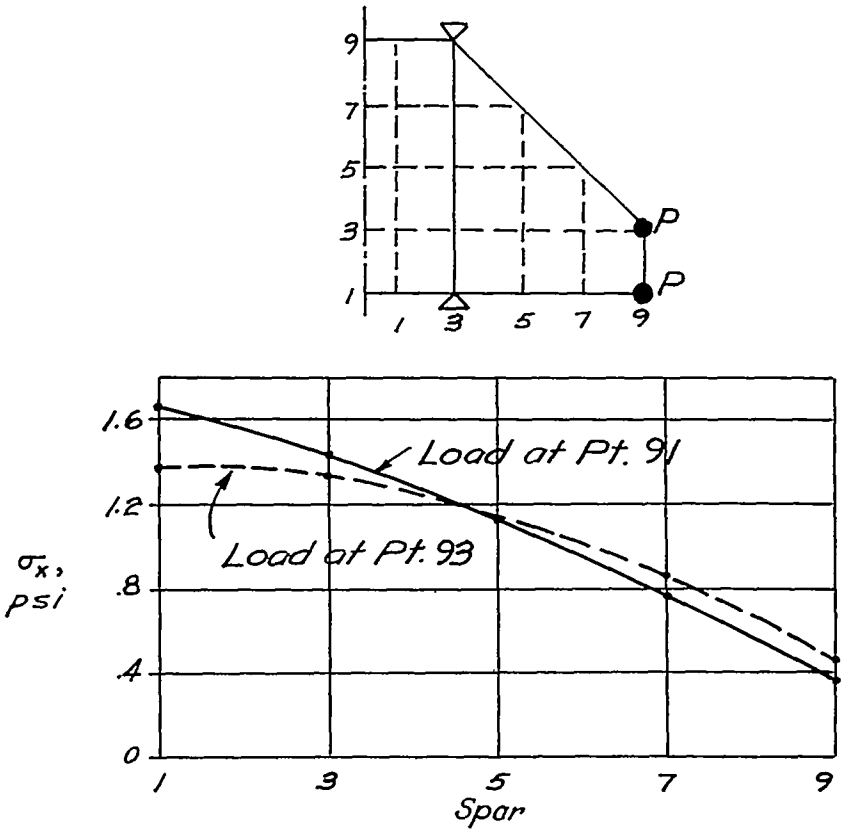

(a) Rectangular section.

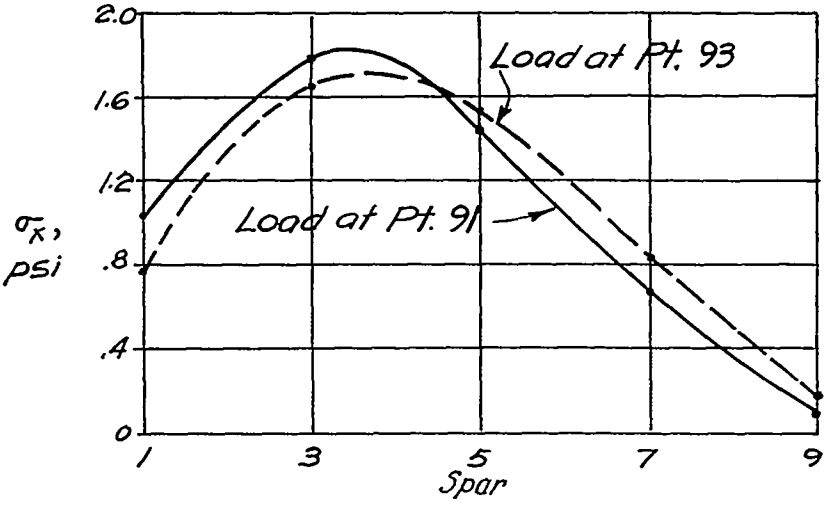

(b) Biconvex section.

Figure 29.- Spanwise normal stress over support. Symmetric loads; P = 1 pound.

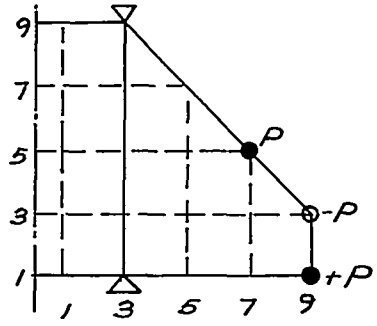

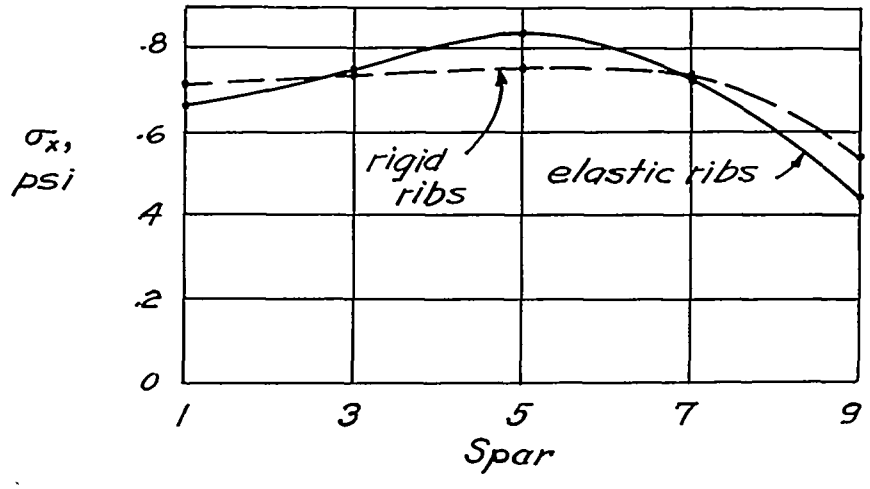

(a) Load at point 75.

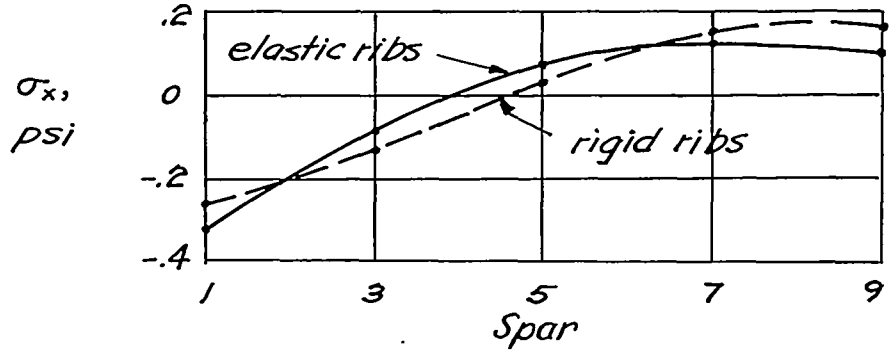

(b) Tip couple.

Figure 30.- Spanwise normal stress over support. Rectangular section; symmetric loads; P = 1 pound.

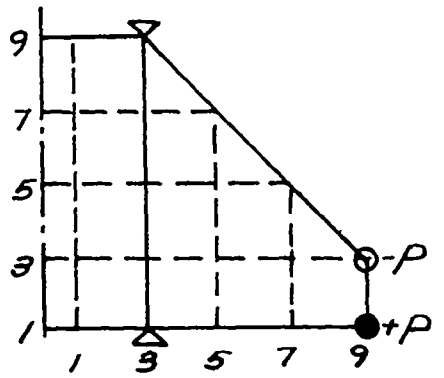

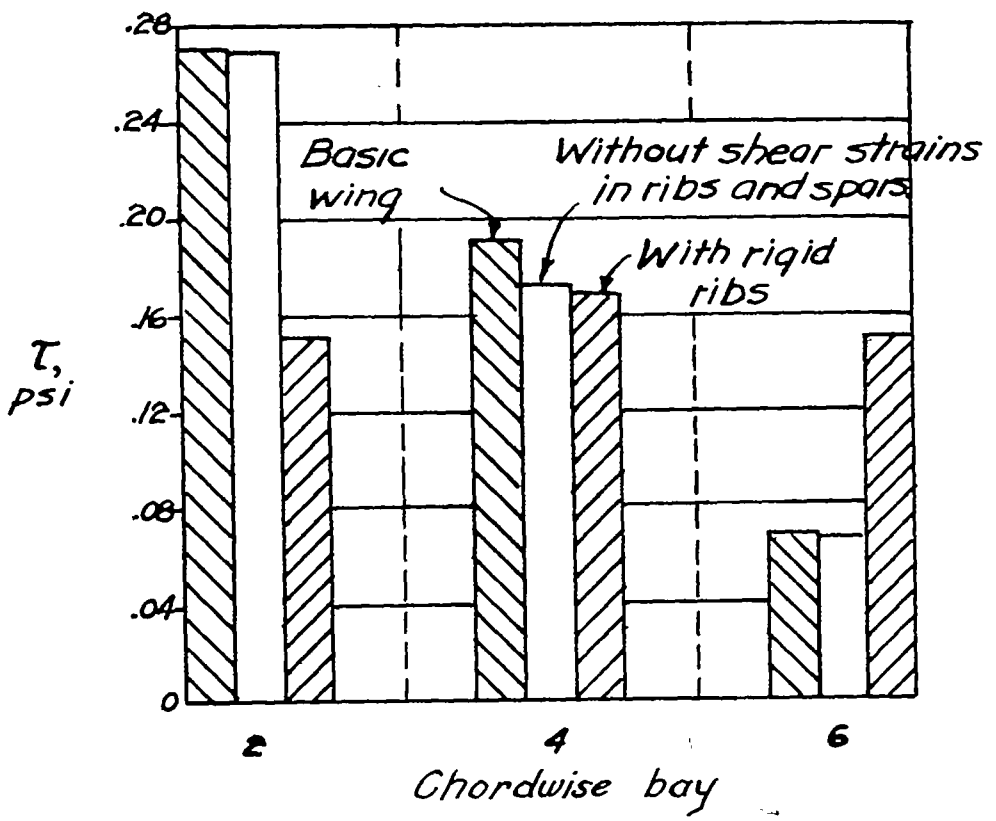

Figure 31.- Shear stress in skin between spars 3 and 5. Rectangular section; symmetric tip couple; P = 1 pound.

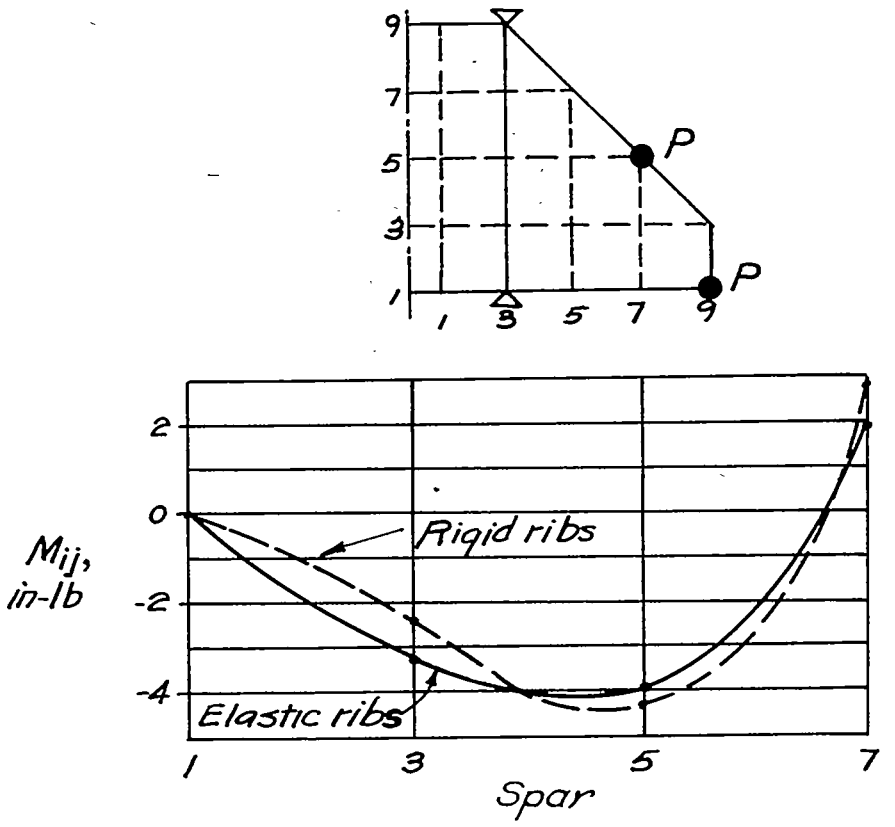

(a) Load at point 91.

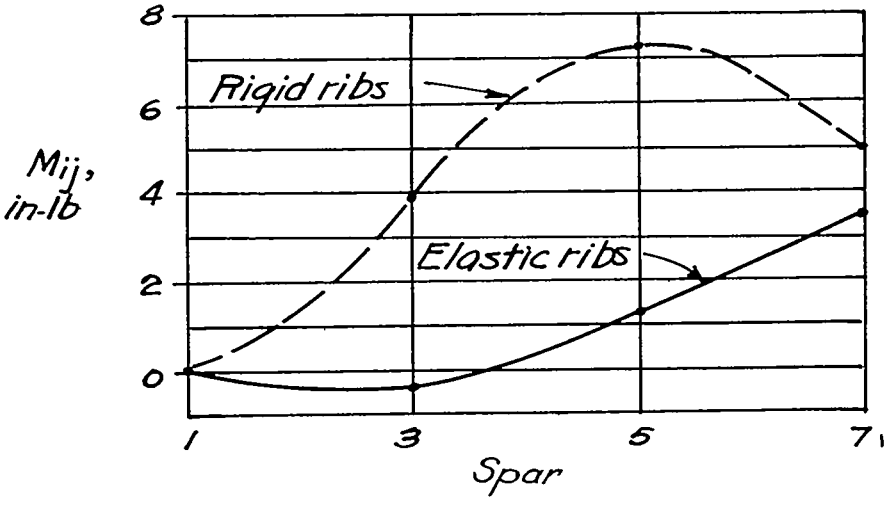

(b) Load at point 75.

Figure 32.- Chordwise bending moments along rib 5. Rectangular section; symmetric loads; P = 1 pound.

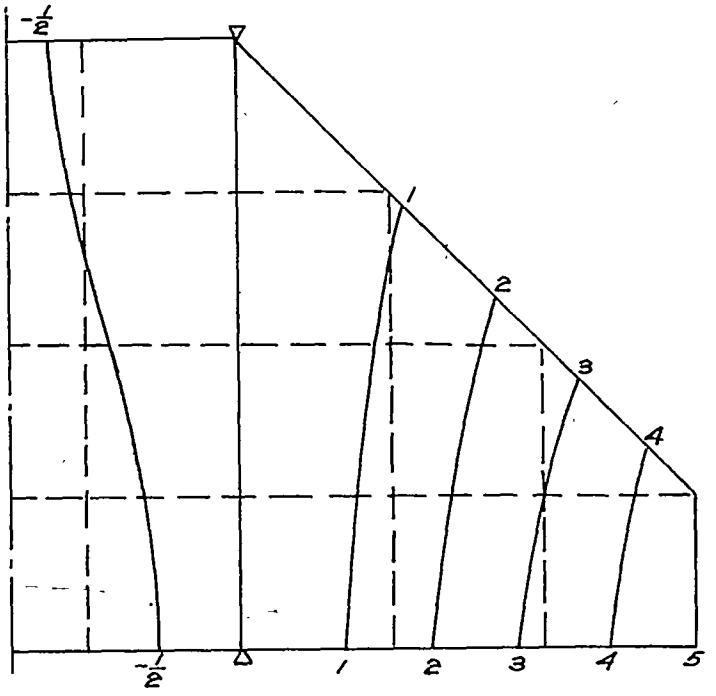

(a) First mode. Frequency is 46.6 cycles per second.

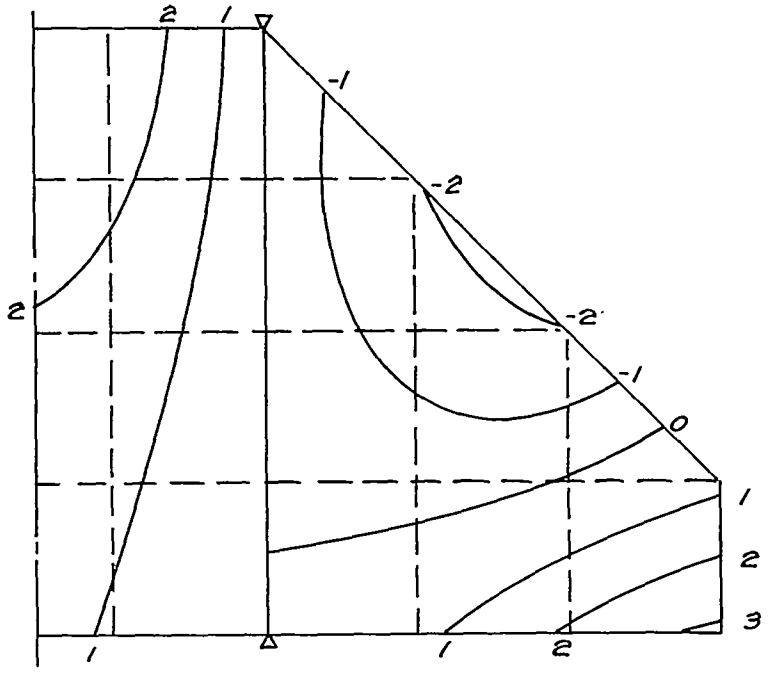

(b) Second mode. Frequency is 163 cycles per second.

Figure 33.- Symmetric vibration modes; rectangular section.

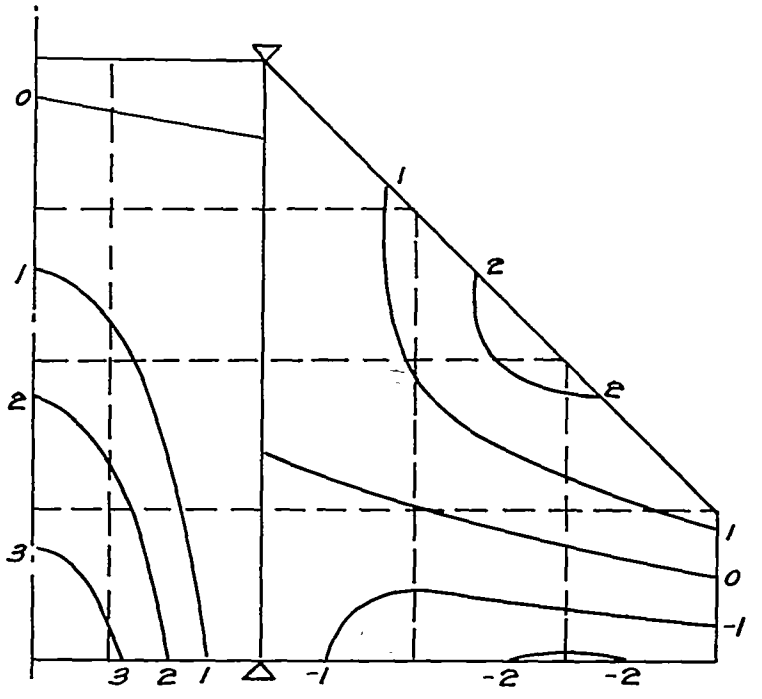

(c) Third mode. Frequency is 206 cycles per second.

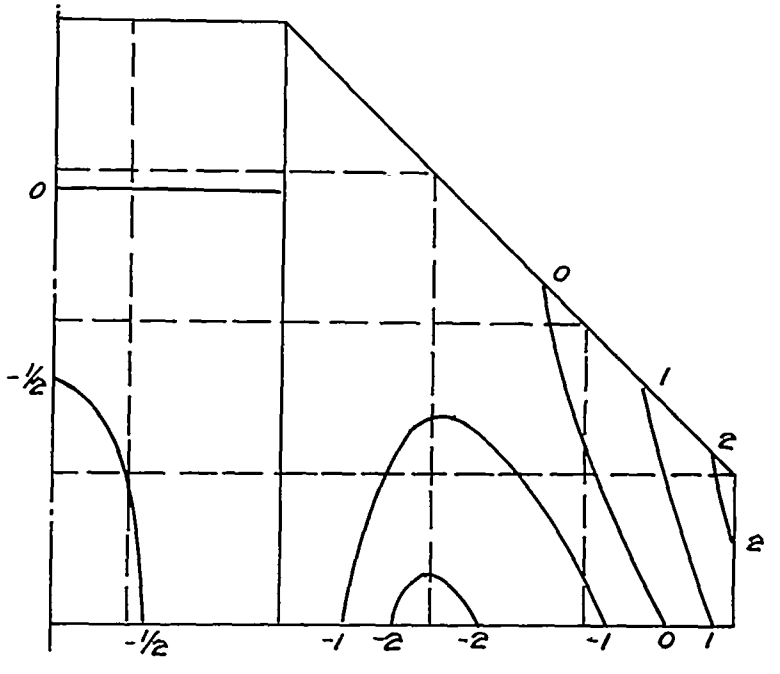

(d) Fourth mode. Frequency is 275 cycles per second.

Figure 33.- Concluded.